VOLUME XXIV JANUARY, 1945 NUMBER 1

THE BELL SYSTEM TECHNICAL JOURNAL

DEVOTED TO THE SCIENTIFIC AND ENGINEERING ASPECTS OF ELECTRICAL COMMUNICATION

AMERICAN TELEPHONE AND TELEGRAPH COMPANY
NEW YORK

50c per copy *$1.50 per Year*

THE BELL SYSTEM TECHNICAL JOURNAL

Published quarterly by the
American Telephone and Telegraph Company
195 Broadway, New York, N. Y.

SUBSCRIPTIONS

Subscriptions are accepted at $1.50 per year. Single copies are 50 cents each. The foreign postage is 35 cents per year or 9 cents per copy.

PRINTED IN U. S. A.

The Bell System Technical Journal

Vol. XXIV *January, 1945* *No. 1*

Intermittent Behavior in Oscillators

By W. A. EDSON

Oscillators of all sorts may, for certain values of the parameters, show low-frequency disturbances. Usually the disturbance takes the form of a low-frequency interruption of the desired oscillation. By the method here presented it is possible to determine whether or not such intermittent behavior will occur in a given oscillator and what circuit modifications are required to promote stability. The intentional generation of a modulated wave by control of the low frequency behavior of an oscillator is also considered. Oscillators of the negative resistance type are not considered.

I. Introduction

IT HAS been known for a long time that all kinds of oscillators are subject to the trouble variously referred to as intermittent oscillation, motor boating, or squegging. In conventional circuits such as the Hartley the phenomenon is most likely to be observed if the grid leak and grid condenser are abnormally large. It is found that the time constant of this combination must be reduced as the frequency is raised and as the Q of the resonant circuit is decreased. At frequencies above a few hundred megacycles the problem of producing a practical circuit with suitable margin of stability is quite difficult.

With the advent of the oscillator having automatic output control the problem assumed a new aspect.[1, 2] By application of an amplified control circuit a high degree of constancy of output together with low harmonic output is obtained. Satisfactory operation is secured, however, only when suitable attention is given to the characteristics of the control circuit.

The intentional generation of pulses by means of intermittent oscillations of relatively high frequency has been studied to some extent, and circuits of this kind are employed in some television systems. Usually the high-frequency oscillation is limited to a small portion of the low-frequency cycle, the charge stored during this period being allowed to dissipate itself relatively slowly during the remainder of the cycle.

In all of these circuits satisfactory performance depends upon a proper proportioning of elements not directly associated with the operating fre-

[1] L. B. Argimbau, "An Oscillator Having a Linear Operating Characteristic," *Proc. I.R.E.*, Vol. 21, p. 14, Jan. 1933.

[2] J. Groszkowski, "Oscillators with Automatic Control of the Threshold of Regeneration," *Proc. I.R.E.*, Vol. 22, p. 145, Feb. 1934.

quency. When continuous oscillation is necessary it is desirable to provide adequate margin against intermittent operation. When intermittent operation is desired the opposite is true. In either case an understanding of the same general problem is necessary.

The present analysis applies only to oscillators of the feedback type. No method of extending it to cover negative resistance oscillators such as the Dynatron and the Transitron has been found. Relaxation oscillators as such are not considered here inasmuch as they are seldom affected by intermittent operation. No specific frequency limits apply but it is sometimes difficult at very high frequencies to achieve desirable values of the constants. At very low frequencies oscillators employing automatic output control are relatively unsuitable because their performance tends to be unduly sluggish.

The term linear oscillator is used to indicate an oscillator in which the range of operation is controlled within such limits that the harmonic content of the output is inappreciable.

The general equation describing a simple amplitude-modulated wave is

$$V = V_0(1 + m \sin 2\pi ft) \sin 2\pi Ft$$

This may be taken as defining the modulation factor m, a complex number which is limited to magnitudes between zero and one.

II. General Theory of Oscillation

It is found that three separate functions are necessary and sufficient for the operation of an oscillator of the feedback type.[3] These are indicated in the block diagram of Fig. 1.

The amplifier must be provided to overcome the losses of the rest of the system. The power output, if any, depends upon the fact that the output of an amplifier is greater than the input.

Selectivity must be provided to insure that the output has a definite frequency. Ordinarily a tuned circuit of relatively high Q is used although some excellent oscillators employ resistance-capacitance networks. The term filter is employed as being sufficiently general to include these extremes.

A limiter of some form is necessary to establish the level at which sustained oscillations occur. In many circuits the functions of amplifier and limiter are performed simultaneously in the vacuum tube. In an important class of oscillators the limiter is a thermal device such as a tungsten lamp. In the Meacham circuit the functions of limiter and filter are combined in a bridge employing a tuned circuit and a tungsten lamp.

To simplify the analysis it is convenient to assume that the amplifier of Fig. 1 is completely linear and operates with equal gain at all frequencies

[3] This topic is discussed more fully in "Hyper and Ultra-High Frequency Engineering," R. I. Sarbacher, and W. A. Edson, John Wiley & Sons, Inc., 1943.

from zero to infinity. Similarly the filter is assumed to consist of linear circuit elements and to have a definite curve of loss versus frequency. Associated with this loss characteristic is some specific phase characteristic.[4] The limiter is assumed to have a loss which is independent of frequency but which is explicitly related to the input (or output) voltage.

Although amplifiers having the ideal performance indicated are not physically realizable there are no new or unfamiliar concepts involved. Similarly the performance of passive networks, such as constitute the filter, has been extensively studied and is well understood. It is therefore appropriate to devote the following section to the third function.

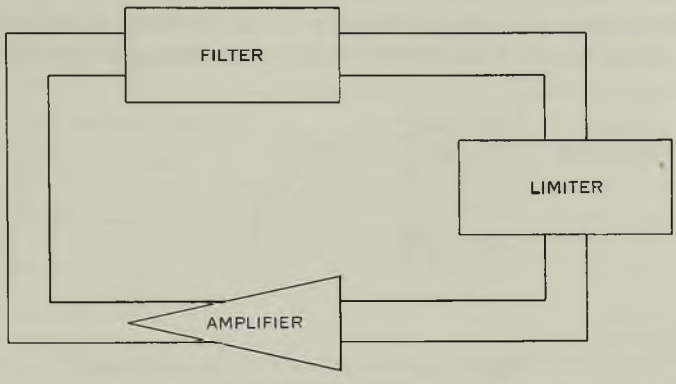

Fig. 1—Functional block diagram of an oscillator.

III. Types of Limiters

The limiters which are now in common use may be separated into four relatively distinct groups.

1. Vacuum tubes in which the gain is decreased by simple overload as the level of oscillation rises. This is the most common form of limiter.

2. Varistors in which the impedance depends upon the instantaneous value of current. Copper oxide, thyrite, and electronic diodes are examples.

3. Thermistors in which the resistance depends upon the rms value of current but does not vary appreciably during any one cycle. Carbon and tungsten filament lamps are the most common examples.

4. Vacuum tubes in which the gain is reduced by application of a bias which depends upon the level of oscillation. Usually the bias is developed by rectifying a portion of the output.

The limiters of the first two groups depend for their operation upon the generation of harmonic voltages and currents. The limiters of the second

[4] H. W. Bode, "Relations Between Attenuation and Phase in Feedback Amplifier Design," *Bell Sys. Tech. Jour.*, Vol. 19, pp. 421–457, July 1940.

two groups operate with very little harmonic distortion. The output of oscillators employing such limiters may, therefore, be made quite free from harmonic voltages. Oscillators of this sort are referred to as linear because the tube or tubes serve as simple Class A linear amplifiers.

IV. Criterion of Self Modulation

The block diagram of Fig. 1 is characterized by the fact that the separate elements are connected to each other in the form of an endless ring. The output may be assumed to come from any of the three junctions. It is this fact of closure which complicates the problem of oscillator study. For purposes of analysis it is convenient to open the loop as shown in Fig. 2. For this example it makes no difference where we choose to make the cut, but in actual circuits some caution must be exercised. This matter is dis-

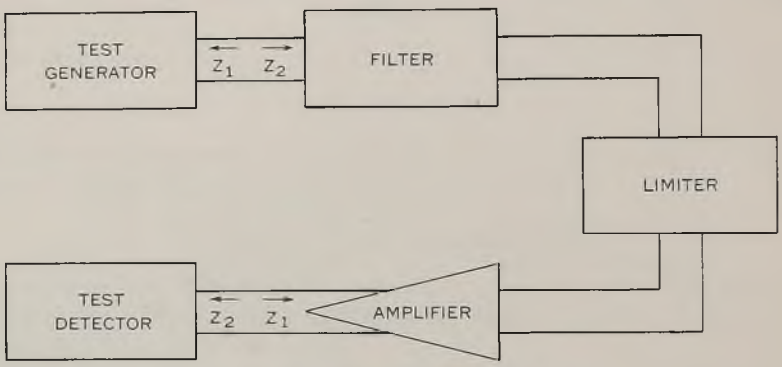

Fig. 2—Test for self-modulation in an oscillator.

cussed more fully later. It is also necessary to choose the impedances of the test generator and test detector so that the operation of the components of the original system is not disturbed.

If a continuous wave of suitable voltage and frequency is supplied by the test generator it will be found that the terminal voltage of the test detector is identical in magnitude and phase with that of the generator. In this condition the requirements which are fundamental to oscillators are satisfied. That is, the frequency and level at which oscillation should occur if the circuit were closed as in Fig. 1 have been established. The net phase shift of the system is zero and the net gain is zero.

Whether the oscillations so produced would be stable or interrupted is now determined by adding amplitude modulation of relatively low frequency and very small magnitude to the test generator. It is clear that this modulation will be transmitted through the amplifier, filter, and limiter to the test detector and that the phase and percentage of the modulation may both be

modified. By examining the transmission of a lightly modulated wave for various frequencies of modulation it is possible to determine whether or not the normal oscillation will be self modulated when the loop is closed as in Fig. 1.

The carrier is held constant at the frequency F and amplitude V for which the input and output are identical, and the frequency f of the modulation is varied from zero to infinity. In the following treatment it is assumed that the significant portion of the characteristic is observed for modulation frequencies small compared to F. The theory is simplified in this way without being seriously restricted in usefulness. The percentage of modulation must be held very low so as not to exceed the normal operating range of the limiter. The criterion is most conveniently stated in terms of the transmission of the modulation envelope which may be considered as a vector quantity.

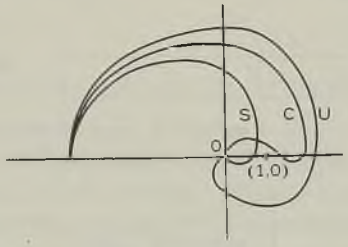

Fig. 3—Nyquist diagram showing magnitude and phase of loop transmission.
Legend: U is unstable
C is conditionally stable
S is absolutely stable

A plot of the vector ratio of output to input modulation for various frequencies is prepared as in Fig. 3. The system characterized by curve U is unstable and will generate a self modulated rather than a continuous wave. The system characterized by curve S is unconditionally stable and will be free from self modulation. The system characterized by curve C is conditionally stable and may generate either a continuous or an interrupted wave depending upon the manner in which the oscillation is started and other factors.

V. Analogy of the Oscillator to the Feedback Amplifier

The behavior of oscillators of the type here considered is entirely dependent upon feedback. It is therefore appropriate to review the fundamental principles which apply to feedback in general.

In the feedback amplifier, negative feedback is applied to improve the linearity, stability, impedance, or frequency characteristics. Considerable improvements in some or all of the properties may be secured if a consider-

able amount of negative feedback is applied and properly controlled. Positive feedback is sometimes used to increase gain or selectivity, but stability under such circumstances is poor. Any considerable amount of positive feedback results in oscillation.

The criterion by which stable feedback systems are distinguished from unstable ones has been presented by Nyquist and verified by others.[5, 6] A closed feedback system having input and output terminals is illustrated in Fig. 4. In Fig. 5 the loop is opened at some arbitrary point and a test

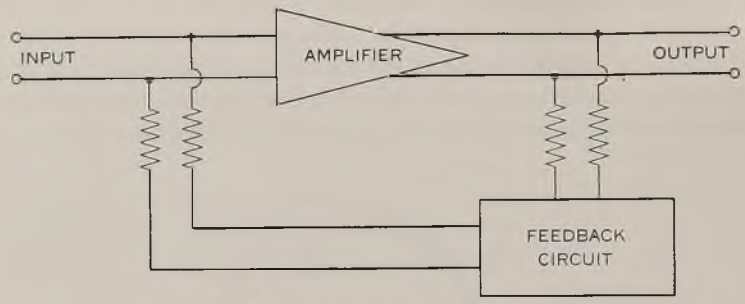

Fig. 4—Typical feedback amplifier.

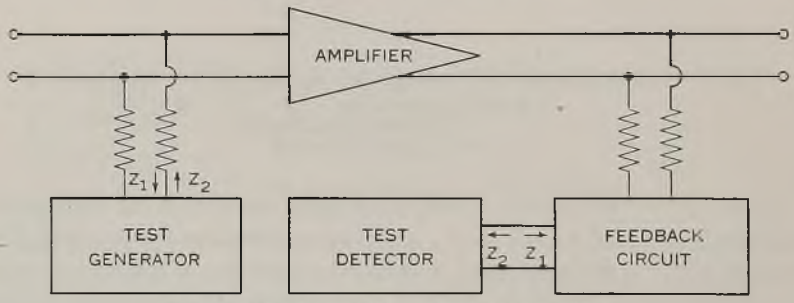

Fig. 5—Test for stability of feedback amplifier.

oscillator and detector are connected. Here as in Fig. 2 certain precautions as to impedance are observed. The test generator must produce a pure sinusoidal wave of such small magnitude that no part of the tested system overloads and the vector ratio of the detector voltage to the generator voltage is observed for a large number of frequencies. The polar plot of Fig. 3 applies directly to the feedback amplifier except that the radius vector represents the transmission of a simple wave rather than of an envelope.

[5] H. Nyquist, "Regeneration Theory," *Bell Sys. Tech. Jour.*, Vol. 11, pp. 126–147, Jan., 1932.

[6] E. Peterson, J. G. Kreer, & L. A. Ware, "Regeneration Theory and Experiment," *Proc. I.R.E.*, Vol. 22, pp. 1191–1210, Oct., 1934.

The conditions of absolute and conditional stability and instability are exactly the same as those already given.

It must be appreciated that Nyquist's criterion supplies no information as to the type or frequency of oscillations which will be generated by an unstable system. This is true because the analysis is limited to linear systems. The only information imparted is that a very small oscillation of some frequency will increase exponentially with time until the amplitude is limited by the action of some non-linear device. A small or relatively large shift of frequency may occur and the oscillation may be regular or intermittent. The present work extends the usefulness of Nyquist's criterion by using it in modified form to determine whether or not a particular unstable system (oscillator) has or lacks stability as to self-modulation. There is no apparent reason why a system lacking in both fundamental and envelope stability might not be analyzed a third time for the stability of the self-modulation.

VI. Analysis of an Oscillator having Automatic Output Control

Figure 6 presents a simple form of feedback oscillator having a separate rectifier as limiter. For small amplitudes of oscillation the tube operates in a linear fashion with cathode self-bias. No bias is produced by the diode rectifier until the peak voltage in the coil L_3 exceeds that of the bias battery B. All voltage in excess of this value is rectified, smoothed by the condenser C, and applied to the resistor r as bias. It is seen that a small percentage change in the output level may result in a large change in the bias. Accordingly an output which is quite stable with respect to the tube condition and applied voltages, except that of B, is to be expected.

The stability of this circuit with respect to self modulation is most conveniently tested by opening the oscillatory loop at the plate of the tube. In so far as the plate resistance of the tube is high with respect to that of the associated circuit it is not necessary to control the impedances of the test generator and detector extremely accurately. A block diagram equivalent to Fig. 6 is presented in Fig. 7. The conditions which must exist for the test of stability are shown in Fig. 8. In both those figures it should be noted that the gain control is actuated by the input, not the output, of the amplifier. It is therefore possible for a marked decrease of output voltage to result from a small increase of input voltage. This behavior is very different from that of the conventional, back-acting, automatic-volume-control amplifier in which the output change is in the same direction as the input change but of reduced magnitude. It is this difference which is the basis of most difficulty with amplitude controlled oscillators.

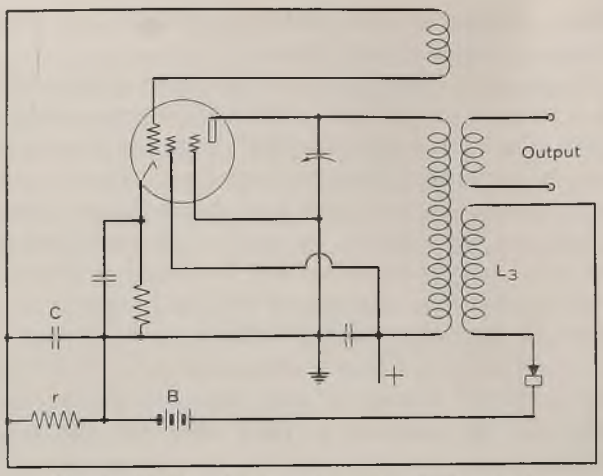

Fig. 6—Oscillator having automatic output control.

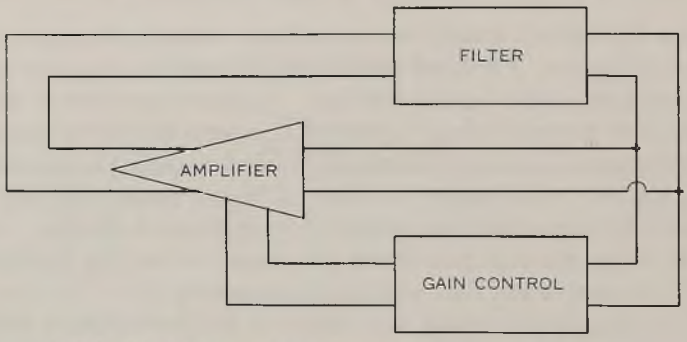

Fig. 7—Block diagram of automatic output control oscillator.

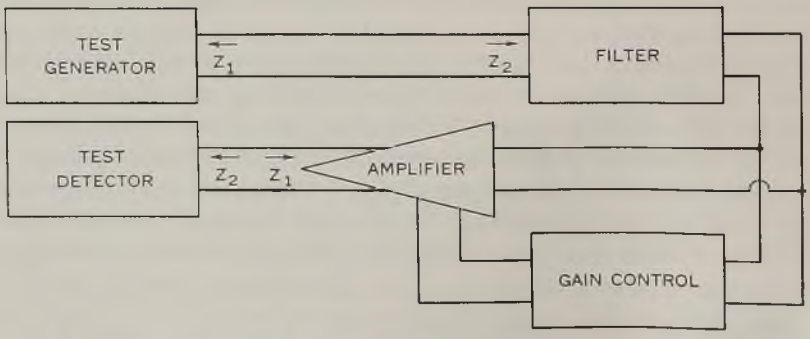

Fig. 8—Test for modulation stability of automatic output control oscillator.

Filter

The filter of Fig. 8 consists of only a single tuned circuit. Its transmission is readily represented in terms of the circuit Q by the familiar universal resonance curve. The transmission of a modulated wave through such a passive network is conveniently determined by separating the wave into its carrier and two sidebands. The carrier will be the frequency F corresponding to zero phase shift which, in this case, is also the frequency of maximum transmission. The sidebands will be shifted in phase by equal

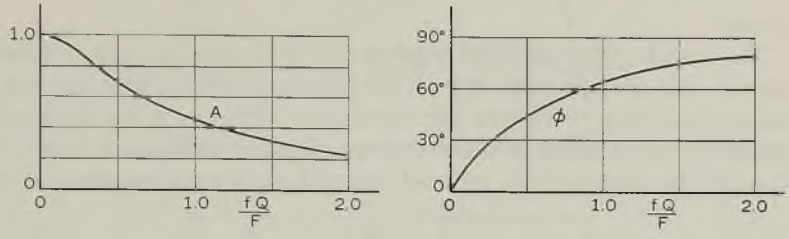

Fig. 9—Envelope transmission of a modulated wave through a single tuned circuit of selectivity Q.

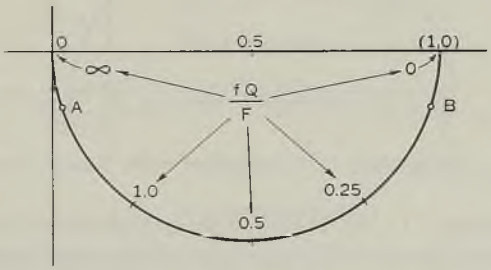

Fig. 10—Data of Fig. 9 plotted in polar form.

and opposite amounts and attenuated according to the frequency f by which they differ from the carrier. This behavior is interpreted in Fig. 9 as transmission and phase shift of the envelope. It is seen that the transmission approaches zero and the phase shift approaches 90° as the modulation frequency is indefinitely increased. The same data is presented in polar form in Fig. 10. Specifically Fig. 10 shows the vector ratio of the modulation factor m of the output wave to that of the input wave for all frequencies. In Fig. 9 the magnitude and phase angle of the ratio are shown separately.

Limiter

The limiting action of the tube and diode combination is determined by direct circuit analysis. For very low modulating frequencies the condenser

C of Fig. 6 serves only as a high-frequency by-pass; the direct voltage across r being the instantaneous difference between the peak voltage induced in L_3 and that of the stabilizing battery B. For very high modulating frequencies the modulation as well as the carrier is by-passed by C and no modulation voltage appears across r. Thus the bias is constant and the output wave is identical with the input wave. This corresponds to an envelope transmission of (1, 0). For intermediate values of the modulating frequency the voltage developed across r varies in magnitude and phase approximately as if a constant current of the modulating frequency f were applied to r and C in parallel.

The output of the amplifier depends not only upon the bias developed across r but also upon the input. For systems having a large amount of control the action of the bias is predominant. Thus for a low modulating frequency the variation of the bias overpowers the initial modulation, the phase of the modulation is reversed, and the percentage magnified by the

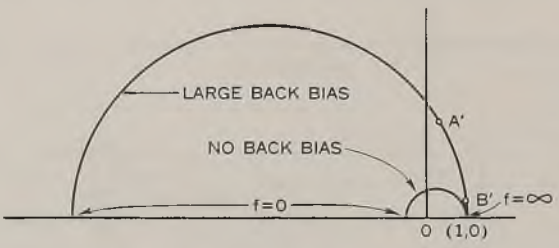

Fig. 11—Envelope transmission of a modulated wave through controlled amplifier.

action of the limiter. In Fig. 11 the envelope transmission is plotted in polar form for conditions of relatively large and relatively small amounts of control.

Loop Transmission

The separate diagrams of Figs. 10 and 11 are combined in Fig. 12 to determine the stability of the system. For any chosen frequency f the vector of Fig. 10 is multiplied by the vector of Fig. 11 corresponding to the same frequency to locate one point of Fig. 12. The resultant vector has an angle which is the sum of the two component angles and a magnitude which is the product of the two component magnitudes.

It is seen that the loop may be made to cross the axis considerably to the left of the point (1, 0) if the points A and A' of the previous figures correspond to the same frequency. Similarly the loop may be made to come very close to the point (1, 0) by increasing the size of C or lowering the Q of the tuned circuit so that the points B and B' correspond to the same frequency. With the circuit elements drawn in Fig. 6 the stability margin

may be reduced to zero, but actual looping of the point (1, 0) is not indicated. Parasitic elements, not here considered, can readily affect the performance enough to produce instability.

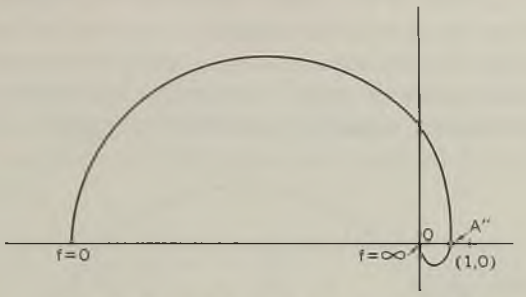

Fig. 12—Nyquist diagram applying to Fig. 6.

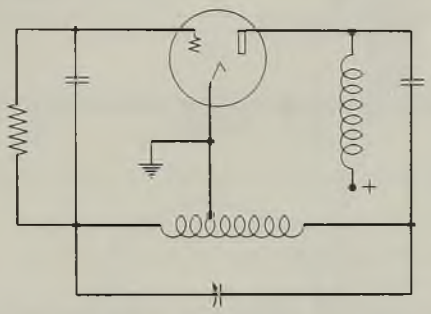

Fig. 13—Hartley circuit.

VII. Analysis of the Hartley Oscillator

The familiar Hartley Oscillator circuit is shown in Fig. 13. In this arrangement the tube serves as amplifier and limiter by the action of overloading. Harmonic voltages and currents are produced but if the selectivity of the tuned circuit is high the voltage returned to the grid of the tube is nearly sinusoidal.

The stability of this circuit is tested in exactly the same way as was that of the previous circuit. The loop is opened at the plate of the tube to determine the transmission of a modulated signal. If, as is usually the case, the coupling of the coil is close, the filter reduces to a single tuned circuit. The limiting action results from bias produced by rectification at the grid. Accordingly the block diagram of Fig. 7 is directly applicable, and the behavior of the filter is correctly given by Fig. 9.

Generally the circuit operates in class "C" with high bias and large grid

voltage swings. If the time constant of the grid-leak-condenser combination is long in comparison to the period of a modulation cycle the bias will not be able to follow the applied voltage and the modulation of the output will be larger than that of the input. Moreover it is in phase with that of the input. When the modulating frequency is low the bias is able to follow the level of modulation and the output modulation is very small. Thus the transmission of a modulated signal is greatest at high modulating frequencies, and the modulation output is in phase with the input. Because of the

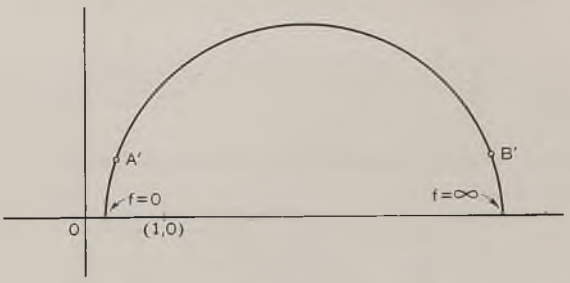

Fig. 14—Envelope transmission of a modulated wave through a grid-leak-biased Class C amplifier.

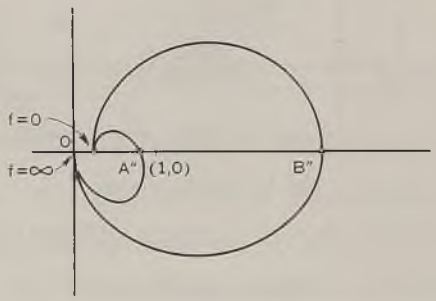

Fig. 15—Nyquist diagram applying to Fig. 13.

action of the grid-leak-condenser network a phase shift at intermediate modulating frequencies occurs. This behavior is represented in polar form in Fig. 14.

The stability of the system is determined by combining in Fig. 15 the separate diagrams of Figs. 14 and 10. As in the previous system a thoroughly stable system results if the element values are such that the points A and A' of Figs. 10 and 14 correspond to the same frequency. If on the other hand the elements are such that B and B' correspond to the same frequency the curve loops (1, 0) indicating instability. In general stability is

promoted by increase of the Q of the tuned circuit and by decrease of the time constant of the grid-leak-condenser combination.

VIII. The Lamp Stabilized Oscillator

The circuit of Fig. 16 is of particular interest because the functions of amplifier, limiter, and filter are performed separately by units which are readily identified with their functions. The present method of analysis was developed in connection with this particular circuit. The output frequency and amplitude are both quite stable and the harmonic content of the output is low.

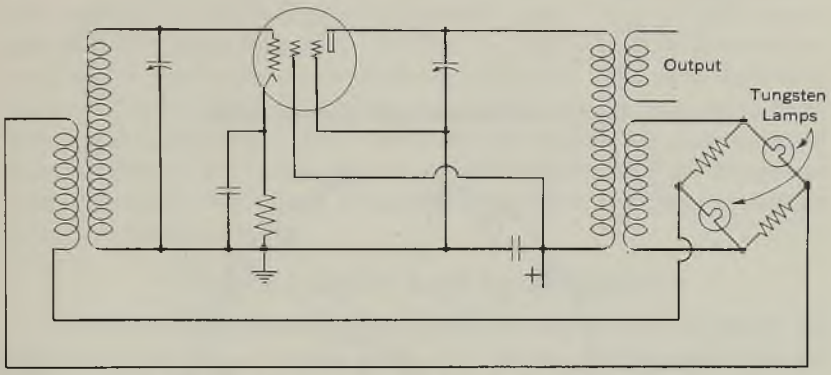

Fig. 16—Schematic diagram of lamp stabilized oscillator.

Under operating conditions the gain of the tuned amplifier, which is ordinarily in the order of 40 db, is equalled by the loss of the lamp bridge. The lamps operate at such a temperature that their resistance is slightly less than that of the associated linear resistors. If the gain of the amplifiers is for any reason somewhat reduced, the current through the lamps decreases, the temperature and resistance of the lamps is reduced, and the loss through the bridge is reduced to the new value of amplifier gain.

The d-c characteristic of a lamp bridge is shown in Fig. 17. A curve identical with Fig. 17 is observed if the measurement is made with an alternating current whose period is very short in comparison to the thermal time-constant of the filaments. Up to L the operation is nearly linear. In the region of M the output is essentially independent of the input. At N the bridge is nearly balanced and a small percentage change in the input voltage results in a large and opposite percentage change in the output. It is thus seen that an alternating current having a small superimposed modulation of low frequency will result in an output having a considerably

larger percentage modulation in the opposite phase. When the modulation frequency exceeds a few hundred cycles the lamps are unable to follow the individual cycles and the output wave is identical in form to the input. At intermediate modulating frequencies the transmission of a modulated wave

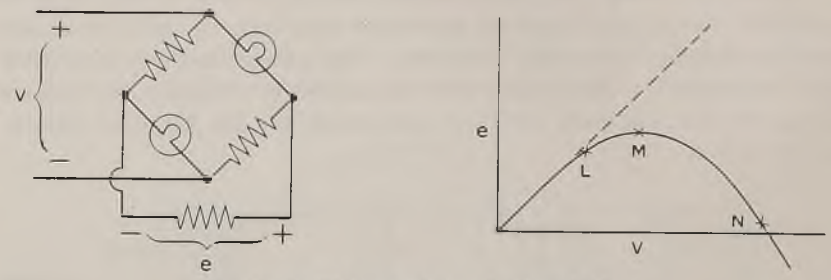

Fig. 17—D-C characteristics of a lamp bridge.

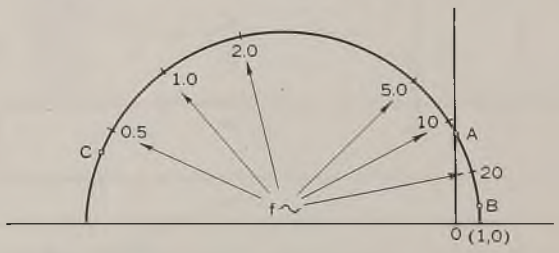

Fig. 18—Envelope transmission of a modulated wave through a lamp bridge.

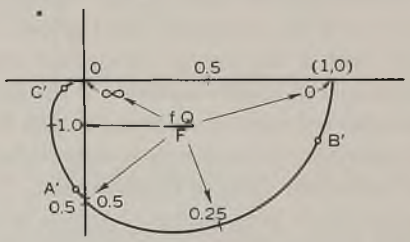

Fig. 19—Envelope transmission of a modulated wave through two similar tuned circuits of selectivity Q.

involves a phase shift. The behavior of a typical lamp bridge is presented in Fig. 18.

If the Q of the grid and plate circuits are both relatively high the filter circuit may be taken as equivalent to two separate tuned circuits. The transmission of each is given by Fig. 9. The combined transmission of the pair is given in polar form in Fig. 19. Because two tuned circuits are

employed, the diagram of Fig. 19 differs markedly from that of Fig. 10. Specifically the phase shift corresponding to a given value of attenuation is greatly increased. As in previous cases the curve of over-all loop transmission may or may not loop the point (1, 0) depending upon the relative frequency scales. Thus if the points A and A' of Figs. 18 and 19 correspond to the same frequency the Nyquist diagram passes near the point (2, 0) indicating instability. If the points B and B' correspond to the same frequency the loop passes very near to the point (1, 0) and instability is likely.

By making the tuned circuits very selective or by reducing the thermal time constant of the lamp circuit the points C and C' may be made to correspond to the same frequency. In this case the loop passes to the left of the point (1, 0) and the system is absolutely stable. The same result may be secured more easily by making one of the tuned circuits much more selective than the other. This is ordinarily accomplished by increasing the Q and impedance level of the grid circuit while keeping the Q and impedance level of the plate circuit much lower so as to provide a suitable power output to operate the lamp bridge.

IX. The Varistor Stabilized Oscillator

A circuit which differs from that of Fig. 16 only in that the lamps are replaced by varistors is shown in Fig. 20. At low levels of oscillation the impedance of the varistors is relatively high, the loss of the limiter is low and the amplitude of oscillation rises. At some higher level the varistor impedance is reduced, the bridge approaches balance to the fundamental frequency, and a stable condition is reached. Because the initial unbalance of the bridge is opposite to that of Fig. 16 a reversal of phase is necessary to establish oscillation.

The stable condition reached differs from that of the lamp stabilized oscillator in that the varistor goes through its entire range during each high-frequency cycle. The lamp resistance changes by only a small amount during any one cycle, its resistance depending on an integration of many previous cycles. Two important facts arise from this difference. Harmonics are produced in the bridge and, in so far as the varistors face reactances of these harmonic frequencies, intermodulation may produce currents of fundamental frequency but shifted in phase with respect to the original. Thus the bridge may produce a phase shift which is a function of level of the oscillation frequency. A degradation of frequency stability results from such a condition. More important to the present problem is the fact that all modulation frequencies are transmitted alike. A small modulation is reversed in phase and magnified by an amount depending upon the bridge balance but not upon the modulation frequency.

Because the limiter introduces no phase shift it follows that the envelope loop transmission is merely an enlarged and reversed copy of that for the filter. This can loop the (1,0) point only if there are at least three shunt elements in the filter section. That is, instability can result only if the phase shift of the filter system exceeds 180° for frequencies relatively near the operating frequency. This circuit is therefore much less likely to produce intermittent operation than any other circuit here considered.

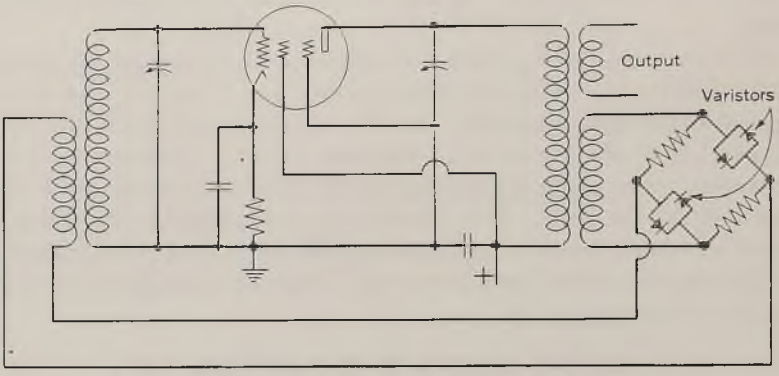

Fig. 20—Schematic diagram of varistor stabilized oscillator.

X. Negative Feedback in Oscillators

Because positive feedback is the necessary condition for the operation of an oscillator it is not obvious that the application of negative feedback is ever desirable. Actually it is frequently possible to introduce negative feedback into an oscillator with no loss of performance and under certain circumstances advantages are gained.

The circuit of Fig. 16 serves as a convenient example. Removal of the cathode by-pass condenser is likely to reduce the amplifier gain by about 6 db and to increase the stability of the gain with respect to applied voltages by a corresponding amount. Coincident with removal of the by-pass condenser the operating level drops a small amount, the bridge loss decreases 6 db to reestablish equilibrium, and the stabilizing effect of the bridge is cut in half. Accordingly the over-all stability of the output with respect to applied voltages is unchanged. The advantages gained are that the loss which must be held in the bridge is reduced so that stray reactances are less likely to disturb the operation, and that the harmonic content of the output is reduced.

Stated in a different way, the output stability of an oscillator using a non-feedback amplifier is limited in practice by the bridge balance which may be maintained. After this value of gain has been reached additional stability

may be secured by supplying increased inherent gain which is offset by direct negative feedback.

XI. Design of a Controlled Oscillator

To clarify the material already presented and to convey some additional concepts an oscillator having a large amount of control will be designed. The block diagram is to be that of Fig. 7 and the circuit is to be similar to that of Fig. 6.

It may readily be seen that the gain control must satisfy two fundamental requirements. It must deliver a d-c bias which increases rapidly with increase of the level of oscillation and it must not return any appreciable voltage of oscillation frequency. Otherwise the frequency will be affected by the elements in the control circuit as well as those in the filter, and the performance will be generally poor. Because of its balance a push-pull rectifier is helpful in meeting the latter requirement. The principal requirement is achieved by amplification and by the use of a constant counter emf or back bias. No bias is produced until the level of oscillation exceeds some threshold value. Above this threshold the bias increases approximately volt for volt with the peak value of the signal. The same amplifier which is used to increase the control may be used advantageously as a buffer so that appreciable power outputs may be produced without degrading the frequency or amplitude stability.

It will be assumed that a Q of 100 is available in the coil and that a frequency of one megacycle is to be generated. The transmission of a modulated wave in terms of the sideband displacement through such a one-circuit filter is shown in Fig. 21. Because the cutoff occurs very slowly it will be convenient to incorporate a rapid cutoff in the auxiliary filter of the gain control, thus avoiding an excessive phase shift at any one frequency.

The circuit features already discussed are shown in Fig. 22. A basic oscillator with a single tuned coil, a buffer amplifier having little selectivity and therefore contributing very little to the equivalent filter section, a source of biasing voltage, a balanced rectifier, and an auxiliary low-pass filter are shown. The condenser C is only large enough to allow the rectifier to be driven without serious loss at one megacycle. It has relatively little effect upon the modulation performance.

It is assumed that the buffer-amplifier, rectifier, etc. are so chosen that a modulation of very low frequency of one part per million applied at the plate terminal of the oscillator will result in a modulation of one part in a thousand returned to that point. This is equivalent to saying that the envelope gain is 60 db at low frequencies, and corresponds to 60 db of negative feedback in a conventional amplifier.

The auxiliary filter will be designed to approximate the attenuation and

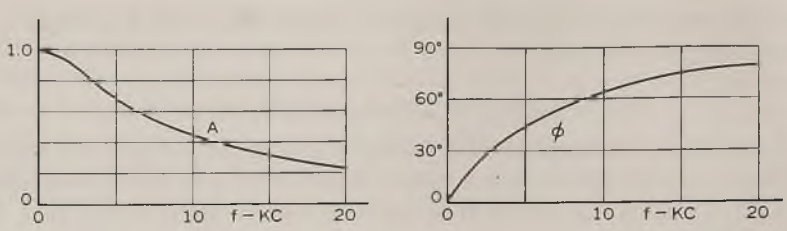

Fig. 21—Envelope transmission through tuned circuit.

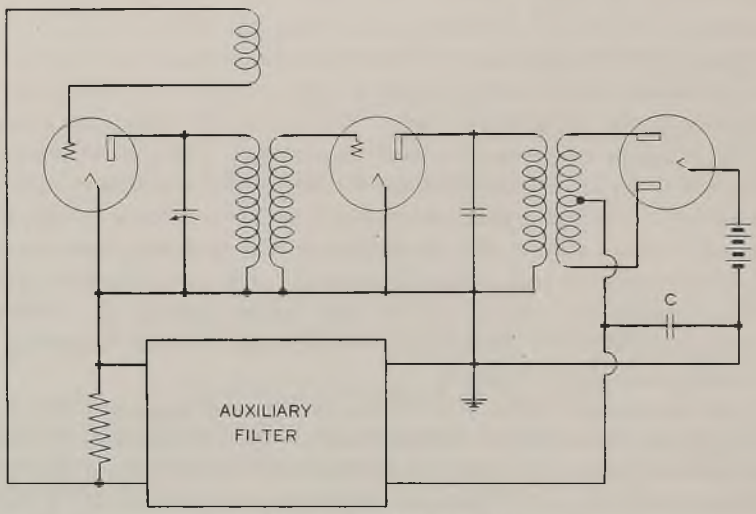

Fig. 22—Special A-V-C oscillator.

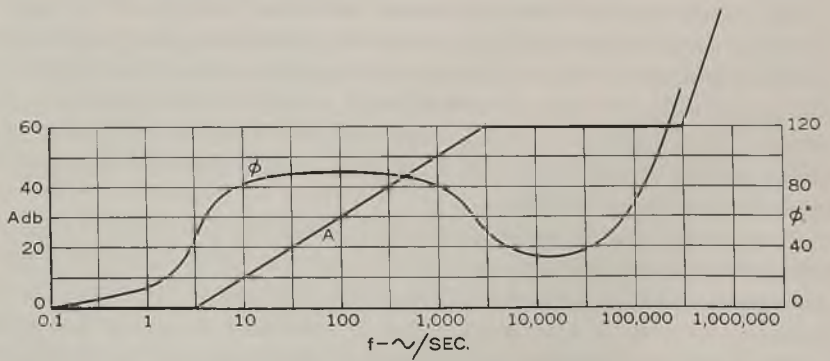

Fig. 23—Characteristics of auxiliary filter.

phase characteristics shown in Fig. 23. The choice of this particular shape is best explained by reference to Fig. 24 which presents the over-all envelope loop transmission of the system. It is seen that the phase shift is relatively constant at 90° over a wide band of frequencies and that the gain falls off approximately linearly over the same band. In particular the gain becomes zero around 5000 cycles whereas the phase does not reach zero below 500,000

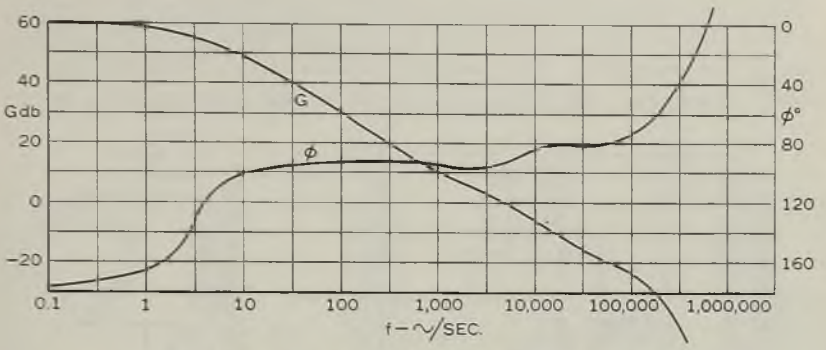

Fig. 24—Overall envelope transmission of Fig. 22.

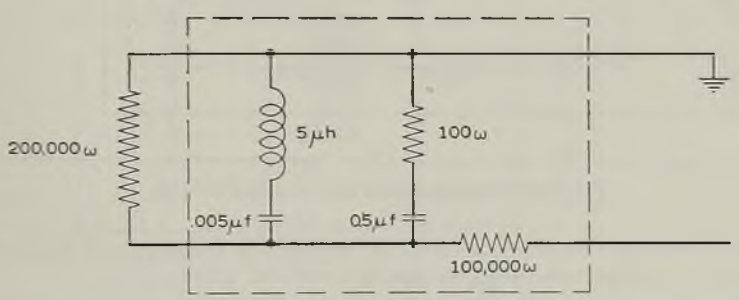

Fig. 25—Configuration of auxiliary filter.

cycles. In terms of Nyquist's criterion this represents a very stable system which is little disturbed by transient effects. A system having even greater stability could be achieved by beginning the cut-off at lower frequencies. It would then be found that the output was somewhat sluggish in reaching a new equilibrium after being disturbed. Such a behavior is not uncommon but is generally undesirable.

Elements which give approximately the characteristics called for in Fig. 23 are shown in Fig. 25. The peak of loss at one megacycle is contributed by the series resonant trap. The rest of the behavior is due to the 0.5 μf condenser in combination with the associated resistors.

XII. Auxiliary Control of Thermally Limited Oscillators

In the Meacham and certain other oscillator circuits a thermistor is associated with reactive elements in a bridge circuit which functions as both limiter and filter. In these circuits a large increase in the frequency stability is observed. This may sometimes be conveniently expressed as a magnification of the effective Q of the filter.

The advantages of great frequency stability and good amplitude stability of these systems are accompanied by an undesirable tendency toward intermittent operation. The thermal constants of the thermistor are not readily adjustable. Moreover adjustment of the reactances to secure

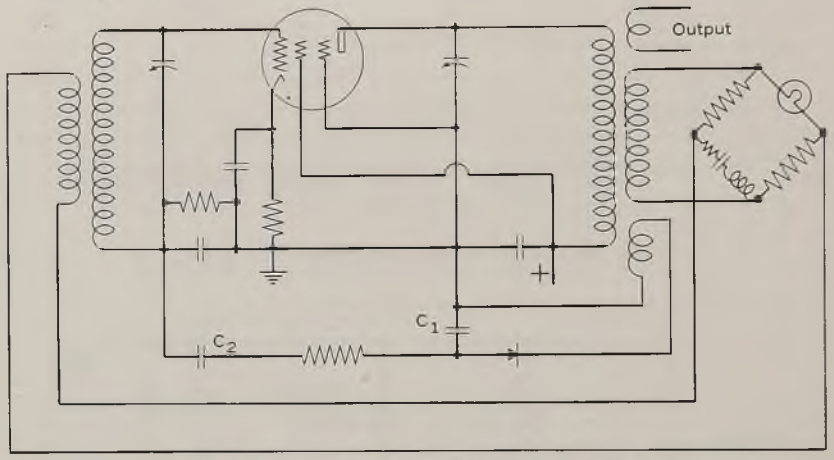

Fig. 26—Meacham circuit with auxiliary control.

suitable envelope stability is likely to impair the frequency or amplitude stability for which the circuit is chosen.

This dilemma may be resolved by the addition of an auxiliary network which does not affect the envelope transmission to very low frequencies but does modify the behavior at higher frequencies in such a way as to promote the stability of the system.

A simple circuit illustrating the principle appears in Fig. 26. It will be noticed that the circuit is so arranged that the average bias applied to the tube is only that due to the cathode resistor. The steady voltage developed across C_1 by the rectifier is unable to affect the bias because of the blocking condenser C_2. Accordingly the rectifier circuit does not affect the normal operating condition, which is characterized by a bridge loss equal to the amplifier gain. The added elements come into play only if there is a tendency toward self-modulation. Then displacement currents of modulation frequency flow through C_2 in such a magnitude and phase as to modify the tube gain and compensate the modulation returned from the bridge.

The exact nature of the control which must be added is best ascertained by opening the circuit at the plate of the tube. The loop transmission of a modulation envelope may then be determined, either experimentally or analytically. If instability is found an auxiliary circuit must be designed to produce an over-all system which is stable. In general the elements of the auxiliary circuit are to be chosen so that the loop transmission is considerably less than unity in the region of zero phase. This is ordinarily accomplished by increasing the final cutoff frequency at which the over-all loop envelope transmission is negligible.

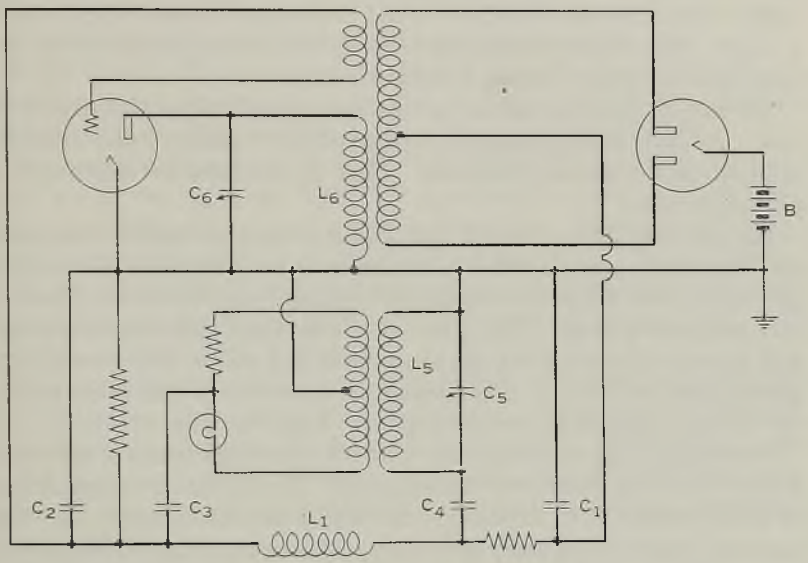

Fig. 27—Self-modulating oscillator.

XIII. A Self Modulated Oscillator

The previous sections have been devoted primarily to the problem of preventing self-modulation in oscillators. Let us now consider an oscillator having envelope instability. The Nyquist diagram indicates that self-modulation will occur and tells the approximate frequency of the envelope wave. More detailed analysis of the circuit is necessary to determine the wave form of the envelope and the manner in which its amplitude is limited.

If a circuit is to function well as an oscillator the Nyquist diagram for the operating frequency must loop the (1, 0) point with considerable margin. This is necessary so that a small loss of gain will not stop oscillation. At the operating level the limiter reduces the loop transmission to unity. In the region of (1, 0) amplitude stability is favored if the rate of change of gain

with respect to level is high. Similarly the frequency stability is favored if the rate of change of phase with respect to frequency is high.

If a circuit is to function well as a self-modulated oscillator, the above conditions must be met and in addition the Nyquist diagram for the envelope must meet similar requirements. That is, there must be a limiter and filter in addition to the effective amplifier in the envelope system.

A circuit which meets these requirements is shown in Fig. 27. It is seen to be similar to that of Fig. 6 but to have a more complicated low-frequency path. The operation is best explained in terms of the relative size of the various elements. The by-pass condensers C_1 and C_2 are comparatively small. The blocking condensers C_3 and C_4 are quite large. The choke L_1 is large. Thus these elements serve as open or short circuits but do not enter into the setting of either of the frequencies.

The stability tests are carried out by opening the mesh at the plate of the tube. At the operating frequency, as defined by the plate coil and condenser the loop gain is high at low levels. Thus the fundamental conditions for oscillation exist.

The next step in the analysis is to supply a signal of suitable magnitude and frequency to reduce the loop transmission to $(1, 0)$. A small modulation of very low frequency is returned magnified and reversed in phase, as with previous systems. The phase of the envelope transmission changes with increase of modulating frequency until it is zero at the resonant frequency of L_5 and C_5. At this frequency a considerable gain exists so that the Nyquist diagram for the envelope also loops the point $(1, 0)$.

The tungsten lamp in conjunction with the other impedances of the bridge serves to limit the degree of self-modulation. The operating frequency may be set by means of C_6 in conjunction with a suitable value of L_6. The operating amplitude may be controlled by adjustment of the bias battery B. The frequency of the self-modulation is set by means of C_5 in conjunction with L_5.

XIV. Conclusions

A method of applying known feedback theory to the problem of self-modulation in oscillators has been presented. Although the discussion has been limited to electrical circuits it is clear that the analysis is applicable to other systems, such as electromechanical or mechanical oscillators.

The analysis has been applied to several familiar oscillators to illustrate the method and to clarify some details of their operation. A sample design of a bias controlled oscillator is presented to show application to new designs.

The application of bias control to thermistor stabilized oscillators is described. The design of a self-modulated oscillator is undertaken to show how intentional modulation may be introduced and controlled.

Evaluating the Relative Bending Strength of Crossarms

By RICHARD C. EGGLESTON

OVER a million crossarms are produced annually in the United States. In the open wire lines of the Bell System alone there are now about 20 million arms in use. It is natural, therefore, that public utility engineers should have an interest in the strength of such an important item of outside plant material; and, consequently, an interest in any tool or means of evaluating the strength of such material. It is believed that the moment diagram is a convenient and reasonably reliable tool for estimating the loads an arm will support, for measuring the effect of knots of various sizes and of pinhole locations on arm strength, and for answering similar questions relating to the bending strength of crossarms under vertical loads.

Two moment diagrams are shown in Fig. 1 for Bell System Type A crossarms; and in the pages that follow are presented the method used in constructing the diagrams and a discussion of their use. While the calculation results apply particularly to the type and quality of arm referred to, they would also be of value as a time saving reference in future studies that may be proposed relating to the strength of the same or other types of arms involving different knot allowances.

The resisting moment of a beam is the product of its section modulus by the unit stress on the remotest fiber of the beam. The section modulus of a beam of uniform cross-section is constant and readily determinable. The section modulus, however, of a beam of nonuniform cross-section, such as a crossarm, varies because of the different cross-sectional shapes and dimensions involved.

In this study the following five different shapes were recognized:

(1) Roofed section between pinholes
(2) Roofed pinhole section
(3) Roofed brace bolt hole section
(4) Rectangular pole bolt hole section
(5) Rectangular section without bolt holes

The dimensions of the sections investigated were as follows:

Section of Arm	Dimensions	
	Minimum	Nominal
	(Inches)	(Inches)
Roofed section, except at end of arm	$3\frac{3}{16} \times 4\frac{3}{32}$	$3\frac{1}{4} \times 4\frac{3}{16}$
Roofed section at end of arm	$3\frac{3}{16} \times 4$	$3\frac{1}{4} \times 4\frac{3}{16}$
Unroofed sections	$3\frac{3}{16} \times 4\frac{3}{16}$	$3\frac{1}{4} \times 4\frac{1}{4}$

Since there is little, if any, engineering interest in the strength of structural members of maximum size, no investigations were made of sections of maximum dimensions.

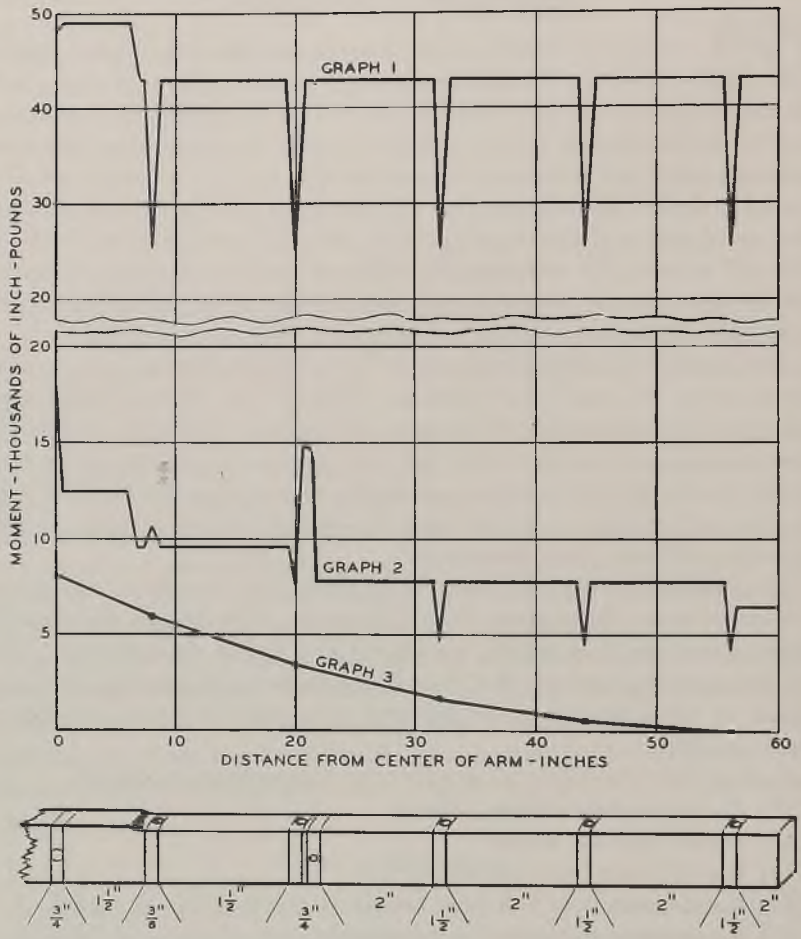

Fig. 1—Moment diagram for Type A southern pine and Douglas fir crossarms per Specification AT-7075:

Graph 1—Resisting moments of arms of nominal dimensions, straight grained and free from knots. (Fiber stress 5000 psi)

Graph 2—Resisting moments of arms of minimum dimensions, having maximum slant grain (1″ in 8″), and containing knots of the maximum sizes permitted (viz., sizes shown at bottom of arm sketch). (Fiber stress 3250 psi)

Graph 3—Bending moments from a load of 50 pounds at each pin position.

Section modulus calculations were made of each shape of minimum and nominal size, both with and without knots. Tests have shown that, be-

cause of the distortion of the grain that occurs around them, knots are fully as injurious to the strength of structural timbers as knot holes.[1] Therefore, in dealing with sections containing knots, it was assumed for the purposes of this study that the knot extended across the section in the same manner as a hole having a diameter equal to the diameter of the knot. It was also assumed that the knot was located in, or reasonably close to, the most damaging position in the arm section.

In the calculations of the section modulus of all roofed arm sections, it was necessary first to compute the moments of inertia of the whole or parts of the top segments of such sections (viz. nominal and minimum sections

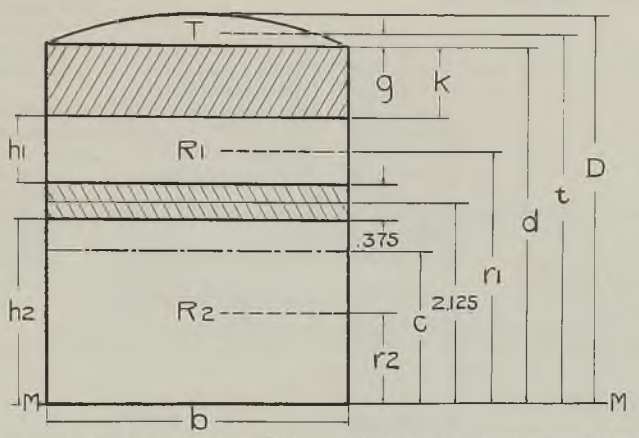

Fig. 2—Brace bolt hole section containing a $\frac{3}{4}$ inch knot located immediately below the top segment (knot and bolt hole shaded).

between pinholes, and nominal and minimum pinhole sections). Accordingly, four such computations were made and the results used in calculating the section moduli of all the roofed sections investigated. The details of the four computations are shown in the Appendix. To insure uniformity in the results, the degree of precision used in these computations was considerably greater than is ordinarily employed in dealing with timber products. All of the work, however, was done on a computing machine, and it was just about as easy to carry the operations to eight decimal places (which was the capacity of the machine used) as to a lesser number. As a matter of interest in this connection, it was found by actual trial in Computation I that absurd results would occur if fewer than five decimal places were used.

For convenience, all of the section modulus calculations were made in tabular form. In such form the procedure employed would not be readily

[1] Pg. 6 Dept. Circular 295, U. S. Dept. of Agriculture, "Basic Grading Rules and Working Stresses for Structural Timbers," by J. A. Newlin and R. P. A. Johnson.

apparent. Therefore, a sample calculation follows showing the method of finding the section modulus of the brace bolt hole section containing a $\frac{3}{4}$ inch knot.

Sample Calculation

Referring to Fig. 2, it will be noted that the knot and bolt hole divide the section into three parts: the top segment (T) and two rectangular portions ($R1$ and $R2$). The moment of inertia (I) of such a compound section about its neutral axis (at a distance c from M-M) is equal to the sum of the moments of inertia (IT, $IR1$ and $IR2$) of the component parts T, $R1$ and $R2$ about axes through their own centers of gravity, plus the areas of the component parts multiplied by the squares of the distances of their own centers of gravity from the neutral axis of the compound section. The section modulus (S) of this section is found, of course, by dividing its moment of inertia by the distance (y) from the neutral axis of the section to the most remote fiber.

Dimensions:

$b = 3.1875''$ (Width of Section)
$k = 0.7500''$ (Diameter of Knot)
$d = 3.7625''$ (See Computation I in Appendix)
$h1 = 0.7000''$ $(d - 2.125'' - 0.1875'' - k)$
$h2 = 1.9375''$ $(2.125'' - 0.1875'')$
$g = 0.1330''$ (See Computation I)
$t = 3.8955''$ $(d + g)$
$r1 = 2.6625''$ $(\frac{1}{2}\, h1 + 2.3125'')$
$r2 = 0.96875''$ $(\frac{1}{2}\, h2)$
$D = 4.09375''$ (Depth of Section)

Areas:

$T = 0.7099$ sq. ins. (See Computation I)
$R1 = 2.2313$ " $(bh1)$
$R2 = 6.1758$ " $(bh2)$

9.1170 sq. ins.

Moments about $M - M$:

$Tt = 2.7654$
$R1r1 = 5.9408$
$R2r2 = 5.9828$

$14.6890 = 9.1170\, c$; and hence
$c = 1.6112$

Moments of Inertia:

$IT = 0.0053$ (See Computation I)
$IR1 = 0.0911$ $(bh1^3 \div 12)$
$IR2 = 1.9319$ $(bh2^3 \div 12)$
$T(t - c)^2 = 3.7043$
$R1(r1 - c)^2 = 2.4661$
$R2(c - r2)^2 = 2.5490$

$I = 10.7477$
$y = 2.48255$ (D − c)

Section Modulus:

$$S = \frac{I}{y} = 4.3293$$

The same general procedure shown in this sample calculation was followed in dealing with the other cross-sectional shapes. For this reason, only the final results of the several calculations are presented; although, for

TABLE 1.—*Section Modulus of Roofed Sections between Pinholes*

	Knot Diameter—Inches								
	No Knot	½	¾	1	1¼	1½	2	2½	3
Calculation 1: (Knots located at top of section) Section Size*:									
Minimum		6.86		5.08		3.57	2.33	1.35	0.64
End. Min.				4.78			2.13		0.53
Nominal		7.37		5.50		3.91	2.59	1.54	0.76
Calculation 2: (Knots located at bottom of section) Section Size*:									
Minimum		6.11	5.24	4.42	3.71	3.05	1.92	1.05	0.47
Calculation 3: (Knots located immediately below top segment) Section Size*:									
Minimum	8.03	5.45	4.56	3.86	3.34	2.95	2.50	2.34	2.37
End. Min.	7.65			3.65					
Nominal	8.60			4.16					

TABLE 2.—*Section Modulus of Roofed Pinhole Sections*

	Knot Diameter—Inches						
	No Knot	¼	½	¾	1	1½	2
Calculation 4: (Knots vertical) Section Size*:							
Minimum	4.50	3.84	3.21	2.63	2.25		
End. Min.	4.29			2.50			
Nominal	5.11			2.88			
Calculation 5: (Knots horizontal) Section Size*:							
Minimum		3.63	2.96	2.40	1.97	1.41	1.11
End. Min.				2.26		1.33	
Nominal				2.76		1.64	

* Section Sizes:
Minimum = $3\frac{3}{16}'' \times 4\frac{3}{32}''$
End. Min. = $3\frac{3}{16}'' \times 4''$ (viz. minimum at end of arm)
Nominal = $3\frac{1}{4}'' \times 4\frac{3}{16}''$

convenience, reference is made to the calculations by number in the pages that follow. These results are shown in Tables 1, 2, 3 and 4, and a brief discussion of the scope and use made of them follows.

TABLE 3.—*Section Modulus of Bolt Hole Sections*

	Knot Diameter—Inches								
	No Knot	$\frac{1}{4}$	$\frac{3}{8}$	$\frac{1}{2}$	$\frac{3}{4}$	1	$1\frac{1}{4}$	$1\frac{1}{2}$	
Calculation 6: Brace bolt hole section									
Section Size*:									
Minimum .	7.97	6.47		5.28	4.33	3.58		2.62	
Nominal . .	8.55				4.71			2.78	
Calculation 7: Pole bolt hole section								$2\frac{1}{2}$" *Knot*	3" *Knot*
Section Size*:									
Minimum .	9.25		7.42		5.63		3.24	1.51	.75
Nominal . .	9.74				6.05		3.61	1.66	.85

* Section Sizes:
Minimum = $3\frac{1}{16}$" x $4\frac{3}{32}$"
End. Min. = $3\frac{3}{16}$" x 4" (viz. minimum at end of arm)
Nominal = $3\frac{1}{4}$" x $4\frac{3}{16}$"

TABLE 4.—*Section Modulus of Rectangular Section without Bolt Holes (Calculation 8)*

Section Size	Knot Diameter	Section Modulus
Minimum ($3\frac{3}{16}$" x $4\frac{3}{16}$")	(No Knot)	9.32
	$\frac{1}{4}$	8.24
	$\frac{1}{2}$	7.22
	$\frac{3}{4}$	6.28
	1	5.40
	$1\frac{1}{2}$	3.84
	2	2.54
	$2\frac{1}{2}$	1.51
	3	.75
Nominal ($3\frac{1}{4}$" x $4\frac{1}{4}$")	(No Knot)	9.78
	$\frac{1}{4}$	8.67
	$\frac{1}{2}$	7.62
	$\frac{3}{4}$	6.64
	1	5.72
	$1\frac{1}{2}$	4.10
	2	2.74
	$2\frac{1}{2}$	1.66
	3	.85

ROOFED SECTIONS BETWEEN PINHOLES

As indicated in Table 1, three tabular calculations were made for roofed sections between pinholes. In Calculations 1, 2 and 3 it was assumed that the knots present were located (1) at the top, (2) at the bottom, and (3) immediately below the top segment of the section, respectively. The results relating to the $3\frac{1}{16}$" x $4\frac{3}{32}$" section are plotted as Curves 1, 2 and 3, respectively, in Fig. 3.

With respect to the knot positions considered, it is apparent from an examination of the three curves (Fig. 3) that knots up to approximately $1\frac{1}{2}$″ in diameter are most damaging when located immediately below the roofed portion of the arm; and that the worst position for knots over $1\frac{1}{2}$″ in diameter is at the bottom of the arm. However, since under usual loading

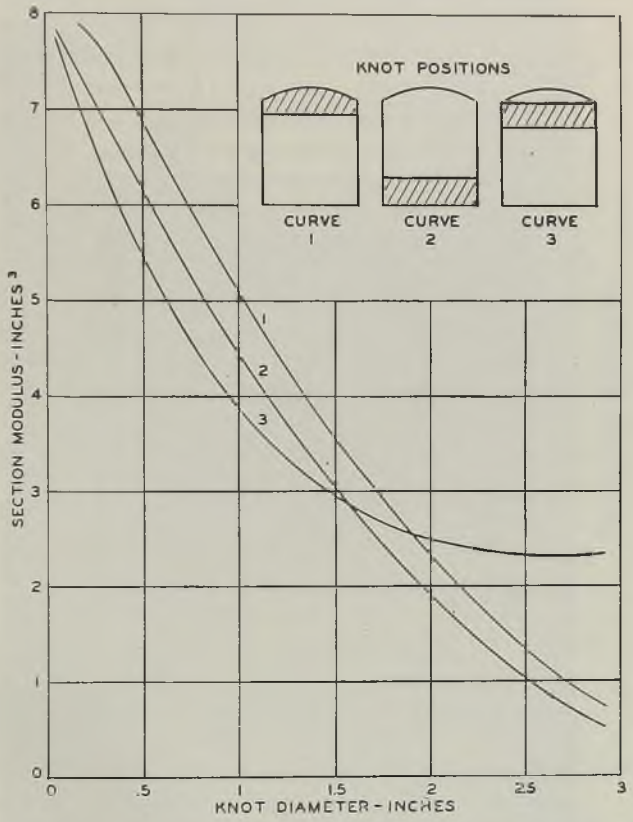

Fig. 3—Sections between pinholes. Section modulus of crossarm sections containing knots of the sizes shown on the base line and located in the positions indicated. The data apply to sections of minimum size ($3\frac{9}{16}$″ x $4\frac{3}{32}$″).

conditions knots at the bottom of an arm section are in compression, and thus would have less influence on strength than they would have on the tension side,[2] it was felt that the strength value shown by Curve 2 may be ignored; and that the values shown by a smooth curve, combining the values

[2] On Page 69 of U. S. Dept. of Agriculture Tech. Bul. 479, "Strength and Related Properties of Woods Grown in the United States" by L. J. Markwardt and T. R. C. Wilson, is the following statement: "Knots have approximately one-half as much effect on compressive as on tensile strength."

of Curve 3 up to the $1\frac{1}{2}''$ knot point with those of Curve 1 for 2″ and larger knots, would be the practical minimum section moduli for roofed sections between pinholes. Accordingly, such a smooth curve was constructed and is shown as Curve 2 in Fig. 4. The results of Calculations 1 and 3 for nom-

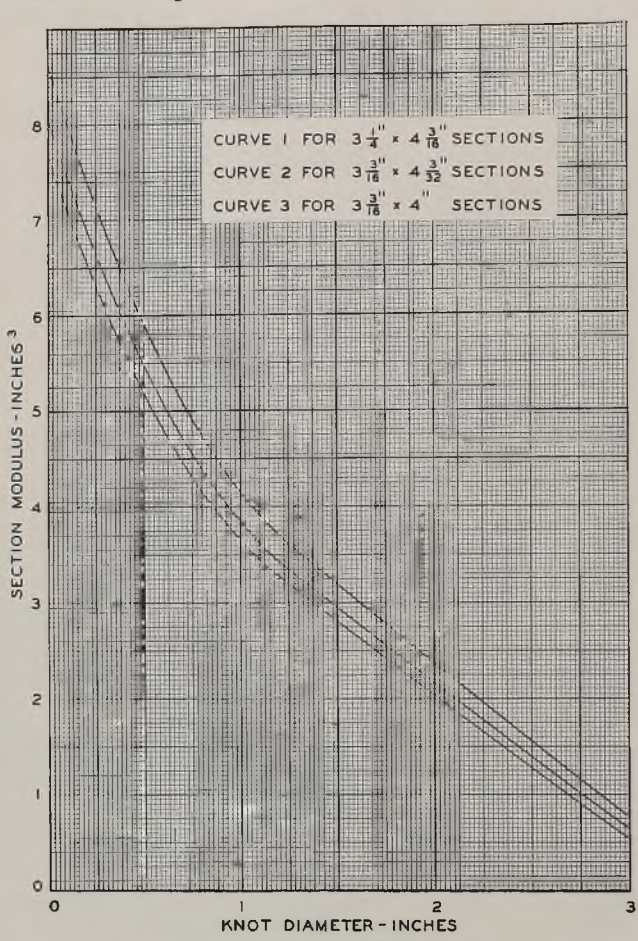

Fig. 4—Sections between pinholes. Section modulus of crossarm sections containing knots of the sizes shown on the base line and located in damaging positions.

inal and arm-end minimum sections were also plotted, and Curves 1 and 3 drawn for those sections.

Roofed Pinhole Sections

Two calculations were made for the pinhole sections: Calculation 4, in which the knots were assumed to be located adjacent to the pinhole in a

vertical position; and Calculation 5, in which the knots were assumed to be immediately below the top segment in a *horizontal* position. The results of these two calculations are shown in Table 2. It has heretofore been generally assumed that in pinhole sections knots less than 1″ in diameter were more damaging in a vertical position than in a horizontal position. The results of Calculations 4 and 5, however, show that the horizontal knots immediately below the top segment are the more damaging. In order to compare the effect of knots so located with the effect of knots at the extreme

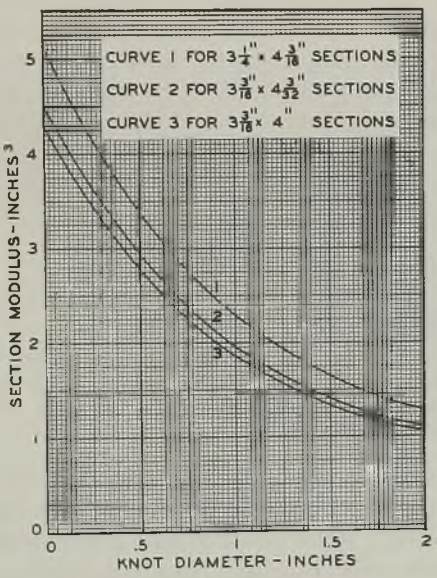

Fig. 5—Pinhole sections. Section modulus of crossarm sections containing knots of the sizes shown on the base line and located in damaging positions.

top of the section, the following two computations assumed 1″ and 2″ horizontal knots at the latter location:

1″ Knot at Section Top:

$$\tfrac{1}{2}S = \frac{.02875\ (3.09375)^2}{6} = 1.48156$$

$$S = 2.9631$$

2″ Knot at Section Top:

$$\tfrac{1}{2}S = \frac{.92875\ (2.09375)^2}{6} = .67857$$

$$S = 1.3571$$

As the section modulus (S) values for sections containing 1″ and 2″ horizontal knots located immediately below the top segment are 1.97 and 1.11, respectively, (Calculation 5, Table 2) it is apparent that in pinhole sections horizontal knots immediately below the top segment are the more damaging. The results of Calculation 5 were accordingly plotted in Fig. 5 and smooth curves drawn to show the section modulus for each of the three sections containing knots of any size.

Roofed Brace Bolt Hole Section

The worst position for knots in the brace bolt hole section was assumed to be substantially the same as in the roofed sections between pinholes; and in Calculation 6, the results of which are shown in Table 3, knots up to $1\frac{1}{2}$″ in diameter were assumed to be so located, viz. immediately below the top segment.

To check this assumption with respect to worst position, the following analysis was made of the minimum sections:

Distance from top of section:

To top of bolt hole	1.78″
To bottom of bolt hole	2.16″

Distance from bottom of top segment:

To top of bolt hole	1.45″
To bottom of bolt hole	1.83″

It is apparent that any knot ranging in diameter from 1.78″ to 2.16″, when located at the top of the section, would enter the bolt hole. The section modulus of any section containing a knot within that size range would be the section modulus of the remaining portion of the section, or $\frac{bd^2}{6}$, where b is the width of the section and d the depth below the bolt hole. Thus

$$S \text{ (minimum arm)} = \frac{3.1875\ (1.9375)^2}{6} = 1.9943$$

It is also evident that any knot from 1.45″ to 1.83″ in diameter, when located immediately below the top segment, would likewise enter the bolt hole; and that the section modulus, on this basis of knot location, would be the same for any section containing a knot within the size range mentioned. Continuing the analysis the following tests were made:

2″ Knot:

The distance between the top segment and the bottom of the bolt hole of a minimum section is 1.83″. Therefore, a 2″ knot located immediately

below the top segment would extend beyond the hole; and its effect would be the same as in Calculation 3 (Table 1), where the section modulus of a section containing a 2″ knot similarly located was found to be 2.50. On the other hand, since a 2″ knot is within the limits 1.78″ and 2.16″, the section modulus of a section containing such a knot located at its top would be 1.99.

1.78″ Knot:

A knot of this size immediately below the top segment would enter the bolt hole since it is within the 1.45″ and 1.83″ limits, and the section modulus value associated with it would be the same as shown in the Calculation 6 results (Table 3) for a section containing a $1\frac{1}{2}$″ knot, or $S = 2.62$. But, as evident from previous discussion, the section modulus associated with this knot, if located at the top of the section, would be 1.99.

1.5″ Knot:

It can be shown that the section modulus of a section containing a knot of this size located at the top of the section would be 2.55; and that the section modulus associated with a similarly located *1″ knot* would be 4.55.

The foregoing analysis for minimum sections may be summarized as follows:

Knot Size	Section Modulus	
	Knot at Top	Knot below Top Segment
(Inches)	(Inches^3)	(Inches^3)
2.0	1.99	2.50
1.78	1.99	2.62
1.5	2.55	2.62
1.0	4.55	3.58

A study of this summary shows that knots $1\frac{1}{2}$″ and over are more damaging when located at the section top; and that knots under $1\frac{1}{2}$″ are more damaging when located immediately below the top segment. The section modulus values associated with $2\frac{1}{2}$″ and 3″ knots would be the same as shown in the Calculation 1 results (Table 1).

By a similar analysis for arms of nominal size it can be shown:

(1) That the more damaging position for knots $1\frac{1}{2}$″ and under is immediately below the top segment;

(2) That the more damaging position for any knot within the diameter range from 1.875″ to 2.25″ and all the larger knots is at the top of the section;

(3) That the section modulus associated with 1.875″ to 2.25″ knots would be $\frac{3.25(1.9375)^2}{6} = 2.0334$; and

(4) That the section modulus values associated with $2\frac{1}{2}$″ and 3″ knots would be the same as shown in the Calculation 1 results (Table 1).

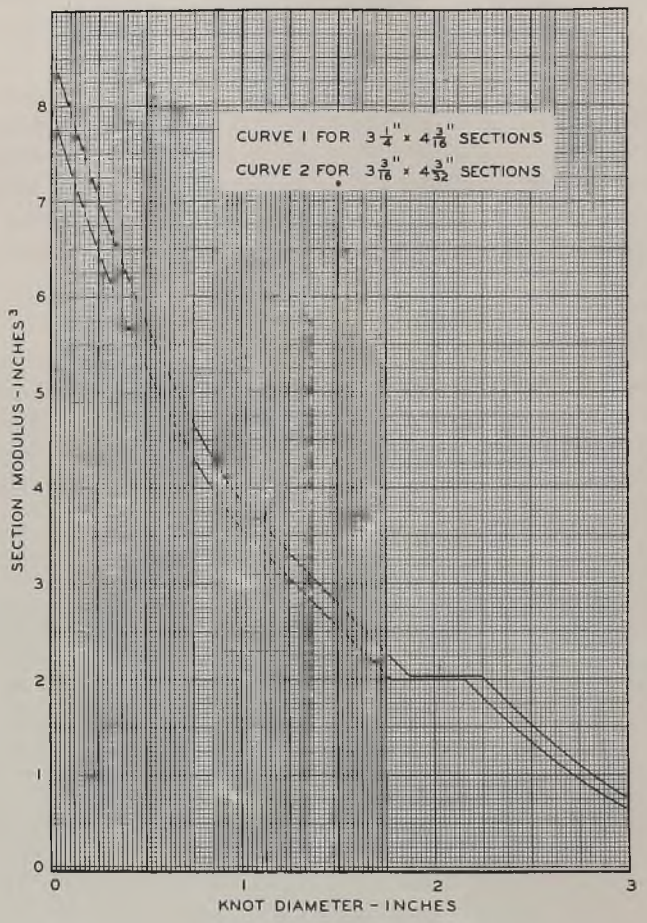

Fig. 6—Brace bolt hole sections. Section modulus of crossarm sections containing knots of the sizes shown on the base line and located in damaging positions.

The results of Calculation 6 (Table 3), and of the foregoing analyses, together with the Calculation 1 results for $2\frac{1}{2}$″ and 3″ knots, were plotted in Fig. 6 for both minimum and nominal sections.

Rectangular Pole Bolt Hole Section

The most damaging position for knots in the pole bolt hole section was assumed to be at the top of the section. They were so figured in Calcula-

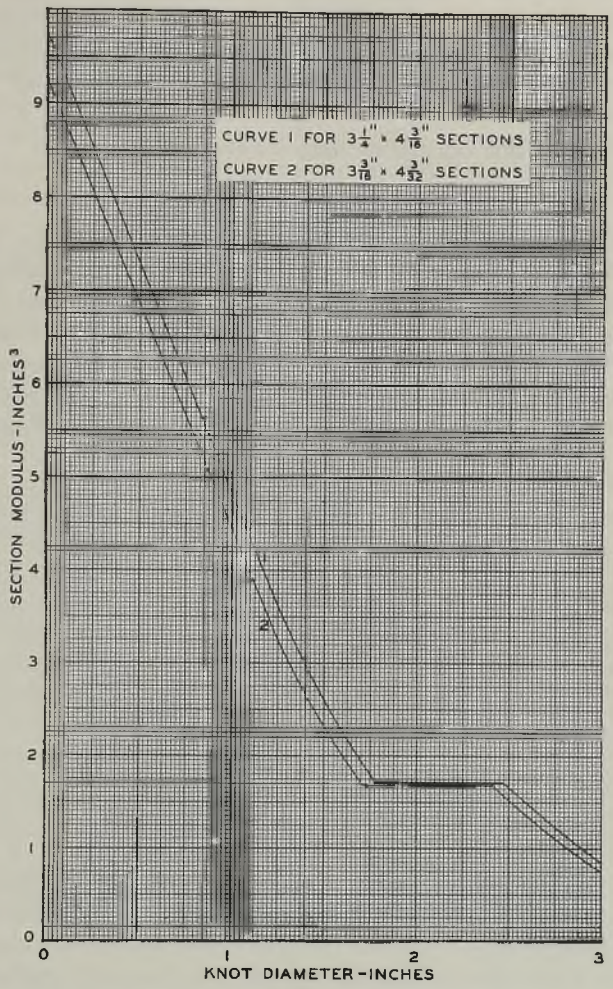

Fig. 7—Pole bolt hole section. Section modulus of crossarm section containing knots of the sizes shown on the base line and located in damaging positions.

tion 7, the results of which are shown in Table 3 and plotted in Fig. 7 for both minimum and nominal arms.

Rectangular Sections without Bolt Holes

Here too the most damaging position for knots was assumed to be at the top of the section. In Calculation 8 the section moduli of sections containing knots from $\frac{1}{4}''$ to $3''$ in diameter were determined for both minimum and nominal sections. The results are shown in Table 4. As section modulus values for sections containing knots of other sizes than those shown may be found so simply by the formula for rectangular sections, $S = \frac{bd^2}{6}$, no curves of the results of this calculation were drawn.

Moment Diagrams

From the results of this study as shown in Table 4 and in Figs. 4, 5, 6 and 7, section modulus values for clear arms and for arms containing knots of various sizes may be read and multiplied by appropriate fiber stresses to determine the resisting moments throughout the length of such arms. For example, the section moduli of clear arms of nominal dimensions, and of arms of minimum dimensions with the maximum knots permitted under the current Bell System crossarm specification (AT-7075) are as follows:

Section of Arm	Arms of nominal size and free from knots	Arms of minimum size with maximum knots	
	Section Modulus	Section Modulus	Diameter of Max. Knots
Pole bolt hole	9.74	5.63	$\frac{3}{4}''$
Brace bolt holes	8.55	4.33	$\frac{3}{4}''$
Pole pinholes	5.11	3.28	$\frac{3}{8}''$
Other pinholes in middle section[3]	5.11	2.38	$\frac{3}{4}''$
End pinholes	5.11	1.33	$1\frac{1}{2}''$
Other pinholes in end sections[3]	5.11	1.41	$1\frac{1}{2}''$
Unroofed part of middle section	9.78	3.84	$1\frac{1}{2}''$
Roofed part of middle section	8.60	2.95	$1\frac{1}{2}''$
Solid part of brace bolt hole zones[4]	8.60	4.56	$\frac{3}{4}''$
Between pinholes in end sections	8.60	2.17	$2''$
Extreme ends	8.60	2.03	$2''$

These section modulus values were used in preparing the moment diagrams shown in Fig. 1. The clear arm of nominal dimensions was also assumed to be straight grained. The fiber stress factor used for it was 5000 psi, which is the ultimate fiber stress value that has been employed in the Bell System for many years for sawn southern pine and Douglas fir. The

[3] For the purposes of specifying knot limitations, crossarms under Specification AT-7075 are divided into a middle section (between brace bolt holes) and end sections (beyond brace bolt holes).

[4] Where a brace bolt hole zone is less than four (4) inches from a pinhole zone, these zones and the portion of the arm between them are considered as a single zone.

fiber stress factor used in computing the resisting moments for the arm of minimum size with maximum slant grain and maximum knots was 3250 psi, which is simply 5000 psi discounted 35% to allow for slant grain of 1″ in 8″, which is the maximum permitted by Specification AT-7075. A discount is, of course, unnecessary for the presence of knots, since allowance for their effect on strength was made in the section modulus values used.

Since the 5000 psi value is an ultimate fiber stress and not a working stress, and since the arms were assumed to be made of clear, straight grained material, Graph 1 (Fig. 1) represents an idealized condition. The resisting moments shown are probably the maximum that may be expected from any commercial lots of southern pine or Douglas fir crossarms,[5] notwithstanding the fact that the dimensions of some of the arms may exceed the nominal specified. With respect to Graph 2 (Fig. 1), the objection may be raised that 35% is not a sufficient discount for a 1″ to 8″ slant of grain and that the 3250 psi value makes no allowance for the effect of long continued loading. On the other hand, the graph assumes the simultaneous occurrence of the maximum knot in a most damaging position in every section of an arm of minimum dimensions and having the maximum slant of grain allowed. Since the probability of such simultaneous occurrence of these defects and conditions is extremely small, it is felt that the resisting moments of Graph 2 represent the minimum strength of any arm of the two species concerned that may be furnished under Specification AT-7075.

Under the assumptions made, Graphs 1 and 2 (Fig. 1) may be regarded as the upper and lower limits of the bending strength of specification crossarms. On the same diagram may be plotted the graph or graphs of the moments resulting from any given load at each pin position, or any single load concentrated at any point on the arm. As an illustration, Graph 3, showing the bending moments from a load of 50 pounds per pin, is shown in the diagram (Fig. 1). A load of 50 pounds per pin is calculated to be the load of size 165 wire coated with ice having a radial thickness of $\frac{1}{4}$ inch in span lengths of 235 feet, or of wire of the same size in 100 foot spans where the radial thickness of the ice coating is $\frac{1}{2}$ inch. Since Graph 3 is wholly below Graph 2, even an arm of lowest specification quality would support the assumed loads with some margin of strength to spare. This margin or factor of safety, would, of course, be increased greatly if the quality of the arm under consideration approached the quality assumed in Graph 1. As previously indicated, the probability is extremely remote that any single arm will ever be furnished of a quality as low as assumed in Graph 2. It

[5] Graphs 1 and 2 (Fig. 1) are for southern pine and Douglas fir crossarms. It is estimated that the resisting moments of comparable graphs for the other woods included in Specification AT-7075 should be about 20% lower.

follows, therefore, that the average strength of any lots of southern pine or Douglas fir arms produced under Specification AT-7075 may be expected to lie well above the Graph 2 limit.

Graph 2 and a bending moment graph for vertical loads at each pin position are of considerable value to the material design engineer, since the degree of parallelism between the two will show whether a consistent strength relationship exists throughout the length of the crossarm. As a matter of interest in this connection, moment diagrams were used as a guide in setting the knot limitations shown in Specification AT-7075.

Resisting and bending moment graphs may also be used to determine the location of the critical section of a crossarm by noting the point of coincidence between a *maximum* bending moment graph and the resisting moment graph for a clear arm. It can be shown by such graphs that this point in all types of Bell System crossarms, designed for vertical loads, is located at the pole pinholes. If the comparison were made between a maximum bending moment graph and the resisting moment graph of an arm containing all of the maximum defects permitted, the location of the point of coincidence between the graphs might or might not fall at the pole pinholes, depending on the magnitude and location of the defects allowed. It should be noted, however, that for such arms the critical section locations so determined apply only when the arms are actually of the assumed minimum quality; and, since the probability of such being the case is so extremely remote, it is concluded that the maximum stress or critical section locations in arms of that quality are of academic interest only, and that for all practical purposes the critical section of any $3\frac{1}{4}''$ x $4\frac{1}{4}''$ x $10'$ crossarm is located at the pole pinhole.

This conclusion does not mean that every arm broken in service or under test will break at the pole pinhole; for, obviously, if some other section is relatively weaker because of some hidden defect which reduces its section modulus or its fiber strength, it will break at such section regardless of any mathematical determination of the break location. But the conclusion does mean that, generally speaking, when a crossarm breaks the break will occur at, or be closely related to, the pole pinholes. To check the accuracy of this conclusion, an examination was made of all available crossarm strength test data in which the break locations were recorded. The examination revealed that, out of 258 arms tested, the breaks in 219, or 85 per cent, were either at, or directly related to, the pole pinholes. Six per cent of the breaks were located between the two pole pinholes, and 9 per cent at points outside the pole pinholes.

As an illustration of another use to which such a moment diagram may be put, the following specific example is cited. Before the present standard Bell System specification for crossarms was drafted, it was decided to

include a new type ("W6") with 16 pin positions. It was felt that, if the additional pin holes in the type W6 did not unduly weaken the arm, it could not only replace the old type "JW" arm with 8 pin positions but also be used in installations where greater flexibility in wire spacings might be required.

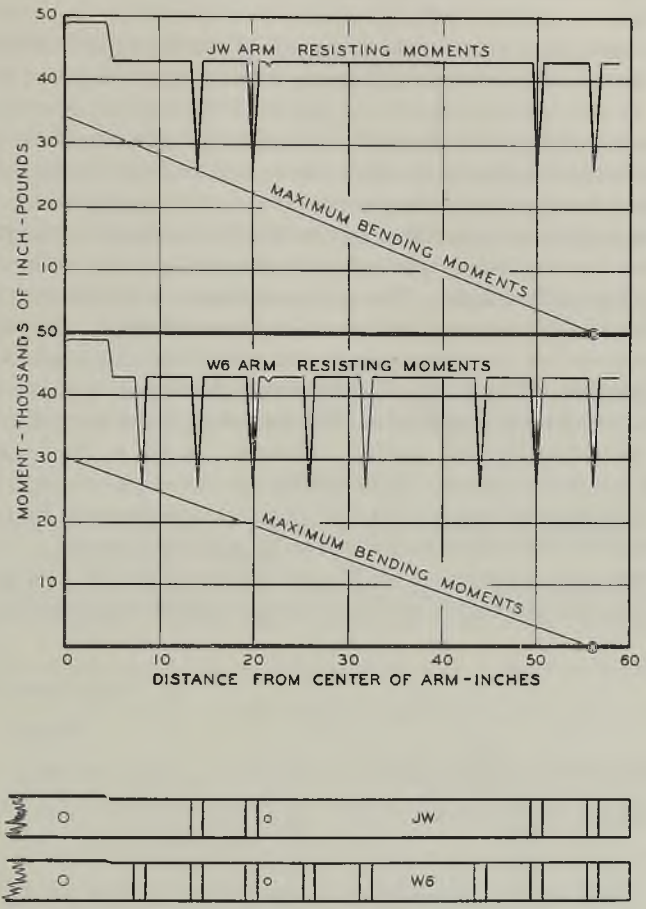

Fig. 8—Resisting moments and maximum bending moments for clear JW and W6 crossarms.

In order to obtain an estimate of the strength relationship between the two types, strength tests were made of 10 matched arms of each type. The test arms were made of air-seasoned, clear Douglas fir. The dimensions of the crossarm blanks were $3\frac{1}{4}''$ x $4\frac{1}{4}''$ x 20′. In selecting the 10 blanks from which the test arms were made, only straight grained pieces free from

evidence of manufacturing and other defects were chosen. Each blank chosen was cut into two 10′ lengths, one of which was made into a JW arm and the other into a W6 arm, making 10 matched arms of each type. The tests were made on an Amsler testing machine. The average breaking load at the end pinholes was 1159 pounds for the JW arms and 1002 pounds for W6 arms.

At the same time an estimate was made of the theoretical *strength relationship* between the two types by means of the moment diagrams shown in Fig. 8. In this figure are shown the graphs of the resisting moments (fiber stress factor—5000 psi) of clear JW and clear W6 arms, together with the graphs of the bending moments due to the maximum loads these arms would withstand when the loads are concentrated at the end pinholes. These maximum loads were determined by dividing the moments at the points of coincidence between the graphs (critical pole pinhole sections) by the distances to the end pinholes. The maximum loads, so determined, are 608 pounds for the JW arm and 532 pounds for the W6 arm. The fact that these loads are low as compared with the actual breaking loads shows, of course, that the average ultimate fiber stress developed by these selected arms was considerably greater than 5000 psi, which is not surprising in view of their exceptionally high quality. However, so far as the information sought is concerned—namely, to determine not the actual strength but the strength relationship between the two types—the result would be the same regardless of the fiber stress factor used in the moment diagram.

The ratio of the strength of the W6 arm to that of the JW arm as shown both by the actual strength tests and by the moment diagrams was as follows:

	Strength Ratio W6 to JW
	(Per cent)
Actual strength tests $-\frac{1002}{1159} \times 100 =$	86.5
Moment diagrams $-\frac{532}{608} \times 100 =$	87.5

These ratios show a remarkably close agreement between theory and actuality and justify the belief that the crossarm moment diagram may be employed to obtain reasonably accurate estimates of relative bending strength.

Summary

The results of this study may be summarized as follows:

1. The moment diagram is a useful guide in setting specification limitations on defects.

2. It is shown that the critical section of a crossarm is located at the pole pinholes. The practical value of this observation is that it emphasizes the need for keeping the pole pinhole sections and the portion of the arm between them reasonably free from strength reducing defects.

3. Only by breaking tests can the *actual* bending strength of crossarms be determined. The *relative* bending strengths, however, of two or more arms of different types or quality may be estimated with sufficient accuracy by means of the moment diagram, regardless of the fiber stress used in its construction.

4. If the fiber stress factor employed is dependable, the moment diagram may be used to estimate the minimum factor of safety that would obtain for an arm of any type or any assumed quality. In this connection, it is believed that the strength of Bell System crossarms is well above the minimum required to support the loads ordinarily carried.

5. The section modulus curves of Figs. 4, 5, 6 and 7 will simplify the construction of moment diagrams for arms of the same sizes shown in the figures but differing with respect to type and quality.

The uses listed lead to the general conclusion that the crossarm moment diagram is a convenient and reasonably reliable engineering tool.

APPENDIX

Computation I. Moment of Inertia of Top Segment of Minimum ($3\frac{3}{16}$" x $4\frac{3}{32}$") Section between Pinholes:

The moment of inertia (IT) of a segment (T) with respect to an axis through its center of gravity and parallel to its base may be found by the formula

$$IT = I_{BB} - Ax^2$$

where I_{BB} is the moment of inertia of the segment about the axis BB, A the area of the segment and x the distance between the two axes. The values I_{BB}, A and x are given by:

$$I_{BB} = \tfrac{1}{4}Ar^2\left[1 + \frac{2\sin^3 a\cos a}{a - \sin a\cos a}\right] \tag{1}$$

$$A = \tfrac{1}{2}r^2(2a - \sin 2a) \tag{2}$$

$$x = \tfrac{2}{3}\frac{r^3\sin^3 a}{A} \tag{3}$$

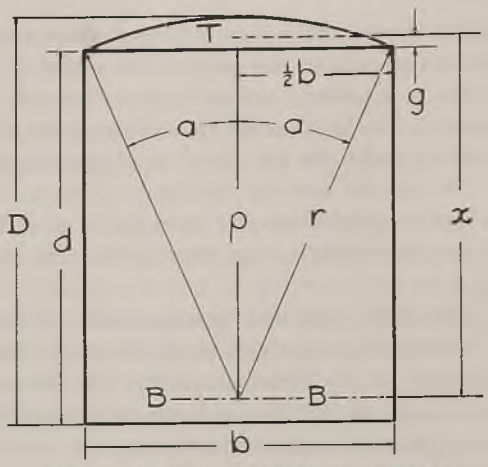

Fig. 9—Crossarm section between pinholes.

The significance of r and a in these formulae, and of the other symbols used in the computations that follow will be clear from a glance at Fig. 9.

$D = 4.09375''$

$b = 3.1875''$

$\frac{1}{2}\,b = 1.59375''$

$r = 4''$

$r^2 = 16.000000$

$(1/2\,b)^2 = 2.540039$

$p^2 = 13.459961$

$p = 3.668782''$

$\text{Sin } a = \dfrac{1/2\,b}{r} = 0.39843750$

$a = 23° 28' 49.93''$

$a = 0.40981266$ radians

$2\,a = 46° 57' 39.86''$

$\text{Sin}^3 a = 0.063252925$

$\text{Sin } 2\,a = 0.73089017$

$\text{Cos } a = 0.91719548$

$\text{Sin } a \text{ Cos } a = 0.36544507$

$d = p + (D - r) = 3.7625''$

$A = 0.7099$ sq. ins. [Area of T by Formula (2)]

$x = 3.8018''$ [By Formula (3)]

$g = x - p = 0.1330''$

$I_{BB} = 10.2654$ [By Formula (1)]

$Ax^2 = 10.2601$

$IT = 0.0053$

(Note: While the results of this and the following computations are shown to four decimal places, the actual work was done by machine and carried to eight decimal places as mentioned in the text.)

Since the width of the section in this computation and the radius of its roof is the same as for the minimum $3\frac{3}{16}''$ x $4''$ section at the end of the arm, the top segments of the two are identical, and the only value that will differ

will be the depth (d) of the rectangular portion of the section, which for the smaller will be $p + (D - r)$, or

$$3.6688 + (4 - 4) = 3.6688''$$

Computation II. Moment of Inertia of Top Segment of Nominal ($3\frac{1}{4}''$ x $4\frac{3}{16}''$) Section between Pinholes:

As this computation was made in exactly the same manner as Computation I, only the results are here shown:

$$d = 3.8593''$$
$$g = 0.1317''$$
$$A = 0.7168 \text{ sq. ins}$$
$$IT = 0.0053$$

Computation III. Moment of Inertia of Top Segment of Minimum ($3\frac{3}{16}''$ x $4\frac{3}{32}''$) Pinhole Section:

It will be noted in Fig. 10 that the top segment is divided into four parts: the small segment (T_1) at the top of the pinhole, the rectangular portion

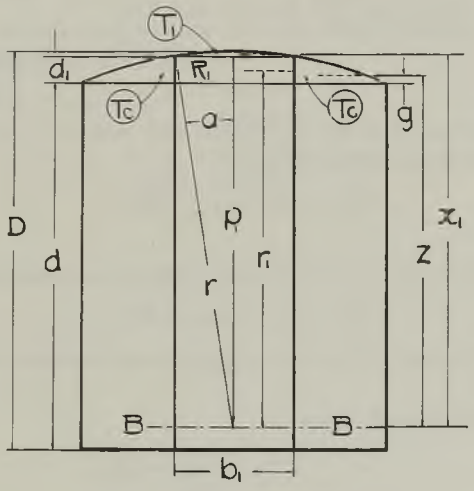

Fig. 10—Crossarm pinhole section.

R_1, with a width of b_1 and a depth of d_1, and two portions designated Tc. The purpose of this computation is to determine the moment of inertia of one of the Tc portions with respect to its gravity axis parallel to its base. The moment of inertia of the two Tc portions about the axis BB may be

found by deducting the moments of inertia of T_1 and R_1 about this axis from the moment of inertia of the entire top segment about the same axis.

$D = 4.09375''$

$b_1 = 1.33''$

$\frac{1}{2} b_1 = 0.665''$

$r = 4.00''$

$r^2 = 16.000000$

$(1/2\ b_1)^2 = 0.442225$

$p_1^2 = 15.557775$

$p_1 = 3.9443345''$

$\text{Sin } a = \dfrac{1/2\ b_1}{r} = 0.16625$

$a = 9° 34' 11.49''$

$a = 0.16702554$ radians

$2a = 19° 8' 22.98''$

$\text{Sin}^3 a = 0.0045949941$

$\text{Sin } 2a = 0.32787285$

$\text{Cos } a = 0.98608364$

$\text{Sin } a \text{ Cos } a = 0.16393640$

d (Computation I) $= 3.7625''$

$d_1 = p_1 + (D - r) - d = 0.2756''$

$r_1 = p_1 - 1/2 d_1 = 3.8065''$

Area $R_1 = b_1 d_1 = 0.3665$ sq. ins.

$A_1 = 0.0494$ sq. ins. [Area of T_1 by Formula (2)]

$x_1 = 3.9666''$ [By Formula (3)]

By Computation I, $IT_{BB} = 10.2654$

IT_{1BB} [Formula (1)] $= 0.7777$

$IR_{1BB} = \dfrac{b_1 d_1^3}{12} + R_1 r_1^2 = 5.3126$

6.0903

$2ITc_{BB} = 4.1751$

The moment of inertia of the 2 Tc areas with respect to the axis through their own centers of gravity is given by

$$2ITc = 2ITc_{BB} - 2Tc\ z^2$$

where

2 Tc is the area of the two Tc portions of the top segment and is given by

$$2Tc = A - (A_1 + R_1)$$

in which A is the area of the entire top segment as shown in Computation I; and

where, by the principle of moments,

$$z = \frac{Tx - T_1 x_1 - R_1 r_1}{2Tc}$$

in which Tx, $T_1 x_1$ and $R_1 r_1$ are the moments of the areas of T, T_1 and R_1, respectively, about the axis BB. ($Tx = Ax$ of Computation I.)

Thus

$2Tc = 0.2940$ sq. ins.

$z = 3.7680''$

As previously shown, $2ITc_{BB} = 4.1751$
$2Tc\,z^2 = 4.1738$

$2ITc = 0.0013$
$ITc = 0.0007$
$D - r = 0.09375''$
$z = 3.7680''$

$3.8618''$
$d = 3.7625''$

g for $Tc = 0.0993''$

The results of this computation apply also to the minimum $3\frac{3}{16}''$ x $4''$ pinhole section at the ends of the arm. The depth (d) of the rectangular portion of the end pinhole sections will be the same as at the extreme ends of the arm, viz. $3.6688''$.

Computation IV. Moment of Inertia of Top Segment of Nominal ($3\frac{1}{4}''$ x $4\frac{3}{16}''$) *Pinhole Section:*

Since this computation was made in the same manner as Computation III, only the results are here shown:

$d = 3.8593''$
$g = 0.1019''$
$Tc = 0.1630$ sq. ins.
$ITc = 0.0008$

Mathematical Analysis of Random Noise

BY S. O. RICE

(*Concluded from July 1944 issue*)

PART III

STATISTICAL PROPERTIES OF RANDOM NOISE CURRENTS

3.0 Introduction

In this section we use the representations of the noise currents given in section 2.8 to derive some statistical properties of $I(t)$. The first six sections are concerned with the probability distribution of $I(t)$ and of its zeros and maxima. Sections 3.7 and 3.8 are concerned with the statistical properties of the envelope of $I(t)$. Fluctuations of integrals involving $I^2(t)$ are discussed in section 3.9. The probability distribution of a sine wave plus a noise current is given in 3.10 and in 3.11 an alternative method of deriving the results of Part III is mentioned. Prof. Uhlenbeck has pointed out that much of the material in this Part is closely connected with the theory of Markoff processes. Also S. Chandrasekhar has written a review of a class of physical problems which is related, in a general way, to the present subject.[22]

3.1 The Distribution of the Noise Current[23]

In section 1.4 it has been shown that the distribution of a shot effect current approaches a normal law as the expected number of events per second, ν, increases without limit.

In line with the spirit of this Part, Part III, we shall use the representation

$$I(t) = \sum_{n=1}^{N} (a_n \cos \omega_n t + b_n \sin \omega_n t) \qquad (2.8\text{–}1)$$

to show that $I(t)$ is distributed according to a normal law. This is obtained at once when the procedure outlined in section 2.8 is followed. Since a_n and b_n are distributed normally, so are $a_n \cos \omega_n t$ and $b_n \sin \omega_n t$ when t is regarded as fixed. $I(t)$ is thus the sum of $2N$ independent normal variates and consequently is itself distributed normally.

[22] Stochastic Problems in Physics and Astronomy, *Rev. of Mod. Phys.*, Vol. 15, pp. 1–89 (1943).

[23] An interesting discussion of this subject by V. D. Landon and K. A. Norton is given in the *I.R.E. Proc.*, 30 (Sept. 1942) pp. 425–429.

The average value of $I(t)$ as given by (2.8–1) is zero since $\bar{a}_n = \bar{b}_n = 0$:

$$\bar{I}(t) = 0 \tag{3.1–1}$$

The mean square value of $I(t)$ is

$$\begin{aligned} \overline{I^2(t)} &= \sum_{n=1}^{N} (\overline{a_n^2} \cos^2 \omega_n t + \overline{b_n^2} \sin^2 \omega_n t) \\ &= \sum_{n=1}^{N} w(f_n)\Delta f \qquad (3.1–2) \\ &\to \int_0^\infty w(f)\, df = \psi(0) \equiv \psi_0 \end{aligned}$$

In writing down (3.1–2) we have made use of the fact that all the a's and b's are independent and consequently the average of any cross product is zero. We have also made use of

$$\overline{a_n^2} = \overline{b_n^2} = w(f_n)\Delta f, \qquad f_n = n\Delta f, \qquad \omega_n = 2\pi f_n$$

which were given in 2.8. $\psi(\tau)$ is the correlation function of $I(t)$ and is related to $w(f)$ by

$$\psi_\tau \equiv \psi(\tau) = \int_0^\infty w(f) \cos 2\pi f\tau \, df \tag{2.1–6}$$

as is explained in section 2.1. In this part we shall write the argument of $\psi(\tau)$ as a subscript in order to save space.

Since we know that $I(t)$ is normal and since we also know that its average is zero and its mean square value is ψ_0, we may write down its probability density function at once. Thus, the probability of $I(t)$ being in the range $I, I + dI$ is

$$\frac{dI}{\sqrt{2\pi\psi_0}} e^{-I^2/2\psi_0} \tag{3.1–3}$$

This is the probability of finding the current between I and $I + dI$ at a time selected at random. Another way of saying the same thing is to state that (3.1–3) is the fraction of time the current spends in the range $I, I + dI$.

In many cases it is more convenient to use the representation (2.8–6)

$$I(t) = \sum_{n=1}^{N} c_n \cos(\omega_n t - \varphi_n), \qquad \overline{c_n^2} = 2w(f_n)\Delta f \tag{2.8–6}$$

in which $\varphi_1, \cdots \varphi_n$ are independent random phase angles. In order to deduce the normal distribution from this representation we first observe

that (2.8–6) expresses $I(t)$ as the sum of a large number of independent random variables

$$I(t) = x_1 + x_2 + \cdots + x_N$$

$$x_n = c_n \cos (\omega_n t - \varphi_n)$$

and hence that as $N \to \infty$ $I(t)$ becomes distributed according to a normal law. In order to make the limiting process definite we first choose N and Δf such that $N\Delta f = F$ where

$$\int_F^\infty w(f)\, df < \epsilon \int_0^\infty w(f)\, df$$

where ϵ is some arbitrarily chosen small positive quantity. We now let $N \to \infty$ and $\Delta f \to 0$ in such a way that $N\Delta f$ remains equal to F. Then

$$\begin{aligned} A &= \overline{x_1^2} + \overline{x_2^2} + \cdots + \overline{x_N^2} = \sum_1^N 2w(f_n)\Delta f\, \overline{\cos^2 (\omega_n t - \varphi_n)} \\ &= \sum_1^N w(f_n)\Delta f \to \int_0^F w(f)\, df \end{aligned} \tag{3.1–4}$$

$$\begin{aligned} B &= \overline{|x_1|^3} + \cdots + \overline{|x_N|^3} = \sum_1^N (2w(f_n)\Delta f)^{3/2}\, \overline{|\cos (\omega_n t - \varphi_n)|^3} \\ &< 4(\Delta f)^{1/2} \int_0^F [w(f)]^{3/2}\, df \end{aligned}$$

where the bars denote averages with respect to the φ's, t being held constant. If we assume that the integrals are proper, the ratio $BA^{-3/2} \to 0$ as $N \to \infty$, and consequently the central limit theorem* may be used if $w(f) = 0$ for $f > F$. Since we may make F as large as we please by choosing ϵ small enough, we may cover as large a frequency range as we wish. For this reason we write ∞ in place of F.

Now that the central limit theorem has told us that the distribution of $I(t)$, as given by (2.8–6), approaches a normal law, there remains only the problem of finding the average and the standard deviation:

$$\begin{aligned} \overline{I(t)} &= \sum_1^N c_n\, \overline{\cos (\omega_n t - \varphi_n)} = 0 \\ \overline{I^2(t)} &= \sum_1^N c_n^2\, \overline{\cos^2 (\omega_n t - \varphi_n)} \\ &\to \int_0^\infty w(f)\, df = \psi_0 \end{aligned} \tag{3.1–5}$$

* Section 2.10.

This gives the probability density (3.1–3). Hence the two representations lead to the same result in this case. Evidently, they will continue to lead to identical results as long as the central limit theorem may be used. In the future use of the representation (2.8–6) we shall merely assume that the central limit theorem may be applied to show that a normal distribution is approached. We shall omit the work corresponding to equations (3.1–4).

The characteristic function for the distribution of $I(t)$ is

$$\text{ave. } e^{iuI(t)} = \exp -\frac{\psi_0}{2} u^2 \tag{3.1–6}$$

3.2 The Distribution of $I(t)$ and $I(t + \tau)$

We require the two dimensional distribution in which the first variable is the noise current $I(t)$ and the second variable is its value $I(t + \tau)$ at some later time τ. It turns out that this distribution is normal[24], as we might expect from the analogy with section 3.1. The second moments of this distribution are

$$\begin{aligned} \mu_{11} &= \overline{I^2(t)} = \psi_0 = \int_0^\infty w(f)\, df \\ \mu_{22} &= \psi_0 \\ \mu_{12} &= \overline{I(t)I(t+\tau)} \\ &= \psi_\tau \end{aligned} \tag{3.2–1}$$

The expression for μ_{12} is in line with our definition (2.1–4) for the correlation function:

$$\psi_\tau \equiv \psi(\tau) = \operatorname*{Limit}_{T\to\infty} \frac{1}{T} \int_0^T I(t)I(t+\tau)\, dt \tag{2.1–4}$$

In order to get the distribution from the representation (2.8–6) we write

$$I_1 = I(t) = \sum_1^N c_n \cos(\omega_n t - \varphi_n)$$

$$I_2 = I(t+\tau) = \sum_1^N c_n \cos(\omega_n t - \varphi_n + \omega_n \tau)$$

[24] It seems that the first person to obtain this distribution in connection with noise was H. Thiede, *Elec. Nachr. Tek.* 13 (1936), 84–95.

From the central limit theorem for two dimensions it follows that I_1 and I_2 are distributed normally. As in (3.1)

$$\mu_{11} = \overline{I_1^2} = \sum_1^N c_n^2 \cdot \tfrac{1}{2} \to \int_0^\infty w(f)\, df = \psi_0$$

$$\mu_{22} = \overline{I_2^2} = \overline{I_1^2} = \psi_0 \tag{3.1-2}$$

$$\mu_{12} = \overline{I_1 I_2} = \sum_1^N c_n^2 \text{ ave. } \{\cos(\omega_n t - \varphi_n) \cos(\omega_n t - \varphi_n + \omega_n \tau)\}$$

Now the quantity within the parenthesis is

$$\cos^2(\omega_n t - \varphi_n) \cos \omega_n \tau - \cos(\omega_n t - \varphi_n) \sin(\omega_n t - \varphi_n) \sin \omega_n \tau$$

and when we take the average with respect to φ_n the second term drops out, giving

$$\mu_{12} = \sum_1^N c_n^2 \cdot \tfrac{1}{2} \cos \omega_n \tau \to \int_0^\infty w(f) \cos 2\pi f\tau\, df = \psi_\tau \tag{3.2-3}$$

where we have used $\omega_n = 2\pi f_n$ and the relation (2.1–6) between $w(f)$ and $\psi(\tau)$.

The probability density function for I_1 and I_2 may be stated. From the discussion of the normal law in 2.9 it is

$$\frac{[\psi_0^2 - \psi_\tau^2]^{-1/2}}{2\pi} \exp\left[\frac{-\psi_0 I_1^2 - \psi_0 I_2^2 + 2\psi_\tau I_1 I_2}{2(\psi_0^2 - \psi_\tau^2)}\right] \tag{3.2-4}$$

For a band pass filter whose range extends from f_a to f_b we have

$$\begin{aligned}
\psi_\tau &= \int_{f_a}^{f_b} w_0 \cos 2\pi f\tau\, df \\
&= w_0 \frac{\sin \omega_b \tau - \sin \omega_a \tau}{2\pi\tau} \qquad (3.2\text{–}5) \\
&= \frac{w_0}{\pi\tau} \sin \pi\tau(f_b - f_a) \cos \pi\tau(f_b + f_a) \\
\psi_0 &= w_0(f_b - f_a)
\end{aligned}$$

where w_0 is the constant value of $w(f)$ in the pass band and

$$\begin{aligned}
\omega_b &= 2\pi f_b \qquad (3.2\text{–}6) \\
\omega_a &= 2\pi f_a
\end{aligned}$$

According to our formula (3.2–4), I_1 and I_2 are independent when ψ_τ is zero. For the τ's which make ψ_τ zero, a knowledge of I_1 does not add to our knowledge of I_2. For example, suppose we have a narrow filter. Then

$$\psi_\tau = 0 \text{ when } \tau = [2(f_b + f_a)]^{-1}$$

$$\psi_\tau \text{ is nearly } -\psi_0 \text{ when } \tau = [f_b + f_a]^{-1}$$

For the first value of τ, all we know is that I_2 is distributed about zero with $\overline{I_2^2} = \psi_0$. For the second value of τ I_2 is likely to be near $-I_1$. This is in line with the idea that the noise current through a narrow filter behaves like a sine wave of frequency $\frac{1}{2}(f_b + f_a)$ (and, incidentally, whose amplitude fluctuates with an irregular frequency of the order of $\frac{1}{2}(f_b - f_a)$). The first value of τ corresponds to a quarter-period of such a wave and the second value to a half-period. By drawing a sine wave and looking at points separated by quarter and half periods, the reader will see how the ideas agree.

The characteristic function for the distribution of I_1 and I_2 is

$$\text{ave. } e^{iuI_1+ivI_2} = \exp\left[-\frac{\psi_0}{2}(u^2 + v^2) - \psi_\tau uv\right] \tag{3.2-7}$$

The three dimensional distribution in which

$$I_1 = I(t)$$

$$I_2 = I(t + \tau_1)$$

$$I_3 = I(t + \tau_1 + \tau_2)$$

where τ_1 and τ_2 are given and t is chosen at random is, as we might expect, normal in three dimensions. The moments, from which the distribution may be obtained by the method of Section 2.9, are

$$\mu_{11} = \mu_{22} = \mu_{33} = \psi_0$$

$$\mu_{12} = \psi_{\tau_1}$$

$$\mu_{23} = \psi_{\tau_2}$$

$$\mu_{13} = \psi(\tau_1 + \tau_2) = \psi_{\tau_1+\tau_2}$$

The characteristic function for I_1, I_2, I_3 is

$$\text{ave. } e^{iz_1I_1+iz_2I_2+iz_3I_3}$$

$$= \exp\left[-\frac{\psi_0}{2}(z_1^2 + z_2^2 + z_3^2) - \mu_{12}z_1z_2 - \mu_{23}z_2z_3 - \mu_{13}z_1z_3\right] \tag{3.2-8}$$

3.3 Expected Number of Zeros per Second

We shall use the following result. Let y be given by

$$y = F(a_1, a_2, \cdots a_N; x), \tag{3.3-1}$$

and let the a's be random variables. For a given set of a's, this equation gives a curve of y versus x. Since the a's are random variables we shall call this curve a random curve. Let us select a short interval x_1, $x_1 + dx$,

and then draw a batch of a's. The probability that the curve obtained by putting these a's in (3.3–1) will have a zero in x_1, $x_1 + dx$ is

$$dx \int_{-\infty}^{+\infty} |\eta| \, p(0, \eta; x_1) \, d\eta \tag{3.3–2}$$

and the expected number of zeros in the interval (x_1, x_2) is

$$\int_{x_1}^{x_2} dx \int_{-\infty}^{+\infty} |\eta| \, p(0, \eta; x) \, d\eta \tag{3.3–3}$$

In these expressions $p(\xi, \eta; x)$ is the probability density function for the variables

$$\begin{aligned} \xi &= F(a_1, \cdots a_N; x) \\ \eta &= \frac{\partial F}{\partial x} \end{aligned} \tag{3.3–4}$$

Since the a's are random variables so are ξ and η, and their distribution will contain x as a parameter. This is indicated by the notation $p(\xi, \eta; x)$.

These results may be proved in much the same manner as are similar results for the distribution of the maxima of a random curve. This method of proof suffers from the restriction that the a's are required to be bounded.[25] Results equivalent to (3.3–2) and (3.3–3) have been obtained independently by M. Kac.[26] His method of proof has the advantage of not requiring the a's to be bounded.

Here we shall sketch the derivation of a closely related result: The probability that y will pass through zero in x_1, $x_1 + dx$ with positive slope is

$$dx \int_0^{\infty} \eta p(0, \eta; x_1) \, d\eta \tag{3.3–5}$$

We choose dx so small that the portions of all but a negligible fraction of the possible random curves lying in the strip $(x_1, x_1 + dx)$ may be regarded as straight lines. If $y = \xi$ at x_1 and passes through zero for $x_1 < x < x_1 + dx$, its intercept on $y = 0$ is $x_1 - \frac{\xi}{\eta}$ where η is the slope. Thus ξ and η must be of opposite sign and

$$x_1 < x_1 - \frac{\xi}{\eta} < x_1 + dx$$

[25] S. O. Rice, *Amer. Jour. Math.* Vol. 61, pp. 409–416 (1939). However, L. A. MacColl has pointed out to me that a set of sufficient conditions for (3.3–5) to hold is: (a) $p(\xi, \eta; x)$ is continuous with respect to (ξ, η) throughout the $\xi\eta$-plane; and (b) that the integral

$$\int_0^{\infty} p(a\eta, \eta; x_1) \, d\eta$$

converges uniformly with respect to a in some interval $-a_1 \leq a \leq a_2$, where a_1 and a_2 are positive. These conditions are satisfied in all the applications we shall make use of (3.3–5).

[26] M. Kac, *Bull. Amer. Math. Soc.* Vol. 49, pp. 314–320 (1943).

According to the statement of our problem, we are interested only in positive values of η, and we therefore write our inequality as

$$-\eta\, dx < \xi < 0$$

For a given random curve i.e. for a given set of a's ξ and η have the values given by

$$\xi = F(a_1, \cdots a_N ; x_1)$$

$$\eta = \left[\frac{\partial F}{\partial x}\right]_{x=x_1}$$

If these values of ξ and η satisfy our inequality, the curve goes through zero in x_1, $x_1 + dx$. The probability of this happening is[27]

$$\int_0^\infty d\eta \int_{-\eta\, dx}^0 d\xi\, p(\xi, \eta; x_1) = \int_0^\infty [0 - (-\eta\, dx)] p(0, \eta; x_1)\, d\eta$$

where we have made use of the fact that dx is so very small that ξ is effectively zero. The last expression is the same as (3.3–5).

In the same way it may be shown that the probability of y passing through zero in x_1, $x_1 + dx$ with a negative slope is

$$-dx \int_{-\infty}^0 \eta p(0, \eta; x_1)\, d\eta \qquad (3.3\text{–}6)$$

Expression (3.3–2) is obtained by adding (3.3–5) and (3.3–6).

We are now ready to apply our formulas. We let t, $I(t)$ and φ_n play the roles of x, y, and a_n, respectively, and use

$$I(t) = \sum_{n=1}^{N} c_n \cos(\omega_n t - \varphi_n), \qquad c_n^2 = 2w(f)\Delta f \qquad (2.8\text{–}6)$$

[27] MacColl has remarked that the step from the double integral on the left hand side of this equation to the final result (3.3–5) may be made as follows:
It is easily seen that the probability density we are seeking is

$$\left[\frac{d}{d(\Delta x)} \int_0^\infty d\eta \int_{-\eta\Delta x}^0 p(\xi, \eta; x)\, d\xi\right]_{\Delta x=0}$$

Proceeding formally, without regard to conditions validating the analytical operations (for such conditions see the footnote on page 52), we have

$$\frac{d}{d\Delta x} \int_0^\infty d\eta \int_{-\eta\Delta x}^0 p(\xi, \eta; x)\, d\xi = \int_0^\infty \eta p(-\eta\Delta x, \eta; x)\, d\eta$$

and hence the required probability density is

$$\int_0^\infty \eta p(0, \eta; x)\, d\eta$$

The first step is to find the probability density function of the two random variables

$$\xi = \sum_{n=1}^{N} c_n \cos(\omega_n t_1 - \varphi_n)$$
$$\eta = l'(t_1) = -\sum_{n=1}^{N} c_n \omega_n \sin(\omega_n t_1 - \varphi_n) \tag{3.3-7}$$

where the prime denotes differentiation with respect t. From section 2.10

$$\mu_{11} = \overline{\xi^2} = \psi_0$$
$$\mu_{22} = \overline{\eta^2} = \sum_{n=1}^{N} c_n^2 \omega_n^2 \overline{\sin^2(\omega_n t_1 - \varphi_n)}$$
$$= \sum_{n=1}^{N} (2\pi f_n)^2 w(f_n)\Delta f$$
$$\to 4\pi^2 \int_0^\infty f^2 w(f)\, df = -\psi_0''$$
$$\mu_{12} = \overline{\xi\eta} = -\sum_{n=1}^{N} c_n^2 \omega_n \overline{\cos(\omega_n t_1 - \varphi_n)\sin(\omega_n t_1 - \varphi_n)}$$
$$= 0$$

The expression for μ_{22} arises from (2.1–6) by differentiation. In this expression ψ_0'' denotes the second derivative of $\psi(\tau)$ with respect to τ at $\tau = 0$:

$$\psi''(\tau) = -4\pi^2 \int_0^\infty f^2 w(f) \cos 2\pi f\tau\, df \tag{3.3-8}$$

Hence the probability density is

$$p(\xi, \eta; t) = \frac{[-\psi_0\psi_0'']^{-1/2}}{2\pi} \exp\left[-\frac{\xi^2}{2\psi_0} + \frac{\eta^2}{2\psi_0''}\right] \tag{3.3-9}$$

where ψ_0'' is negative. It will be observed that the expression on the right is independent of t. Hence the probability of having a zero in t_1, $t_1 + dt$,

$$dt \int_{-\infty}^{+\infty} |\eta| \frac{[-\psi_0\psi_0'']^{-1/2}}{2\pi} e^{\eta^2/2\psi_0''} d\eta = \frac{dt}{\pi}\left[-\frac{\psi''(0)}{\psi(0)}\right]^{1/2} \tag{3.3-10}$$

which follows from (3.3–3), is independent of t.

The expected number of zeros per second, which may be obtained from (3.3–3) by integrating (3.3–10) over an interval of one second, is

$$\frac{1}{\pi}\left[-\frac{\psi''(0)}{\psi(0)}\right]^{1/2} = 2\left[\frac{\int_0^\infty f^2 w(f)\, df}{\int_0^\infty w(f)\, df}\right]^{1/2} \tag{3.3-11}$$

For an ideal band pass filter whose pass band extends from f_a to f_b the expected number of zeros per second is

$$2\left[\frac{1}{3}\frac{f_b^3 - f_a^3}{f_b - f_a}\right]^{1/2} \tag{3.3-12}$$

When f_a is zero this becomes $1.155\, f_b$ and when f_a is very nearly equal to f_b it approaches $f_b + f_a$.

In a recent paper M. Kac[28] has given a result which, after a slight generalization, leads to

$$e^{-I^2/2\psi_0}\frac{1}{2\pi}\left[-\frac{\psi_0''}{\psi_0}\right]^{1/2} dt \tag{3.3-13}$$

for the probability that the noise current will pass through the value I with positive slope during the interval $t, t + dt$. The expected number of such passages per second is

$$e^{-I^2/2\psi_0} \times [\tfrac{1}{2} \text{ the expected number of zeros per second}] \tag{3.3-14}$$

The expression (3.3–13) may also be derived from analogue of (3.3–5) obtained by replacing the zero in $p(0, \eta; x_1)$ by y.

In some cases the integral

$$\psi_0'' = -4\pi^2 \int_0^\infty f^2 w(f)\, df$$

does not converge.

An example occurs when we apply a broad band noise voltage to a resistance and condenser in series. The power spectrum of the voltage across the condenser is of the form

$$w(f) = \frac{1}{f^2 + a^2} \tag{3.3-15}$$

Although ψ_0'' is infinite, ψ_0 is finite and equal to $\pi/2a$. A straightforward substitution in our formula (3.3–11) gives infinity as the expected number of zeros per second.

Some light is thrown on this breakdown of our formula when we consider a noise current consisting of two bands of noise. One band is confined to relatively low frequencies, and its power spectrum will be denoted by $w_1(f)$. The other band is very narrow and is centered at the relatively high frequency f_2. The complete power spectrum of our noise is then

$$w(f) = w_1(f) + A^2\delta(f - f_2)$$

[28] On the Distribution of Values of Trigonometric Sums with Linearly Independent Frequencies, *Amer. Jour. Math.*, Vol. LXV, pp 609–615, (1943).

where the unit impulse function δ is used to represent the very narrow band. The power spectrum of the narrow band is approximately the same as that of the wave $A\sqrt{2}\cos 2\pi f_2 t$.

The integrals occurring in our formula are

$$\int_0^\infty w(f)\,df = \int_0^\infty w_1(f)\,df + A^2$$

$$= W + A^2$$

$$\int_0^\infty w(f)f^2\,df = \int_0^\infty f^2 w_1(f)\,df + A^2 f_2^2$$

$$= U + A^2 f_2^2$$

We suppose that A and f_2 are such that

$$W \gg A^2$$

$$U \ll A^2 f_2^2 .$$

Then our formula (3.3–11) gives us the expected number of zeros

$$2\frac{Af_2}{W^{1/2}}$$

We may give a qualitative explanation of this formula if we regard our noise current as composed of a small component

$$I_2 = 2^{1/2} A \cos 2\pi f_2 t$$

due to the narrow band superposed on a large, slowly varying component due to the lower band. Since the r.m.s. value of the second component is $W^{1/2}$ we may assign it a representative frequency f_1 and write it approximately as

$$I_1 = (2W)^{1/2} \cos 2\pi f_1 t$$

The zeros of the noise current are clustered around the zeros of the second wave. Near such a zero

$$I_1 = \pm(2W)^{1/2} 2\pi f_1 \Delta t$$

where Δt is the distance from the zero. The oscillations of I_1 produce zeros when $|I_1|$ is less than the amplitude of I_2 or when

$$A > W^{1/2} 2\pi f_1 |\Delta t|$$

and the interval over which zeros are produced is given by

$$2\Delta t = \frac{AW^{-1/2}}{\pi f_1}$$

The number of zeros is this multiplied by $2f_2$. Since there are $2f_1$ such intervals per second the number of zeros per second is

$$\frac{4}{\pi} A W^{-1/2} f_2$$

This differs from the result given by our formula by a factor of $2/\pi$. This discrepancy is due to our representing the two bands by the sine waves I_1 and I_2.

From this example we obtain the picture that when the integral for ψ_0 converges corresponding to $A \to 0$, while at the same time the integral for ψ_0'' diverges, corresponding to $f_2 \to \infty$ in such a way that $Af_2 \to \infty$, the noise current behaves something like a continuous function which has no derivative. It seems that for physical systems the integrals will always converge since parasitic effects will have the effect of making $w(f)$ tend to zero rapidly enough. The frequency which represents the region where this occurs is of the order of the frequency of the microscopic wiggles.

So far we have been considering the formulas of this section in the most favorable light possible. There are experiments which indicate the possibility of the formulas breaking down in some cases. Prof. Uhlenbeck has pointed out that if a very broad band fluctuation current be forced[29] to flow through a circuit consisting of a condenser, C, in parallel with a series combination of inductance, L, and resistance, R, equation (3.3–11) says that the expected number of zeros per second of the current, I, flowing through R (and L) is independent of R. It is simply $\frac{1}{\pi}(LC)^{-1/2}$. The differential equation for I is the same as that which governs the Brownian motion of a mirror suspended in a gas[30], the gas pressure playing the role of R. Curves are available for this motion and it is seen that their character depends greatly upon the pressure[31]. Unfortunately, it is difficult to tell from the curves whether the expected number of zeros is independent of the pressure. The differences between the curves for various pressures indicates that there may be some dependence*.

3.4 The Distribution of Zeros

The problem of determining the distribution function for the distance between two successive zeros seems to be quite difficult and apparently

[29] For example, by putting the circuit in series with a diode.

[30] This problem in Brownian motion is discussed by G. E. Uhlenbeck and S. Goudsmit, *Phys., Rev.*, 34 (1929), 145–151.

[31] E. Kappler, *Annalen d. Phys.*, 11 (1931) 233–256.

* Since this was written M. Kac and H. Hurwitz have studied the problem of the expected number of zeros using quite a different method of approach which employs the "shot-effect" representation (Sec. 3.11). Their results confirm the correctness of (3.3–11) when the integrals converge. When the integrals diverge the average number of electrons, per sec. producing the shot effect must be considered.

nobody has as yet given a satisfactory solution. Here we shall give some results which are related to the general problem and which give an idea of the form of the distribution for the region of small spacings between the zeros.

We shall show (in the work starting with equation (3.4–12)) that the probability of the noise current, I, passing through zero in the interval $\tau, \tau + d\tau$ with a negative slope, when it is known that I passes through zero at $\tau = 0$ with a positive slope, is

$$\frac{d\tau}{2\pi}\left[\frac{\psi_0}{-\psi_0''}\right]^{1/2}\left[\frac{M_{23}}{H}\right](\psi_0^2 - \psi_\tau^2)^{-3/2}[1 + H\cot^{-1}(-H)] \quad (3.4\text{–}1)$$

where M_{22} and M_{23} are the cofactors of $\mu_{22} = -\psi_0''$ and $\mu_{23} = -\psi_\tau''$ in the matrix

$$M = \begin{bmatrix} \psi_0 & 0 & \psi_\tau' & \psi_\tau \\ 0 & -\psi_0'' & -\psi_\tau'' & -\psi_\tau' \\ \psi_\tau' & -\psi_\tau'' & -\psi_0'' & 0 \\ \psi_\tau & -\psi_\tau' & 0 & \psi_0 \end{bmatrix}, \quad (3.4\text{–}2)$$

$$H = M_{23}[M_{22}^2 - M_{23}^2]^{-1/2}.$$

We choose $0 \leq \cot^{-1}(-H) \leq \pi$, the value π being taken at $\tau = 0$, and the value $\pi/2$ being approached as $\tau \to \infty$. It should be remembered that we are writing the arguments of the correlation functions as subscripts, e.g., $-\psi_\tau''$ is really

$$-\psi''(\tau) = 4\pi^2 \int_0^\infty f^2 w(f) \cos 2\pi f\tau \, df \quad (3.3\text{–}8)$$

As τ becomes larger and larger the behavior of I at τ is influenced less and less by the fact that it goes through zero with a positive slope at $\tau = 0$. Hence (3.4–1) should approach the probability that, for any interval of length $d\tau$ chosen at random, I will go through zero with a negative slope. Because of symmetry, this is half the probability that it will go through zero. Thus (3.4–1) should approach, from (3.3–10),

$$\frac{d\tau}{2\pi}\left[\frac{-\psi_0'''}{\psi_0}\right]^{1/2} \quad (3.4\text{–}3)$$

as $\tau \to \infty$. It actually does this since M approaches a diagonal matrix and both M_{23} and H approach zero with $M_{23}/H \to M_{22} \to -\psi_0^2\psi_0''$. For a low pass filter cutting off at f_b (3.4–3) is

$$d\tau f_b 3^{-1/2} \quad (3.4\text{–}4)$$

The behavior of (3.4–1) as $\tau \to 0$ is quite a bit more difficult to work out.

M_{22} and M_{23} go to zero as τ^4, $M_{22}^2 - M_{23}^2$ as τ^{10}, and consequently H goes to infinity as τ^{-1}. The final result is that (3.4–1) approaches

$$d\tau \frac{\tau}{8}\left[\frac{\psi_0\psi_0^{(4)} - \psi_0''^2}{-\psi_0\psi_0''}\right] \tag{3.4–5}$$

as $\tau \to 0$, assuming $\psi^{(4)}$ exists. Here the superscript (4) indicates the fourth derivative at $\tau = 0$,

$$\psi_0^{(4)} = 16\pi^4 \int_0^\infty f^4 w(f)\, df \tag{3.4–6}$$

For a low pass filter cutting off at f_b (3.4–5) is

$$d\tau \frac{\tau}{30}(2\pi f_b)^2 \tag{3.4–7}$$

When (3.4–1) is applied to a low pass filter, it turns out that instead of τ the variable

$$\varphi = 2\pi f_b \tau, \qquad d\varphi = 2\pi f_b\, d\tau \tag{3.4–8}$$

is more convenient to handle. Thus, if we write (3.4–1) as $p(\varphi)\, d\varphi$, it follows from (3.4–4) and (3.4–7) that

$$\begin{aligned} p(\varphi) &\to \frac{1}{2\pi\sqrt{3}} = .0919 \quad \text{as} \quad \varphi \to \infty \\ p(\varphi) &\to \frac{\varphi}{30} \quad \text{as} \quad \varphi \to \infty \end{aligned} \tag{3.4–9}$$

$p(\varphi)$ has been computed and plotted on Fig. 1 as a function of φ for the range 0 to 9. From the curve and the theory it is evident that beyond 9 $p(\varphi)$ oscillates about 0.0919 with ever decreasing amplitude.

We may take $p(\varphi)\, d\varphi$ to be the probability that I goes through zero in $\varphi, \varphi + d\varphi$, when it is known that I goes through zero at $\varphi = 0$ with a slope opposite to that at φ. $p(\varphi)\, d\varphi$ exceeds the probability that I goes through zero at $\varphi = 0$ and in $\varphi, \varphi + d\varphi$ with no zeros in between. This is because $p(\varphi)\, d\varphi$ includes all curves of the latter class and in addition those which may have an even number of zeros between 0 and φ. From this it follows that the curve giving the probability density of the intervals between zeros must be underneath the curve of $p(\varphi)$.

A partial check on the curve for $p(\varphi)$ may be obtained by comparing it with a probability density function obtained experimentally by M. E. Campbell for the intervals between 754 successive zeros. He passed thermal noise through a band pass filter, the lower cutoff being around 200 cps and the upper cutoff being around 3000 cps. The upper cutoff was rather grad-

ual and it is difficult to assign a representative value. The crosses on figure 1 are obtained from his data when we assume that his filter behaves like a low pass filter with a cutoff at $f_b = 2850$, this choice being made in order to make the maximum of his curve coincide with that of $p(\varphi)$.

It is seen that some of the crosses lie above $p(\varphi)$. This is probably due to the fact that the actual filter differs somewhat from the assumed low pass filter.

On Fig. 1 there is also plotted a function closely related to (3.4–1). It is the low pass filter form of the following: The probability of I passing

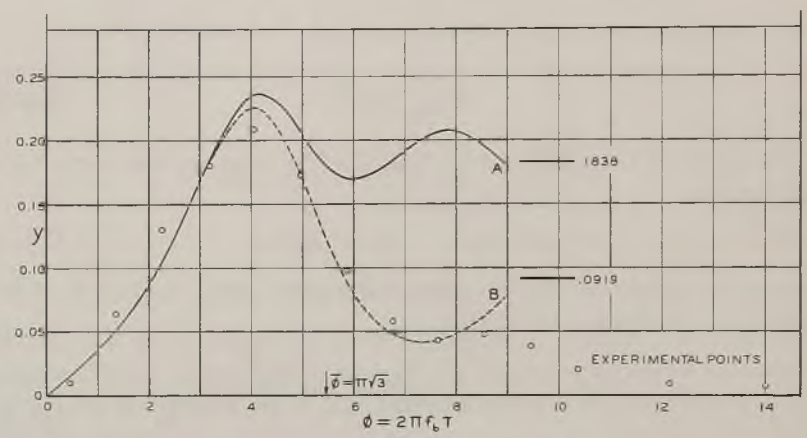

Fig. 1—Distribution of intervals between zeros—low-pass filter
$y_A \Delta\varphi$ is probability of a zero in $\Delta\varphi$ when a zero is at origin.
$y_B \Delta\varphi$ is probability of a zero in $\Delta\varphi$ when a zero is at origin and slopes at zeros are of opposite signs.
$y_B = p(\varphi), f_b$ = filter cutoff, τ = time between zeros.

through zero in τ, $\tau + d\tau$ when it is known that I passes through zero at $\tau = 0$ is

$$\frac{d\tau}{\pi}\left[\frac{\psi_0}{-\psi_0''}\right]^{1/2}\left[\frac{M_{23}}{H}\right](\psi_0^2 - \psi_\tau^2)^{-3/2}[1 + H \tan^{-1} H] \qquad (3.4\text{–}10)$$

where the notation is the same as in (3.4–1) and $-\frac{\pi}{2} \leq \tan^{-1} H \leq \frac{\pi}{2}$. This curve should always lie above $p(\varphi)$ and the small difference between the curves out to $\varphi = 4$ indicates that the true distribution of zeros is given closely by $p(\varphi)$ out to this point.

When (3.4–1) is applied to a relatively narrow band pass filter or some similar device we may make some approximations and obtain an expression somewhat simpler than (3.4–1). As a guide we consider our usual ideal

band pass filter whose range extends from f_a to f_b. The correlation function is given by (3.2–5).

$$\psi_\tau = \frac{w_0}{\pi\tau} \sin \pi\tau(f_b - f_a) \cos \pi\tau(f_b + f_a)$$
$$\psi_0 = w_0(f_b - f_a) \tag{3.2–5}$$

From physical considerations we know that in a narrow filter most of the distances between zeros will be nearly equal to

$$\tau_1 = \frac{1}{f_b + f_a}$$

i.e., nearly equal to the distance between the zeros of a sine wave having the mid-band frequency. We therefore expect (3.4–1) to have a peak very close to τ_1. We also expect peaks at $3\tau_1$, $5\tau_1$ etc. but we shall not consider these. We wish to examine the behavior of (3.4–1) near τ_1.

It turns out that M_{23} is nearly equal to M_{22} so that H is large and (3.4–1) becomes approximately

$$\frac{d\tau}{2}\left[\frac{\psi_0}{-\psi_0''}\right]^{1/2} \frac{M_{23}}{[\psi_0^2 - \psi_\tau^2]^{3/2}}$$

where τ is near τ_1.

In order to see that M_{23} is nearly equal to M_{22} we use the expressions

$$M_{22} = -\psi_0''(\psi_0^2 - \psi_\tau^2) - \psi_0\psi_\tau'^2$$
$$M_{23} = \psi_\tau''(\psi_0^2 - \psi_\tau^2) + \psi_\tau\psi_\tau'^2$$
$$M_{22} + M_{23} = (\psi_0 - \psi_\tau)[(\psi_0 + \psi_\tau)(\psi_\tau'' - \psi_0'') - \psi_\tau'^2]$$
$$= (\psi_0 - \psi_\tau)[B + C]$$
$$M_{22} - M_{23} = (\psi_0 + \psi_\tau)[(\psi_0 - \psi_\tau)(-\psi_\tau'' - \psi_0'') - \psi_\tau'^2]$$
$$= (\psi_0 + \psi_\tau)[-B + C]$$
$$B = \psi_0\psi_\tau'' - \psi_\tau\psi_0''$$
$$C = -\psi_0\psi_0'' + \psi_\tau\psi_\tau'' - \psi_\tau'^2$$

From (3.2–5) it is seen that ψ_τ may be written as

$$\psi_\tau = A \cos \beta\tau, \qquad \beta = \pi(f_b + f_a)$$

where $\beta\tau_1 = \pi$ and A is a function of τ which varies slowly in comparison with $\cos \beta\tau$. We see that near τ_1, ψ_τ is nearly equal to $-\psi_0$. Likewise

ψ_τ' hovers around zero and ψ_τ'' is nearly equal to $-\psi_0''$. Differentiating with respect to τ gives

$$\psi_\tau' = A' \cos \beta\tau - A\beta \sin \beta\tau$$

$$\psi_\tau'' = (A'' - A\beta^2) \cos \beta\tau - 2A'\beta \sin \beta\tau$$

$$\psi_0'' = A_0'' - A_0\beta^2, \qquad \psi_0 = A_0$$

where A_0 and A_0'' are the values of A and its second derivative at τ equal to zero. These lead to

$$B = (A_0A'' - AA_0'') \cos \beta\tau - 2A_0A'\beta \sin \beta\tau$$

$$C = (AA'' - A'^2) \cos^2 \beta\tau - A_0A_0'' + (A_0^2 - A)^2\beta^2$$

We wish to show that $C + B$ and $C - B$ are of the same order of magnitude. If we can do this, it follows that $M_{22} - M_{23}$ is much smaller than $M_{22} + M_{23}$ since $\psi_0 - \psi_{\tau_1}$ is approximately $2\psi_0$ while $\psi_0 + \psi_{\tau 1}$ is quite small. Consequently we will have shown that M_{23} is nearly equal to M_{22}.

So far we have made no approximations. We now express the slowly varying function A as a power series in τ. Since ψ_0' and ψ_0''' must be zero for the type of functions we consider, it follows that

$$A = A_0 + \frac{\tau^2}{2} A_0'' + \cdots$$

$$A' = \tau A_0'' + \cdots$$

$$A'' = A_0'' + \frac{\tau^2}{2} A_0^{(4)} + \cdots$$

where we neglect all powers higher than the second. Multiplication and squaring gives

$$A^2 - A_0^2 = \tau^2 A_0 A_0''$$

$$AA'' - A'^2 = A_0 A_0'' + \frac{\tau^2}{2} (A_0 A_0^{(4)} - A_0''^2)$$

$$= A_0 A_0'' + F$$

$$A_0 A'' - AA_0'' = \frac{\tau^2}{2} (A_0 A_0^{(4)} - A_0''^2) = F$$

Since, for small τ, A and A'' are nearly equal to A_0 and A_0'', respectively we see that the difference on the left is small relative to $A_0 A_0''$, i.e.,

$$|F| << |A_0 A_0''|$$

Our expression for B and C become approximately

$$B = F \cos \beta\tau - 2A_0 A_0'' \beta\tau \sin \beta\tau$$

$$C = F \cos^2 \beta\tau - A_0 A_0'' \sin^2 \beta\tau - A_0 A_0'' \beta^2 \tau^2$$

When τ is near τ_1, $\beta\tau$ is approximately π. Hence both $C + B$ and $C - B$ are approximately $-A_0 A_0'' \pi^2$ and are of the same order of magnitude. Consequently M_{22} and M_{23} are both nearly equal and

$$M_{23} = \psi_0[C + B]$$

$$= -A_0^2 A_0'' \pi^2$$

When this expression for M_{23} is used our approximation to (3.4–1) gives us the result: If the correlation function is of the form

$$\psi_\tau = A \cos \beta\tau$$

where A is a slowly varying function of τ, the probability that the distance between two successive zeros lies between τ and $\tau + d\tau$ is approximately

$$\frac{d\tau}{2} \frac{a}{[1 + a^2(\tau - \tau_1)^2]^{3/2}}$$

where a is positive and

$$a^2 = \frac{A_0 \beta^2}{-A_0'' \tau_1^2}, \qquad \tau_1 = \frac{\pi}{\beta}$$

For our ideal band pass filter with the pass band $f_b - f_a$,

$$a = \sqrt{3}\, \frac{(f_b + f_a)^2}{f_b - f_a}, \qquad \tau_1 = \frac{1}{f_b + f_a}$$

and the average value of $|\tau - \tau_1|$ is a^{-1}. Thus

$$\frac{\text{ave. } |\tau - \tau_1|}{\tau_1} = \frac{1}{a\tau_1} = \frac{f_b - f_a}{\sqrt{3}\,(f_b + f_a)} = \frac{1}{2\sqrt{3}} \frac{\text{band width}}{\text{mid-frequency}}$$

When the correlation function cannot be put in the form assumed above but still behaves like a sinusoidal wave with slowly varying amplitude we may use our first approximation to (3.4–1). Thus, the probability that the distance between two successive zeros lies between τ and $\tau + d\tau$ is approximately

$$\frac{b\, d\tau}{[\psi_0^2 - \psi_\tau^2]^{3/2}}$$

when τ lies near τ_1 where τ_1 is the smallest value of τ which makes ψ_τ approximately equal to $-\psi_0$. This probability is supposed to approach

zero rapidly as τ departs from τ_1, and b is chosen so that the integral over the effective region around τ_1 is unity.

It seems to be especially difficult to get an expression for the distribution of zeros for large spacing. One method, suggested by Prof. Goudsmit, is to amend the conditions leading to (3.4–1) by adding conditions that I be positive at equally spaced points along the time axis between 0 and τ. This leads to integrals which are hard to evaluate. For one point between 0 and τ the integral is of the form (3.5-7).

Another method of approach is to use the method of "in and exclusion" of zeros between 0 and τ. Consider the class of curves of I having a zero at $\tau = 0$. Then, in theory, our methods will allow us to compute the functions $p_0(\tau)$, $p_1(r, \tau)$, $p_2(r, s, \tau)$, associated with this class where

$p_0(\tau)\, d\tau$ is probability of curve having zero in $d\tau$

$p_1(r, \tau)\, d\tau\, dr$ is probability of curve having zeros in $d\tau$ and dr

$p_2(r, s, \tau)\, d\tau\, dr\, ds$ is probability of curve having zeros in $d\tau$, dr, and ds

In fact $p_0(\tau)\, d\tau$ is expression (3.4–10). The method of in and exclusion then leads to an expression for $P_0(\tau)\, d\tau$, the probability of having a zero at 0 and a zero in τ, $\tau + d\tau$ but none between 0 and τ. It is

$$P_0(\tau) = p_0(\tau) - \frac{1}{1!}\int_0^\tau p_1(r, \tau)\, dr + \frac{1}{2!}\int_0^\tau\int_0^\tau p_2(r, s, \tau)\, dr\, ds - \frac{1}{3!}\int_0^\tau\int_0^\tau\int_0^\tau p_3(r, s, t, \tau)\, dr\, ds\, dt + \cdots \tag{3.4–11}$$

Here again we run into difficult integrals. Incidentally, (3.4–11) may be checked for events occurring independently at random. Thus if $\nu\, d\tau$ is the probability of an event happening in $d\tau$, then, if ν is a constant and the events are independent, we have p_0, p_1, p_2, $\cdots$ given by ν, ν^2, ν^3, $\cdots$. From (3.4–11) we obtain the known result $P_0(\tau) = \nu e^{-\nu\tau}$.

We shall now derive (3.4–1). The work is based upon a generalization of (3.3–5): If y is a random curve described by (3.3–1), the probability that y will pass through zero in x_1, $x_1 + dx_1$ with a positive slope and through zero in x_2, $x_2 + dx_2$ with a negative slope is

$$-dx_1\, dx_2 \int_0^{+\infty} d\eta_1 \int_{-\infty}^{0} d\eta_2\, \eta_1\, \eta_2\, p(0, \eta_1, x_1; 0, \eta_2, x_2) \tag{3.4–12}$$

where $p(\xi_1, \eta_1, x_1; \xi_2, \eta_2, x_2)$ is the probability density function for the four random variables

$$\xi_i = F(a_1, a_2, \cdots, a_N; x_i)$$

$$\eta_i = \left[\frac{\partial F}{\partial x}\right]_{x=x_i}, \qquad i = 1, 2.$$

The x_1 and x_2 play the role of parameters in (3.4–12). This result may be established in much the same way as (3.3–5).

When we identify F with one of our representations, (2.8–1) or (2.8–6), of the noise current $I(t)$ it is seen that p is normal in four dimensions. We may obtain the second moments directly from this representation, as has been done in the equations just below (3.3–7). The same results may be obtained from the definition of $\psi(\tau)$, and for the sake of variety we choose this second method. We set $x_1 = t_1$, $x_2 = t_1 + \tau$. Then

$$\begin{aligned} \overline{\xi_1^2} &= \overline{\xi_2^2} = \overline{I^2(t)} = \psi_0 \\ \overline{\xi_1 \xi_2} &= \overline{I(t)I(t+\tau)} = \psi_\tau \\ \overline{\eta_1 \eta_2} &= \overline{\left(\frac{\partial I}{\partial t}\right)_t \left(\frac{\partial I}{\partial t}\right)_{t+\tau}} = \operatorname*{Limit}_{T\to\infty} \frac{1}{T}\int_0^T I'(t+\tau)I'(t)\,dt \end{aligned} \tag{3.4–13}$$

where primes denote differentiation with respect to the arguments. Integrating by parts:

$$\int_0^T I'(t+\tau)\,dI(t) = [I'(t+\tau)I(t)]_0^T - \int_0^T I''(t+\tau)I(t)\,dt$$

We assume that I and its derivative remains finite so that the integrated portion vanishes, when divided by T, in the limit. Since

$$I''(t+\tau) = \frac{\partial^2}{\partial \tau^2} I(t+\tau)$$

we have

$$\overline{\eta_1 \eta_2} = -\frac{\partial^2}{\partial \tau^2}\psi(\tau) = -\psi_\tau''$$

Setting $\tau = 0$ gives

$$\overline{\eta_1^2} = \overline{\eta_2^2} = -\psi_0''$$

in agreement with the value of μ_{22} obtained from (3.3–7). In the same way

$$\begin{aligned} \overline{\xi_1 \eta_2} &= \operatorname*{Limit}_{T\to\infty} \frac{1}{T}\int_0^T I'(t+\tau)I(t)\,dt = \frac{\partial}{\partial \tau}\psi(\tau) \\ &= \psi_\tau' \\ \overline{\xi_2 \eta_1} &= \operatorname*{Limit}_{T\to\infty} \frac{1}{T}\int_0^T I'(t)I(t+\tau)\,dt \\ &= \text{“} \quad (-)\frac{1}{T}\int_0^T I'(t+\tau)I(t)\,dt \\ &= -\psi_\tau' \end{aligned}$$

where we have integrated by parts in getting $\overline{\xi_2\eta_1}$. Setting $\tau = 0$ and using $\psi_0' = 0$ gives

$$\overline{\xi_1\eta_1} = \overline{\xi_2\eta_2} = 0$$

In order to obtain the matrix M of the second moments μ_{rs} in a form fairly symmetrical about its center we choose the 1, 2, 3, 4 order of our variables to be ξ_1, η_1, η_2, ξ_2. From equations (3.4–13) etc. it is seen that this choice leads to the expression (3.4–2) for M.

When we put ξ_1 and ξ_2 equal to zero, we obtain for the probability density function in (3.4–12) the expression

$$\frac{|M|^{-1/2}}{4\pi^2} \exp\left[-\frac{1}{2|M|}(M_{22}\eta_1^2 + 2M_{23}\eta_1\eta_2 + M_{33}\eta_2^2)\right]$$

Because of the symmetry of M, M_{22} is equal to M_{33}. When, in the integral (3.4–12) we make the change of variable

$$x = \left[\frac{M_{22}}{2|M|}\right]^{1/2}\eta_1, \qquad y = -\left[\frac{M_{22}}{2|M|}\right]^{1/2}\eta_2$$

we obtain

$$\frac{dx_1\,dx_2}{\pi^2}\frac{|M|^{3/2}}{M_{22}^2}\int_0^\infty x\,dx\int_0^\infty dy\,ye^{-x^2-y^2+2(M_{23}/M_{22})xy}$$

The double integral may be evaluated by (3.5–4). Let

$$\varphi = \cos^{-1}\left(-\frac{M_{23}}{M_{22}}\right) = \cot^{-1}(-H), \qquad H = M_{23}[M_{22}^2 - M_{23}^2]^{-1/2}$$

where H is the same as that given in (3.4–2). Our expression now becomes

$$\frac{dx_1\,dx_2}{4\pi^2}\frac{|M|^{3/2}}{M_{22}^2 - M_{23}^2}[1 + H\cot^{-1}(-H)]$$

From a property of determinants

$$M_{22}M_{33} - M_{23}^2 = |M|(\psi_0^2 - \psi_\tau^2)$$

Using this to eliminate $|M|$ and dividing by

$$\frac{dx_1}{2\pi}\left[\frac{-\psi_0''}{\psi_0}\right]^{1/2}$$

which, from (3.3–10), is the probability of going through zero in x_1, $x_1 + dx_1$ with positive slope, gives the probability of going through zero in dx_2 with

negative slope when it is known that I goes through zero at x_1 with positive slope:

$$\frac{dx_2}{2\pi}\left[\frac{\psi_0}{-\psi_0''}\right]^{1/2}[M_{22}^2 - M_{23}^2]^{1/2}(\psi_0^2 - \psi_\tau^2)^{-3/2}[1 + H\cot^{-1}(-H)]$$

This is the same as (3.4–1).

The expression (3.4–10) is the same as the probability of I going through zero in $d\tau$ when it is known that I goes through zero at the origin with positive slope. This second probability may be obtained from (3.4–1) by adding the probability that I goes through $d\tau$ with positive slope when it is known to go through zero with positive slope. Thus we must add the expression containing the integral in which the integration in both η_1 and η_2 run from 0 to ∞. In terms of x and y this integral is

$$\int_0^\infty x\,dx \int_0^\infty dy\, y e^{-x^2-y^2-2(M_{23}/M_{22})xy}$$

This is equivalent to a change in the sign of M_{23} and hence of H. After this addition we must consider

$$\begin{aligned} &1 + H\cot^{-1}(-H) + 1 - H\cot^{-1}H \\ &= 2 + H[\cot^{-1}(-H) - \cot^{-1}H] \\ &= 2 + H[\pi - 2\cot^{-1}H] \\ &= 2[1 + H\tan^{-1}H] \end{aligned}$$

and this leads to (3.4–10).

3.5 Multiple Integrals

We wish to evaluate integrals of the form

$$J = \int_0^\infty dx_1 \int_0^\infty dx_2\, e^{-x_1^2 - 2ax_1x_2 - x_2^2} \tag{3.5–1}$$

Our method of procedure is to first reduce the exponent to the sum of squares by a suitable linear change of variable and then change to polar coordinates. This method appears to work also for triple integrals of the same sort, but when it is applied to a four-fold integral, the last integration apparently cannot be put in closed form.

The reduction of the exponent to the sum of squares is based upon the transformation: If*

$$\begin{aligned} x_1 &= h_1 y_1 + h_2 D_{21} y_2 + h_3 D_{31} y_3 + \cdots + h_n D_{n,1} y_n \\ x_2 &= 0 \quad + h_2 D_{22} y_2 + \cdots \quad + h_n D_{n,2} y_n \\ &\cdots\cdots\cdots\cdots\cdots\cdots\cdots\cdots\cdots\cdots\cdots\cdots \\ x_n &= 0 \quad + 0 \quad + \cdots + 0 \quad + h_n D_{n,n} y_n \end{aligned} \tag{3.5–2}$$

* T. Fort, Am. Math. Monthly, 43 (1936), pp. 477–481. See also Scott and Mathews, Theory of Determinants, Cambridge (1904), Prob. 63, p. 276.

where $D_0 = 1$, $D_1 = a_{11}$, $D_{r,r} = D_{r-1}$, and D_{rs} is the cofactor of a_{sr} (or of a_{rs} because they are equal) in D_r :

$$D_r = \begin{vmatrix} a_{11} & a_{12} \cdots & a_{1r} \\ a_{12} & a_{22} & \\ a_{1r} & \cdots & a_{rr} \end{vmatrix}, \qquad h_r = [D_{r-1}D_r]^{-1/2},$$

then, if none of the D_r's is zero,

$$\sum_1^n a_{rs} x_r x_s = y_1^2 + y_2^2 + \cdots + y_n^2$$

From (3.5–2); the Jacobian $\partial(x_1, \cdots x_n)/\partial(y_1, \cdots y_n)$ is equal to $D_n^{-1/2}$.

Applying our transformation to the exponent:

$$x_1 = y_1 - aD_2^{-1/2}y_2$$

$$x_2 = 0 + D_2^{-1/2}y_2$$

$$D_2 = 1 - a^2$$

Since x_2 runs from 0 to ∞ so must y_2. The expression for x_1 shows that y_1 runs from $a\,D_2^{-1/2}y_2$ to ∞. The integral is therefore

$$J = D_2^{-1/2} \int_0^\infty dy_2 \int_{aD_2^{-1/2}y_2}^\infty e^{-y_1^2 - y_2^2}\, dy_1$$

We now change to polar coordinates:

$$\begin{aligned} y_1 &= \rho \cos\theta \\ y_2 &= \rho \sin\theta \end{aligned} \qquad dy_1\, dy_2 = \rho\, d\rho\, d\theta$$

$y_2 \geq 0$ gives $0 \leq \theta \leq \pi$

$y_1 \geq aD_2^{-1/2}y_2$ gives $\cot\theta \geq aD_2^{-1/2}$

and obtain

$$J = D_2^{-1/2} \int_0^{\cot^{-1} aD_2^{-1/2}} d\theta \int_0^\infty \rho e^{-\rho^2}\, d\rho$$

$$= \tfrac{1}{2} D_2^{-1/2} \cot^{-1}(aD_2^{-1/2})$$

where the arc-cotangent lies between 0 and π. This may be written in the simpler form

$$J = \tfrac{1}{2}(1 - a^2)^{-1/2} \cos^{-1} a = \tfrac{1}{2}\varphi \csc\varphi$$

where

$$a = \cos\varphi,$$

it being understood that $0 \leq \varphi \leq \pi$.

Other integrals may be obtained by differentiation. Thus from

$$\int_0^\infty dx \int_0^\infty dy\, e^{-x^2-y^2-2xy\cos\varphi} = \tfrac{1}{2}\varphi \csc\varphi \tag{3.5-3}$$

we obtain

$$\int_0^\infty dx \int_0^\infty dy\, xy\, e^{-x^2-y^2-2xy\cos\varphi} = \tfrac{1}{4}\csc^2\varphi(1 - \varphi\cot\varphi) \tag{3.5-4}$$

By using the same transformation we may obtain

$$\int_0^\infty dx \int_0^\infty dy\, ye^{-x^2-y^2-2axy} = \frac{\sqrt{\pi}}{4}\frac{1}{1+a} \tag{3.5-5}$$

Of course, we may expand part of the exponential in a power series and integrate termwise but this leads to a series which has to be summed in each particular case:

$$\int_0^\infty dx \int_0^\infty dy\, x^n y^m e^{-x^2-y^2-2axy}$$

$$= \frac{1}{4}\sum_{r=0}^{\infty}\frac{(-2a)^r}{r!}\Gamma\left(\frac{n+r+1}{2}\right)\Gamma\left(\frac{m+r+1}{2}\right)$$

If we take $-1 < R(m) < -\frac{1}{2}$, $-1 < R(m) < -\frac{1}{2}$, the series may be summed when $a = 1$. The result stated just below equation (3.8–9) is obtained by continuing m and n analytically.

The same methods will work when the limits are $\pm\infty$. We obtain, when m and n are integers,

$$\int_{-\infty}^{+\infty} dx \int_{-\infty}^{+\infty} dy\, x^n y^m e^{-x^2-y^2-2xy\cos\varphi}$$

$$= \begin{cases} 0, & n+m \text{ odd} \\ (-)^n\sqrt{\pi}\,\dfrac{\Gamma\left(\dfrac{m+n+1}{2}\right)}{(\sin\varphi)^{n+m+1}} & \\ \qquad F\left(-n, -m; \dfrac{1-n-m}{2}; \dfrac{1-\cos\varphi}{2}\right), & n+m \text{ even} \end{cases} \tag{3.5-6}$$

The hypergeometric function may also be written as

$$F\left(-\frac{n}{2}, -\frac{m}{2}; \frac{1-n-m}{2}; \sin^2\varphi\right)$$

By transformations of this we are led to the following expression for the integral

$$\begin{cases} 0, & n+m \text{ odd}, \\ \dfrac{\Gamma\left(\dfrac{m+1}{2}\right)\Gamma\left(\dfrac{n+1}{2}\right)}{(\sin\varphi)^{n+m+1}} F\left(-\frac{n}{2}, -\frac{m}{2}, \frac{1}{2}; \cos^2\varphi\right), & m, n \text{ both even}, \\ -2\dfrac{\Gamma\left(1+\dfrac{n}{2}\right)\Gamma\left(1+\dfrac{m}{2}\right)}{(\sin\varphi)^{n+m+1}} \cos\varphi F\left(\dfrac{1-m}{2}, \dfrac{1-n}{2}; \dfrac{3}{2}; \cos^2\varphi\right), & m, n \text{ odd} \end{cases}$$

As was mentioned earlier, the method used to evaluate the double integrals may also be applied to similar triple integrals. Here we state two results obtained in this way.

$$\int_0^\infty dx \int_0^\infty dy \int_0^\infty dz \exp\left[-x^2 - y^2 - z^2 - 2cxy - 2bzx - 2ayz\right]$$
$$= \frac{1}{4}\left[\frac{\pi}{D_3}\right]^{1/2} [\alpha + \beta + \gamma - \pi]$$
$$\int_0^\infty dx \int_0^\infty dy \int_0^\infty dz\, yz \exp\left[-x^2 - y^2 - z^2 - 2cxy - 2bzx - 2ayz\right]$$
$$= \frac{\sqrt{\pi}}{8D_3}\left[\frac{1+a-b-c}{1+a} - \frac{a-bc}{D_3^{1/2}}(\alpha+\beta+\gamma-\pi)\right] \qquad (3.5\text{–}7)$$

where β and γ are obtained by cyclic permutation of a, b, c from

$$\alpha = \cos^{-1}\frac{a-cb}{(1-c^2)^{1/2}(1-b^2)^{1/2}} = \sin^{-1}\left[\frac{D_3}{(1-c^2)(1-b^2)}\right]^{1/2}$$
$$= \cot^{-1}\frac{a-bc}{D_3^{1/2}}$$

where α, β, γ all lie in the range 0, π and where

$$D_3 = \begin{vmatrix} 1 & c & b \\ c & 1 & a \\ b & a & 1 \end{vmatrix} = 1 + 2abc - a^2 - b^2 - c^2$$

For reference we state the integrals which arise from the definition of the normal distribution given in section (2.9)

$$\int_{-\infty}^{+\infty} dx_1 \cdots \int_{-\infty}^{+\infty} dx_n \exp\left[-\sum_1^n a_{rs}x_r x_s\right] = \left[\frac{\pi^n}{|a|}\right]^{1/2}$$
$$\int_{-\infty}^{+\infty} dx_1 \cdots \int_{-\infty}^{+\infty} dx_n\, x_t x_u \exp\left[-\sum^n a_{rs}x_r x_s\right] = \left[\frac{\pi^n}{|a|^3}\right]^{1/2}\frac{A_{tu}}{2} \qquad (3.5\text{–}8)$$

where the quadratic form is positive definite and $|a|$ is its determinant. A_{tu} is the cofactor of a_{tu}. Incidentally, these may be regarded as special cases of

$$\int_{-\infty}^{+\infty} dx_1 \cdots \int_{-\infty}^{+\infty} dx_n f\left(\sum_1^n a_{rs}x_r x_s\right) F\left(\sum_1^n b_r x_r\right)$$

$$= \frac{2}{\Gamma\left(\frac{n-1}{2}\right)}\left[\frac{\pi^{n-1}}{|a|}\right]^{1/2} \int_{-\infty}^{+\infty} dx \int_0^{\infty} dy\, y^{n-2} f(x^2+y^2) \tag{3.5-9}$$

$$F\left\{x\left[\frac{\sum_1^n A_{rs}b_r b_s}{|a|}\right]^{1/2}\right\},$$

which is a generalization of a result given by Schlömilch.*

3.6 Distribution of Maxima of Noise Current

Here we shall use a result similar to those used in sections 3.3 and 3.4. Let y be a random curve given by (3.3–1),

$$y = F(a_1 \cdots a_N ; x). \tag{3.3-1}$$

If suitable conditions are satisfied, the probability that y has a maximum in the rectangle $(x_1, x_1 + dx_1, y_1, y_1 + dy_1)$, dx_1 and dy_1 being of the same order of magnitude, is[**]

$$-dx_1\, dy_1 \int_{-\infty}^{0} p(y_1, 0, \zeta)\zeta\, d\zeta \tag{3.6-1}$$

and the expected number of maxima of y in $a \leq x \leq b$ is obtained by integrating this expression over the range $-\infty \leq y_1 \leq \infty$, $a \leq x_1 \leq b$. $p(\xi, \eta, \zeta)$ is the probability density function for the random variables

$$\begin{aligned} \xi &= F(a_1, \cdots, a_N ; x_1) \\ \eta &= \left(\frac{\partial F}{\partial x}\right)_{x=x_1} \\ \zeta &= \left(\frac{\partial^2 F}{\partial x^2}\right)_{x=x_1} \end{aligned} \tag{3.6-2}$$

* Höheren Analysis, Braunschweig (1879), Vol. 2, p. 494, equ. (29).

[**] *Am. Jour. Math.*, Vol. 61 (1939) 409–416. A similar problem has been studied by E. L. Dodd, The Length of the Cycles Which Result From the Graduation of Chance Elements. Ann. Math. Stat., Vol. 10 (1939) 254–264. He gives a number of references to the literature dealing with the fluctuations of time series.

In our application of this result we replace x and y by t and I as before. Then

$$\xi = I = \sum_1^N c_n \cos(\omega_n t - \varphi_n)$$

$$\eta = I'$$

$$\zeta = I''$$

where the primes denote differentiation with respect to t. According to the central limit theorem the distribution of ξ, η, ζ approaches a normal law. The second moments defining this law may be obtained either from the above definitions of ξ, η, ζ, or may be obtained from the correlation function as was done in the work following equation (3.4–13).

$$\overline{\xi^2} = \psi_0, \qquad \overline{\eta^2} = -\psi_0'', \qquad \overline{\xi\eta} = 0$$

$$\overline{\eta\zeta} = \overline{I'(t)I''(t)} = \operatorname*{Limit}_{T\to\infty} \frac{1}{T}\int_0^T I'(t)I''(t)\,dt$$

$$= \operatorname*{Limit}_{T\to\infty} \frac{1}{2T}[I'^2(T) - I'^2(0)] = 0$$

$$\overline{\xi\zeta} = \operatorname*{Limit}_{T\to\infty} \frac{1}{T}\int_0^T I(t)I''(t)\,dt$$

$$= \operatorname*{Limit}_{\tau\to 0} \frac{\partial^2\psi(\tau)}{\partial\tau^2} = \psi_0''$$

$$\overline{\zeta^2} = \operatorname*{Limit}_{T\to\infty} \frac{1}{T}\int_0^T I''(t)I''(t)\,dt$$

$$= \operatorname*{Limit}_{T\to\infty} \frac{1}{T}\int_0^T I^{(4)}(t)I(t)\,dt$$

$$= \psi_0^{(4)}$$

where the superscript (4) represents the fourth derivative. The matrix M of the moments is thus

$$M = \begin{bmatrix} \psi_0 & 0 & \psi_0'' \\ 0 & -\psi_0'' & 0 \\ \psi_0'' & 0 & \psi_0^{(4)} \end{bmatrix}$$

The determinant $|M|$ and the cofactors of interest are

$$|M| = -\psi_0''(\psi_0\psi_0^{(4)} - \psi_0''^2) \tag{3.6–3}$$

$$M_{11} = -\psi_0''\psi_0^{(4)}, \qquad M_{13} = \psi_0''^2, \qquad M_{33} = -\psi_0''\psi_0$$

The probability density function in (3.6–1) is

$$p(I, 0, \zeta) = (2\pi)^{-3/2} \mid M \mid^{-1/2} \exp \left[-\frac{1}{2 \mid M \mid} (M_{11} I^2 + M_{33} \zeta^2 + 2M_{13} I\zeta) \right] \tag{3.6–4}$$

and when this is put in (3.6–1) and the integration with respect to ζ performed we get

$$dI\, dt \frac{(2\pi)^{-3/2}}{M_{33}} \left[\mid M \mid^{1/2} e^{-M_{11} I^2/2 \mid M \mid} + M_{13} I \left(\frac{\pi}{2M_{33}} \right)^{1/2} e^{-I^2/2\psi_0} \left(1 + \operatorname{erf} \frac{M_{13} I}{[2 \mid M \mid M_{33}]^{1/2}} \right) \right] \tag{3.6–5}$$

for the probability of a maximum occurring in the rectangle $dI\, dt$. As is mentioned just below expression (3.6–1), the expected number of maxima in the interval t_1, t_2 may be obtained by integrating (3.6-1) from t_1 to t_2 after replacing x by t, and I from $-\infty$ to $+\infty$ after replacing y by I. When we use (3.6–4) it is easier to integrate with respect to I first. The expected number is then

$$-\int_{t_1}^{t_2} dt \frac{M_{11}^{-1/2}}{2\pi} \int_{-\infty}^{0} \zeta \exp \left[-\frac{\zeta^2}{2 \mid M \mid} \left(M_{33} - \frac{M_{13}^2}{M_{11}} \right) \right] d\zeta = (t_2 - t_1) \frac{\psi_0^{(4)}}{2\pi} M_{11}^{-1/2} = \frac{t_2 - t_1}{2\pi} \left[\frac{\psi_0^{(4)}}{-\psi_0''} \right]^{1/2}$$

Hence the expected number of maxima per second is

$$\frac{1}{2\pi} \left[\frac{\psi_0^{(4)}}{-\psi_0''} \right]^{1/2} = \left[\frac{\int_0^\infty f^4 w(f)\, df}{\int_0^\infty f^2 w(f)\, df} \right]^{1/2} \tag{3.6–6}$$

For a band pass filter, the expected number of maxima per second is

$$\left[\frac{3}{5} \frac{f_b^5 - f_a^5}{f_b^3 - f_a^3} \right]^{1/2} \tag{3.6–7}$$

where f_b and f_a are the cut-off frequencies. Putting $f_a = 0$ so as to get a low pass filter,

$$f_b \left[\frac{3}{5} \right]^{1/2} = .775 f_b \tag{3.6–8}$$

From (3.6–8) and (3.6–5) we may obtain the probability density function for the maxima in the case of a low pass filter. Thus the probability that a maximum selected at random from the universe of maxima will lie in I, $I + dI$ is

$$\frac{dI}{3\sqrt{2\pi\psi_0}}\left[2e^{-3y^2/8} + \left(\frac{5\pi}{2}\right)^{1/2} ye^{-y^2/2}\left(1 + \operatorname{erf} y\left(\frac{5}{8}\right)^{1/2}\right)\right] \tag{3.6–9}$$

where

$$y = \frac{I}{\sqrt{\psi_0}}$$

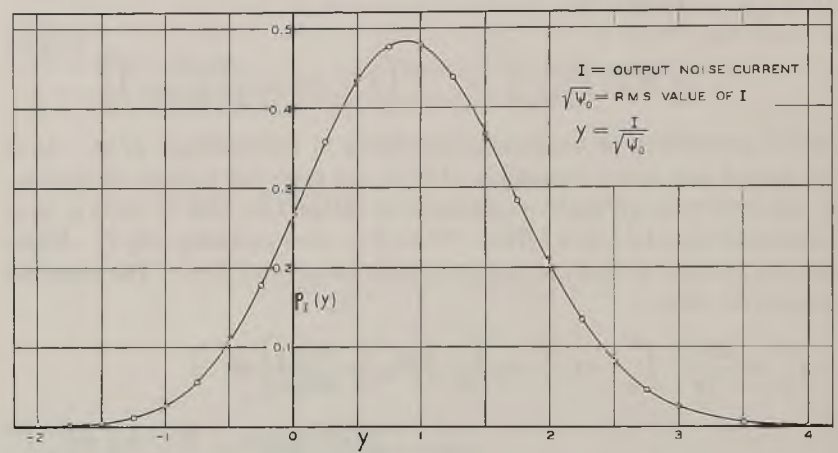

Fig. 2—Distribution of maxima of noise current. Noise through ideal low-pass filter. $\frac{p_I(y)}{\sqrt{\psi_0}}\,dI$ = probability that a maximum of I selected at random lies between I and $I + dI$.

When y is large and positive (3.6–9) is given asymptotically by

$$\frac{dI}{\sqrt{\psi_0}}\,\frac{\sqrt{5}}{3}\,ye^{-y^2/2}$$

If we write (3.6–9) as $p_I(y)\,dy$, the probability density $p_I(y)$ of y may be plotted as a function of y. This plot is shown in Fig. 2. The distribution function $P(I_{\max} < y\sqrt{\psi_0})$ defined by

$$P(I_{\max} < y\sqrt{\psi_0}) = \int_{-\infty}^{y} p_I(y)\cdot dy$$

and which gives the probability that a maximum selected at random is less than a specified $y\sqrt{\psi_0} = I$, is one of the four curves plotted in Fig. 4.

If I is large and positive we may obtain an approximation from (3.6–5). We observe that

$$\frac{M_{11}}{|M|} = \frac{\psi_0^{(4)}}{\psi_0\psi_0^{(4)} - \psi_0''^2} > \frac{1}{\psi_0}$$

so that when I is large and positive

$$e^{-M_{11}I^2/2|M|} \ll e^{-I^2/2\psi_0}$$

Also, in these circumstances the 1 + erf is nearly equal to two. Thus retaining only the important terms and using the definitions of the M's gives the approximation to (3.6–5):

$$\frac{dI\,dt}{2\pi\psi_0}\left[\frac{-\psi_0''}{\psi_0}\right]^{1/2} Ie^{-I^2/2\psi_0} \tag{3.6–10}$$

From this it follows that the expected number of maxima per second lying above the line $I = I_1$ is approximately[33] when I_1 is large,

$$\frac{1}{2\pi}\left[\frac{-\psi_0''}{\psi_0}\right]^{1/2} e^{-I_1^2/2\psi_0} \tag{3.6–11}$$
$$= e^{-I_1^2/2\psi_0} \times \tfrac{1}{2}[\text{the expected number of zeros of } I \text{ per second}]$$

It is interesting to note that the approximation (3.6–11) for the expected number of maxima above I_1 is the same as the exact expression (3.3–14) for the expected number of times I will pass through I_1 with positive slope.

3.7 Results on the Envelope of the Noise Current

The noise current flowing in the output of a relatively narrow band pass filter has the character of a sine wave of, roughly, the midband frequency whose amplitude fluctuates irregularly, the rapidity of fluctuation being of the order of the band width. Here we study the fluctuations of the envelope of such a wave.

First we define the envelope. Let f_m be a representative midband frequency. Then if

$$\omega_m = 2\pi f_m \tag{3.7–1}$$

the noise current may be represented, see (2.8–6), by

$$\begin{aligned} I &= \sum_{n=1}^{N} c_n \cos(\omega_n t - \omega_m t - \varphi_n + \omega_m t) \\ &= I_c \cos \omega_m t - I_s \sin \omega_m t \end{aligned} \tag{3.7–2}$$

where the components I_c and I_s are

$$\begin{aligned} I_c &= \sum_{n=1}^{N} c_n \cos(\omega_n t - \omega_m t - \varphi_n) \\ I_s &= \sum_{n=1}^{N} c_n \sin(\omega_n t - \omega_m t - \varphi_n) \end{aligned} \tag{3.7–3}$$

[33] This expression agrees with an estimate made by V. D. Landon, *Proc. I. R. E.*, 29 (1941), 50–55. He discusses the number of crests exceeding four times the r.m.s. value of I. This corresponds to $I_1^2 = 16\psi_0$.

The envelope, R, is a function of t defined by

$$R = [I_c^2 + I_s^2]^{1/2} \tag{3.7-4}$$

It follows from the central limit theorem and the definitions (3.7–3) of I_c and I_s that these are two normally distributed random variables. They are independent since $\overline{I_c I_s} = 0$. They both have the same standard deviation, namely the square root of

$$\overline{I_c^2} = \overline{I_s^2} = \overline{I^2} = \int_0^\infty w(f)\, df = \psi_0 \tag{3.7-5}$$

Consequently, the probability that the point (I_c, I_s) lies within the elementary rectangle $dI_c dI_s$ is

$$\frac{dI_c\, dI_s}{2\pi\psi_0} \exp\left[-\frac{I_c^2 + I_s^2}{2\psi_0}\right] \tag{3.7-6}$$

In much of the following work it is convenient to introduce another random variable θ where

$$\begin{aligned} I_c &= R\cos\theta \\ I_s &= R\sin\theta \end{aligned} \tag{3.7-7}$$

Since I_c and I_s are random variables so are R and θ. The differentials are related by

$$dI_c dI_s = R d\theta dR \tag{3.7-8}$$

and the distribution function for R and θ is obtainable from (3.7–6) when the change of variables is made:

$$\frac{d\theta}{2\pi}\,\frac{R\,dR}{\psi_0}\, e^{-R^2/2\psi_0} \tag{3.7-9}$$

Since this may be expressed as a product of terms involving R only and θ only, R and θ are independent random variables, θ being uniformly distributed over the range 0 to 2π and R having the probability density[34]

$$\frac{R}{\psi_0}\, e^{-R^2/2\psi_0} \tag{3.7-10}$$

Expression (3.7–10) gives the probability density for the value of the envelope. Like the normal law for the instantaneous value of I, it depends only upon the average total power

$$\psi_0 = \int_0^\infty w(f)\, df$$

[34] See V. D. Landon and K. A. Norton, *I.R.E. Proc.*, 30 (1942), 425–429.

We now study the correlation between R at time t and its value at some later time $t + \tau$. Let the subscripts 1 and 2 refer to the times t and $t + \tau$, respectively. Then from (3.7–3) and the central limit theorem it follows that the four random variables I_{c1}, I_{s1}, I_{c2}, I_{s2} have a four dimensional normal distribution. This distribution is determined by the second moments

$$\overline{I_{c1}^2} = \overline{I_{s1}^2} = \overline{I_{c2}^2} = \overline{I_{s2}^2} = \psi_0 = \mu_{11}$$

$$\overline{I_{c1} I_{s1}} = \overline{I_{c2} I_{s2}} = 0$$

$$\overline{I_{c1} I_{c2}} = \overline{I_{s1} I_{s2}} = \frac{1}{2} \sum_{n=1}^{N} c_n^2 \cos (\omega_n \tau - \omega_m \tau)$$

$$\rightarrow \int_0^\infty w(f) \cos 2\pi (f - f_m)\tau \, df = \mu_{13} \tag{3.7–11}$$

$$\overline{I_{c1} I_{s2}} = -\overline{I_{c2} I_{s1}} = \frac{1}{2} \sum_{n=1}^{N} c_n^2 \sin (\omega_n \tau - \omega_m \tau)$$

$$\rightarrow \int_0^\infty w(f) \sin 2\pi (f - f_m)\tau \, df = \mu_{14}$$

The moment matrix for the variables in the order I_{c1}, I_{s1}, I_{c2}, I_{s2} is

$$M = \begin{bmatrix} \psi_0 & 0 & \mu_{13} & \mu_{14} \\ 0 & \psi_0 & -\mu_{14} & \mu_{13} \\ \mu_{13} & -\mu_{14} & \psi_0 & 0 \\ \mu_{14} & \mu_{13} & 0 & \psi_0 \end{bmatrix}.$$

and from this it follows that the cofactors of the determinant $| M |$ are

$$\begin{aligned} M_{11} = M_{22} = M_{33} = M_{44} &= \psi_0(\psi_0^2 - \mu_{13}^2 - \mu_{14}^2) \\ &= \psi_0 A, \qquad A = \psi_0^2 - \mu_{13}^2 - \mu_{14}^2 \\ M_{12} = \quad M_{34} &= 0 \\ M_{13} = \quad M_{24} &= -\mu_{13} A \\ M_{14} = -M_{23} &= -\mu_{14} A \\ | M | &= A^2 \end{aligned} \tag{3.7–12}$$

The probability density of the four random variables is therefore

$$\frac{1}{4\pi^2 A} \exp - \frac{1}{2A} [\psi_0(I_1^2 + I_2^2 + I_3^2 + I_4^2)$$

$$- 2\mu_{13}(I_1 I_3 + I_2 I_4) - 2\mu_{14}(I_1 I_4 - I_2 I_3)]$$

where we have written I_1, I_2, I_3, I_4 for I_{c1}, I_{s1}, I_{c2}, I_{s2}. We now make the transformation

$$I_1 = R_1 \cos \theta_1 \qquad I_3 = R_2 \cos \theta_2$$

$$I_2 = R_1 \sin \theta_1 \qquad I_4 = R_2 \sin \theta_2$$

and average the resulting probability density over θ_1 and θ_2 in order to get the probability that R_1 and R_2 lie in dR_1 and dR_2. It is

$$\frac{R_1 R_2 \, dR_1 \, dR_2}{4\pi^2 A} \int_0^{2\pi} d\theta_1 \int_0^{2\pi} d\theta_2 \exp$$

$$- \frac{1}{2A} [\psi_0 R_1^2 + \psi_0 R_2^2 - 2\mu_{13} R_1 R_2 \cos (\theta_2 - \theta_1) - 2\mu_{14} R_1 R_2 \sin (\theta_2 - \theta_1)]$$

Since the integrand is a periodic function of θ_2 we may integrate from $\theta_2 = \theta_1$ to $\theta_2 = \theta_1 + 2\pi$ instead of from 0 to 2π. This integration gives the Bessel function, I_0, of the first kind with imaginary argument. The resulting probability density for R_1 and R_2 is

$$\frac{R_1 R_2}{A} I_0 \left(\frac{R_1 R_2}{A} [\mu_{13}^2 + \mu_{14}^2]^{1/2} \right) \exp - \frac{\psi_0}{2A} (R_1^2 + R_2^2) \qquad (3.7\text{–}13)$$

where, from (3.7–12),

$$A = \psi_0^2 - \mu_{13}^2 - \mu_{14}^2$$

μ_{13} and μ_{14} are given by (3.7–11). Of course, R_1 and R_2 are always positive.

For an ideal band pass filter with cut-offs at f_a and f_b we set

$$f_m = \frac{f_b + f_a}{2}, \qquad w(f) = w_0 \quad \text{for} \quad f_a < f < f_b$$

and obtain

$$\psi_0 = w_0 (f_b - f_a)$$

$$\mu_{13} = \int_{f_a}^{f_b} w_0 \cos 2\pi (f - f_m)\tau \, df = \frac{w_0 \sin \pi (f_b - f_a)\tau}{\pi \tau}$$

$$\mu_{14} = \int_{f_a}^{f_b} w_0 \sin 2\pi (f - f_m)\tau \, df = 0$$

The I_0 term in (3.7–13), which furnishes the correlation between R_1 and R_2, becomes

$$I_0 \left(\frac{R_1 R_2}{\psi_0} \frac{\frac{\sin x}{x}}{1 - \frac{\sin^2 x}{x^2}} \right)$$

where x is $\pi(f_b - f_a)\tau$. When x is a multiple of π, R_1 and R_2 are independent random variables. When x is zero R_1 and R_2 are equal. Hence we may say, roughly, that the period of fluctuation of R is the time it takes x to increase from 0 to π or $(f_b - f_a)^{-1}$. This is related to the result given in the next section, namely that the expected number of maxima of the envelope is .641 $(f_b - f_a)$ per second.

3.8 Maxima of R

Here we wish to study the distribution of the maxima of R.* Our work is based upon the expression, cf. (3.6–1),

$$-dR\,dt \int_{-\infty}^{0} p(R, 0, R'')R''\,dR'' \tag{3.8–1}$$

for the probability that a maximum of R falls within the elementary rectangle $dR\,dt$. $p(R, R', R'')$ is the probability density for the three dimensional distribution of R, R', R'' where the primes denote differentiation with respect to t.

We shall determine $p(R, R', R'')$ from the probability density of I_c, I_s', I_c'', I_s, I_c', I_s'', which we shall denote by $x_1, x_2, \cdots x_6$. The interchange of I_s' and I_c' is suggested by the later work. It is convenient to introduce the notation

$$\begin{aligned} b_n &= (2\pi)^n \int_0^\infty w(f)(f - f_m)^n\,df \\ b_0 &= \psi_0 \end{aligned} \tag{3.8–2}$$

where f_m is the mid-band frequency, i.e., the frequency chosen in the definition of the envelope R. b_n is seen to be analogous to the derivatives of $\psi(\tau)$ at $\tau = 0$.

From the definitions (3.7–3) of I_c and I_s we obtain the second moments

$$\begin{aligned} \overline{x_1^2} &= \overline{I_c^2} = \psi_0 = b_0 \\ \overline{x_4^2} &= \overline{I_s^2} = b_0 \\ \overline{x_2^2} &= \overline{I_s'^2} = \sum_1^N w(f_n)\Delta f 4\pi^2(f_n - f_m)^2 = b_2 \\ \overline{x_5^2} &= \overline{I_c'^2} = b_2 \\ \overline{x_3^2} &= \overline{I_c''^2} = b_4 \\ \overline{x_6^2} &= \overline{I_s''^2} = b_4 \end{aligned}$$

* Incidentally, most of the analysis of this section was originally developed in a study of the stability of repeaters in a loaded telephone transmission line. The envelope, R, was associated with the "returned current" produced by reflections from line irregularities. However, the study fell short of its object and the only results which seemed worth salvaging at the time were given in reference[25] cited in Section 3.3.

$$\overline{x_1 x_2} = \overline{I_c I_s'} = \sum_1^N w(f_n)\Delta f 2\pi(f_n - f_m) = b_1$$

$$\overline{x_4 x_5} = \overline{I_s I_c'} = -b_1$$

$$\overline{x_1 x_3} = \overline{I_c I_c''} = -\sum_1^N w(f)\Delta f 4\pi^2(f_n - f_m)^2 = -b_2$$

$$\overline{x_4 x_6} = \overline{I_s I_s''} = -b_2$$

$$\overline{x_2 x_3} = \overline{I_s' I_c''} = -b_3$$

$$\overline{x_5 x_6} = \overline{I_c' I_s''} = b_3$$

All of the other second moments are zero. The moment matrix M is thus

$$M = \begin{bmatrix} b_0 & b_1 & -b_2 & 0 & 0 & 0 \\ b_1 & b_2 & -b_3 & 0 & 0 & 0 \\ -b_2 & -b_3 & b_4 & 0 & 0 & 0 \\ 0 & 0 & 0 & b_0 & -b_1 & -b_2 \\ 0 & 0 & 0 & -b_1 & b_2 & b_3 \\ 0 & 0 & 0 & -b_2 & b_3 & b_4 \end{bmatrix}$$

The adjoint matrix is

$$\begin{bmatrix} B_0 & B_1 & -B_2 & 0 & 0 & 0 \\ B_1 & B_{22} & -B_3 & 0 & 0 & 0 \\ -B_2 & -B_3 & B_4 & 0 & 0 & 0 \\ 0 & 0 & 0 & B_0 & -B_1 & -B_2 \\ 0 & 0 & 0 & -B_1 & B_{22} & B_3 \\ 0 & 0 & 0 & -B_2 & B_3 & B_4 \end{bmatrix}$$

$$B_0 = (b_2 b_4 - b_3^2)B \qquad B_{22} = (b_0 b_4 - b_2^2)B$$

$$B_1 = -(b_1 b_4 - b_2 b_3)B \qquad B_3 = -(b_0 b_3 - b_1 b_2)B$$

$$B_2 = (b_1 b_3 - b_2^2)B \qquad B_4 = (b_0 b_2 - b_1^2)B \qquad (3.8\text{–}3)$$

$$B = b_0 b_2 b_4 + 2\, b_1 b_2 b_3 - b_2^3 - b_0 b_3^2 - b_4 b_1^2$$

$$|M| = B^2$$

where B is the determinant of the third order matrices in the upper left and lower right corners of M.

As in the earlier work, the distribution of $x_1, \cdots, x_6$ is normal in six dimensions. The exponent is $-[2\,|\,M\,|\,]^{-1}$ times

$$B_0(x_1^2 + x_4^2) + 2B_1(x_1 x_2 - x_4 x_5) - 2B_2(x_1 x_3 + x_4 x_6) + B_{22}(x_2^2 + x_5^2) - 2B_3(x_2 x_3 - x_5 x_6) + B_4(x_3^2 + x_6^2) \qquad (3.8\text{–}4)$$

In line with the earlier work we set

$$x_1 = I_c = R\cos\theta \qquad x_4 = I_s = R\sin\theta$$

$$x_2 = I_s' = R'\sin\theta + R\cos\theta\theta'$$

$$x_5 = I_c' = R'\cos\theta - R\sin\theta\theta'$$

$$x_3 = I_c'' = R''\cos\theta - 2R'\sin\theta\theta' - R\cos\theta\theta'^2 - R\sin\theta\theta''$$

$$x_6 = I_s'' = R''\sin\theta + 2R'\cos\theta\theta' - R\sin\theta\theta'^2 + R\cos\theta\theta''$$

The angle θ varies from 0 to 2π and θ' and θ'' vary from $-\infty$ to $+\infty$. By forming the Jacobian it may be shown that

$$dx_1\,dx_2\cdots dx_6 = R^3\,dR\,dR'\,dR''\,d\theta\,d\theta'\,d\theta''$$

Also, the quantities in (3.8–4) are

$$x_1^2 + x_4^2 = R^2 \qquad x_1x_3 + x_4x_6 = RR'' - R^2\theta'^2$$

$$x_1x_2 - x_4x_5 = R^2\theta' \qquad x_2^2 + x_5^2 = R'^2 + R^2\theta'^2$$

$$x_2x_3 - x_5x_6 = RR''\theta' - 2R'^2\theta' - R'R\theta'' - R^2\theta'^3$$

$$x_3^2 + x_6^2 = R''^2 - 2RR''\theta'^2 + 4R'^2\theta'^2 + 4RR'\theta'\theta'' + R^2\theta'^4 + R^2\theta''^2$$

The expression for $p(R, 0, R'')$ is obtained when we set these values of the x's in (3.8–4) and integrate the resulting probability density over the ranges of θ, θ', θ'':

$$p(R, 0, R'') = \frac{R^3}{8\pi^3 B}\int_0^{2\pi} d\theta \int_{-\infty}^{+\infty} d\theta' \int_{-\infty}^{+\infty} d\theta'' \qquad (3.8\text{–}5)$$

$$\exp -\frac{1}{2B^2}[B_0R^2 + 2B_1R^2\theta' - 2B_2(RR'' - R^2\theta'^2) + B_{22}R^2\theta'^2 - 2B_3R\theta'(R'' - R\theta'^2) + B_4(R''^2 - 2RR''\theta'^2 + R^2\theta'^4 + R^2\theta''^2)]$$

The integrations with respect to θ and θ'' may be performed at once leaving $p(R, 0, R'')$ expressed as a single integral which, unfortunately, appears to be difficult to handle. For this reason we assume that $w(f)$ is symmetrical about the mid-band frequency f_m. From (3.8–2), b_1 and b_3 are zero and from (3.8–3), B_1 and B_3 are zero.

With this assumption (3.8–5) yields

$$p(R, 0, R'') = R^2(2\pi)^{-3/2} B_4^{-1/2} \int_{-\infty}^{+\infty} d\theta' \tag{3.8–6}$$

$$\exp -\frac{1}{2B^2}[B_0 R^2 + R([B_{22} + 2B_2]R\theta'^2 - 2B_2 R'') + B_4(R'' - R\theta'^2)^2]$$

The probability that a maximum occurs in the elementary rectangle $dR\ dt$ is, from (3.8–1), $p(t, R)\ dR\ dt$ where

$$p(t, R) = -\int_{-\infty}^{0} p(R, 0, R'')R''\ dR'' \tag{3.8–7}$$

We put (3.8–6) in this expression and make the following change of variables.

$$\begin{aligned} x &= \frac{B_4^{1/2}}{\sqrt{2}\,B} R\theta'^2, \qquad y = -\frac{B_4^{1/2}}{\sqrt{2}\,B} R'' \\ z &= -\frac{B_2}{\sqrt{2B_4}\,B} R = \frac{b_2^2}{\sqrt{2B_4}} R \\ b &= -\frac{(B_{22} + 2B_2)}{2B\,b_2^2} = \left[\frac{3}{2} - \frac{b_0 b_4}{2b_2^2}\right] = \tfrac{1}{2}(3 - a^2) \\ a^2 &= \frac{B_0}{2B^2}\frac{2B_4}{b_2^4} = \frac{b_0 b_4}{b_2^2} \end{aligned} \tag{3.8–8}$$

where we have used the expressions for the B's obtained by setting b_1 and b_3 to zero in (3.8–3). Thus

$$p(t, R) = \frac{4}{b_0 b_2^4}\left(\frac{Bz}{2\pi}\right)^{3/2} \int_0^\infty y\,dy \int_0^\infty x^{-1/2}\,dx \tag{3.8–9}$$

$$\exp\left[-a^2 z^2 + 2bzx + 2zy - (x + y)^2\right]$$

As was to be expected, this expression shows that $p(t, R)$ is independent of t.

A series for $p(t, R)$ may be obtained by expanding $\exp 2z(y + bx)$ and then integrating termwise. We use

$$\int_0^\infty dy \int_0^\infty dx\, x^\mu y^\gamma e^{-(x+y)^2} = \frac{\sqrt{\pi}}{2^{\mu+\gamma+2}} \frac{\Gamma(\gamma + 1)\Gamma(\mu + 1)}{\Gamma\left(\frac{\mu + \gamma + 3}{2}\right)}$$

which may be evaluated by setting

$$x = \rho^2 \cos^2 \varphi, \qquad y = \rho^2 \sin^2 \varphi$$

The double integral in (3.8–9) becomes

$$e^{-a^2z^2}\sqrt{\frac{\pi}{2}}\sum_{n=0}^{\infty}\frac{(2z)^n}{n!}\sum_{m=0}^{n}\frac{n!\,b^m}{m!\,(n-m)!}\frac{\Gamma(m+\frac{1}{2})\Gamma(n-m+2)}{2^{n+2}\Gamma\left(\frac{n}{2}+\frac{7}{4}\right)}$$

$$=\pi 2^{-5/2}\sum_{n=0}^{\infty}\frac{z^n e^{-a^2z^2}}{\Gamma\left(\frac{n}{2}+\frac{7}{4}\right)}A_n$$

where $A_0 = 1$ and

$$A_n=\sum_{m=0}^{n}\frac{(\frac{1}{2})(\frac{3}{2})\cdots(m-\frac{1}{2})}{m!}(n-m+1)b^m, \qquad 0<n \tag{3.8–10}$$

$$A_n \sim (n+1)(1-b)^{-1/2}-\frac{b}{2}\,(1-b)^{-3/2}, \qquad n \text{ large}$$

The term corresponding to $m = 0$ in (3.8–10) is $n + 1$.

We thus obtain

$$p(t,R)=\frac{e^{-a^2z^2}}{4b_0b_2^{\frac{1}{2}}}\frac{(Bz)^{3/2}}{\sqrt{\pi}}\sum_{n=0}^{\infty}\frac{z^n}{\Gamma\left(\frac{n}{2}+\frac{7}{4}\right)}A_n$$

$$=\frac{e^{-a^2z^2}}{4\sqrt{\pi}}\frac{b_2^{1/2}}{b_0}(a^2-1)^{3/2}z^{3/2}\sum_{n=0}^{\infty}\frac{z^nA_n}{\Gamma\left(\frac{n}{2}+\frac{7}{4}\right)} \tag{3.8–11}$$

We are interested in the expected number, N, of maxima per second. From the similar work for I, it follows that N is the coefficient of dt when (3.8–1) is integrated with respect to R from 0 to ∞. Thus from (3.8–7) and

$$dR=\sqrt{2B_4}\,b_2^{-2}\,dz=(2b_0B)^{1/2}b_2^{-3/2}\,dz$$

$$=[2b_0(a^2-1)]^{1/2}\,dz$$

we find

$$N=\int_0^{\infty}p(t,R)\,dR$$

$$=\frac{(a^2-1)^{\frac{5}{2}}}{(2a)^{5/2}}\left(\frac{b_2}{\pi b_0}\right)^{1/2}\sum_{n=0}^{\infty}\frac{\Gamma\left(\frac{n}{2}+\frac{5}{4}\right)}{\Gamma\left(\frac{n}{2}+\frac{7}{4}\right)}\frac{A_n}{a^n} \tag{3.8–12}$$

Equations (3.8–11) and (3.8–12) have been derived on the assumption that $w(f)$ is symmetrical about f_m, i.e. the band pass filter attenuation is

symmetrical about the mid-band frequency. We now go a step further and assume an ideal band pass filter:

$$\begin{aligned} w(f) &= w_0 \qquad f_a < f < f_b \\ w(f) &= 0 \qquad \text{otherwise} \\ 2f_m &= f_a + f_b \end{aligned} \tag{3.8–13}$$

Putting these in (3.8–2) we obtain zero for b_1 and b_3 and also

$$\begin{aligned} b_0 &= w_0(f_b - f_a) = \psi_0 \\ b_2 &= \frac{\pi^2 w_0}{3}(f_b - f_a)^3 \\ b_4 &= \frac{\pi^4 w_0}{5}(f_b - f_a)^5 \\ a^2 &= \tfrac{9}{5} \\ b &= \tfrac{1}{2}(3 - a^2) = \tfrac{3}{5} \\ R &= [2b_0(a^2 - 1)]^{1/2} z = [\tfrac{8}{5}\psi_0]^{1/2} z \\ \left(\frac{b_2}{\pi b_0}\right)^{1/2} &= \left[\frac{\pi}{3}\right]^{1/2}(f_b - f_a), \qquad a^2 z^2 = \frac{9R^2}{8\psi_0} \end{aligned} \tag{3.8–14}$$

n	A_n	n	A_n
0	1	4	6.775
1	2.3	5	8.333
2	3.735	6	9.9002
3	5.238	7	11.4736

$A_n \sim 1.5811\, n + .3953$

From (3.8–12) we find that the expected number of maxima per second of the envelope is

$$N = .64110\,(f_b - f_a) \tag{3.8–15}$$

assuming an ideal band pass filter.

The distribution of the maxima of R for an ideal band pass filter may be obtained by placing the results of (3.8–14) in (3.8–11). This gives

$$p(t, R)\, dR = \frac{dR}{\psi_0^{1/2}} \frac{(f_b - f_a)}{4} \sqrt{\frac{\pi}{3}} \left(\frac{4z}{5}\right)^{3/2} e^{-a^2 z^2} \sum_{n=0}^{\infty} \frac{z^n A_n}{\Gamma\left(\frac{n}{2} + \frac{7}{4}\right)}$$

It is convenient to define y as the ratio

$$y = \frac{R}{\text{r.m.s. } I(t)} = \frac{R}{\psi_0^{1/2}} = \left(\frac{\pi}{2}\right)^{1/2} z$$

where R is understood to correspond to a maximum of the envelope. Since the value of R corresponding to a maximum of the envelope selected at random is a random variable, y is also a random variable. Its probability density is $p_R(y)$, where

$$p_R(y)\, dy = \frac{p(t, R)\, dR}{0.64110(f_b - f_a)}$$

$p_R(y)$ has been computed and is plotted as a function of y in Fig. 3.

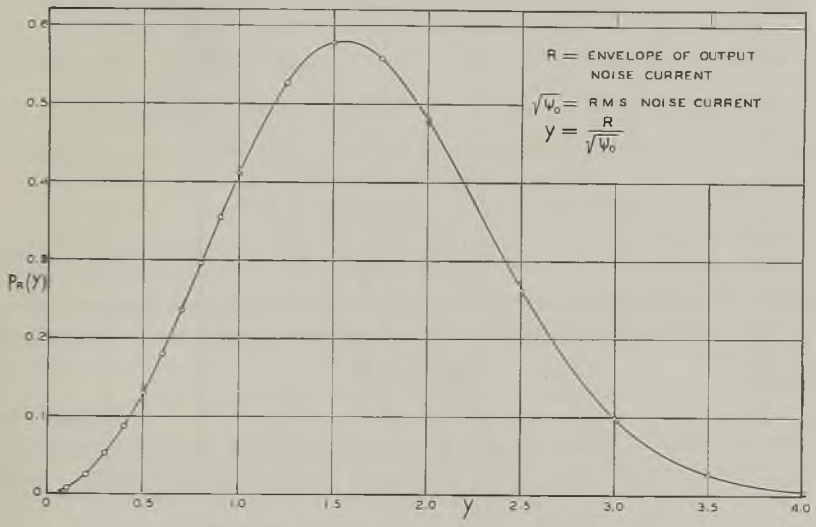

Fig. 3—Distribution of maxima of envelope of noise current. Noise through ideal band-pass filter.

$\frac{p_R(y)}{\sqrt{\psi_0}}\, dR$ = probability that a maximum of R selected at random lies between R and $R + dR$.

The distribution function $P(R_{\max} < y\sqrt{\psi_0})$ defined by

$$P(R_{\max} < y\sqrt{\psi_0}) = \int_0^y p_R(y)\, dy$$

and which gives the probability that a maximum of the envelope selected at random is less than a specified value $y\sqrt{\psi_0} = R$, is plotted in Fig. 4 together with other curves of the same nature.

When y is large, say greater than 2.5,

$$\psi_R(y) \sim \frac{\sqrt{\frac{\pi}{6}}}{.64110}(y^2 - 1)e^{-y^2/2}$$

$$P(R_{\max} < y\sqrt{\psi_0}) \sim 1 - \frac{\sqrt{\frac{\pi}{6}}}{.64110} ye^{-y^2/2}$$

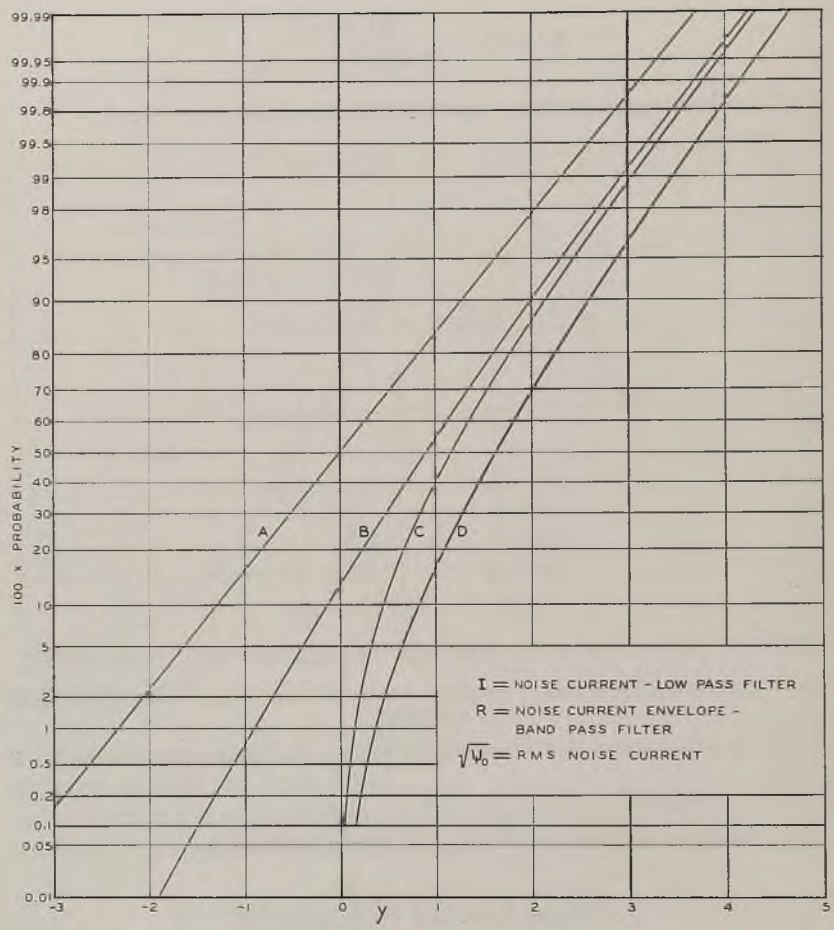

Fig. 4—Distribution of maxima

$A = P(I < y\sqrt{\psi_0})$ = probability of I being less than $y\sqrt{\psi_0}$. Similarly $C = P(R < y\sqrt{\psi_0})$.

$B = P(I \max < y\sqrt{\psi_0})$ = probability of random maximum of I being less than $y\sqrt{\psi_0}$. Similarly $D = P(R \max < y\sqrt{\psi_0})$.

The asymptotic expression for $p_R(y)$ may be obtained from the integral (3.8–9) for $p(t, R)$. Indeed, replacing the variables of integration x, y in (3.8–9) by

$$x' = x$$

$$y' = x + y,$$

integrating a portion of the y' integral by parts, and assuming $b < 1$ ($a^2 \geq 1$, by Schwarz's inequality, so that $b \leq 1$ always) leads to

$$p(t, R) \sim \left(\frac{b_2}{2\pi}\right)^{\frac{1}{2}} \frac{e^{-R^2/2\psi_0}}{\psi_0} \left(\frac{R^2}{\psi_0} - 1\right)$$

when R is large.

If, instead of an ideal band pass filter, we assume that $w(f)$ is given by

$$w(f) = \frac{1}{\sigma\sqrt{2\pi}} e^{-(f-f_m)^2/2\sigma^2}, \qquad f_m \gg \sigma \tag{3.8–16}$$

we find that

$$b_0 = 1$$

$$b_2 = 4\pi^2\sigma^2$$

$$b_4 = 16\pi^4 \cdot 3\sigma^4$$

$$a^2 = 3, b = 0$$

$$A_n = (n + 1)$$

Some rough work indicates that the sum of the series in (3.8–12) is near 3.97. This gives the expected number of maxima of the envelope as

$$N = 2.52\sigma \tag{3.8–17}$$

per second.

The pass band is determined by σ. It appears difficult to compare this with an ideal band pass filter. If we use the fact that the filter given by

$$w(f) = w_0 \exp\left[-\pi\left(\frac{f - f_m}{f_b - f_a}\right)^2\right]$$

passes the same average amount of power as does an ideal band pass filter whose pass band is $f_b - f_a$, we have

$$f_b - f_a = \sigma\sqrt{2\pi}$$

and the expression for N becomes 1.006 $(f_b - f_a)$.

3.9 Energy Fluctuation

Some information regarding the statistical behavior of the random variable

$$E = \int_{t_1}^{t_1+T} I^2(t)\, dt \tag{3.9–1}$$

where $I(t)$ is a noise current and t_1 is chosen at random, has been given in a recent article.[35] Here we study this behavior from a somewhat different point of view.

If we agree to use the representations (2.8-1) or (2.8–6) we may write, as in the paper, the random variable E as

$$E = \int_{-T/2}^{T/2} I^2(t)\, dt \tag{3.9–2}$$

where the randomness on the right is due either to the a_n's and b_n's if (2.8–1) is used or to the φ_n's if (2.8–6) is used.

The average value of E is m_T where, from (3.1–2),

$$\begin{aligned} \bar{E} = m_T &= \int_{-T/2}^{T/2} \overline{I^2(t)}\, dt = \int_{-T/2}^{T/2} \psi(0)\, dt = T\psi_0 \\ &= T\int_0^\infty w(f)\, df \end{aligned} \tag{3.9–3}$$

The second moment of E is

$$\overline{E^2} = \int_{-T/2}^{T/2} dt_1 \int_{-T/2}^{T/2} dt_2\, \overline{I^2(t_1) I^2(t_2)} \tag{3.9–4}$$

If, for the time being, we set t_2 equal to $t_1 + \tau$, it is seen from section 3.2 that we have an expression for the probability density of $I(t_1)$ and $I(t_1 + \tau)$ and hence we may obtain the required average:

$$\begin{aligned} \overline{I_1^2 I_2^2} = \frac{1}{2\pi A} \int_{-\infty}^{+\infty} dI_1 \int_{-\infty}^{+\infty} dI_2\, I_1^2 I_2^2 \exp \\ \left(-\frac{1}{2A^2}\left(\psi_0 I_1^2 + \psi_0 I_2^2 - 2\psi_\tau I_1 I_2\right)\right) \end{aligned} \tag{3.9–5}$$

$$A^2 = \psi_0^2 - \psi_\tau^2, \quad I_1 = I(t_1), \quad I_2 = I(t_1 + \tau) = I(t_2)$$

The integral may be evaluated by (3.5–6) when we set

$$\begin{aligned} I_1 &= Ax\sqrt{\frac{2}{\psi_0}}, \qquad I_2 = Ay\sqrt{\frac{2}{\psi_0}} \\ \psi_\tau &= -\psi_0 \cos\varphi \\ A &= \psi_0 \sin\varphi \end{aligned} \tag{3.9–6}$$

[35] "Filtered Thermal Noise—Fluctuation of Energy as a Function of Interval Length", *Jour. Acous. Soc. Am.*, 14 (1943), 216–227.

Thus

$$\begin{aligned}\overline{I_1^2 I_2^2} &= \psi_0^2(1 + 2\cos^2\varphi) \\ &= \psi_0^2 + 2\psi_\tau^2\end{aligned} \tag{3.9-7}$$

Incidentally, this gives an expression for the correlation function of $I^2(t)$. Replacing τ by its value of $t_2 - t_1$ and returning to (3.9–4),

$$\overline{E^2} = T^2\psi_0^2 + 2\int_{-T/2}^{T/2} dt_1 \int_{-T/2}^{T/2} dt_2 \psi^2(t_2 - t_1) \tag{3.9-8}$$

When we introduce σ_T, the standard deviation of E, and use

$$\sigma_T^2 = \overline{E^2} - m_T^2$$

we obtain

$$\begin{aligned}\sigma_T^2 = \overline{(E - \overline{E})^2} &= 2\int_{-T/2}^{T/2} dt_1 \int_{-T/2}^{T/2} dt_2 \psi^2(t_2 - t_1) \\ &= 4\int_0^T (T - x)\psi^2(x)\, dx\end{aligned}$$

where the second line may be obtained from the first either by changing the variables of integration, as in (3.9–27), or by the method used below in dealing with $\overline{E^3}$. I am indebted to Prof. Kac for pointing out the advantage obtained by reducing the double integral to a single integral. It should be noted that the limits of integration $-T/2$, $T/2$ in the double integral may be replaced by 0, T by making the change of variable $t = t' - T/2$ for both t_1 and t_2.

When we use

$$\psi(\tau) = \int_0^\infty w(f) \cos 2\pi f\tau\, df \tag{2.1-6}$$

we obtain the result stated in the paper, namely,

$$\begin{aligned}\sigma_T^2 = \int_0^\infty w(f_1)\, df_1 \int_0^\infty w(f_2)\, df_2 \Bigg[&\frac{\sin^2 \pi(f_1 + f_2)T}{\pi^2(f_1 + f_2)^2} \\ &+ \frac{\sin^2 \pi(f_1 - f_2)T}{\pi^2(f_1 - f_2)^2}\Bigg]\end{aligned} \tag{3.9-9}$$

If this formula is applied to a relatively narrow band-pass filter and if $T(f_b - f_a) >> 1$ the contribution of the $f_1 + f_2$ term may be neglected and we have the approximation

$$\begin{aligned}\sigma_T^2 &= \int_{f_a}^{f_b} w_0\, df_1 \int_{-\infty}^{+\infty} w_0\, df_2 \frac{\sin^2 \pi(f_1 - f_2)T}{\pi^2(f_1 - f_2)^2} \\ &= w_0^2 T(f_b - f_a) \\ &= w_0 m_T\end{aligned} \tag{3.9-10}$$

where, from (3.9–3)

$$m_T = w_0 T(f_b - f_a) \tag{3.9–11}$$

The third moment $\overline{E^3}$ may be computed in the same way. However, in this case it pays to introduce the characteristic function for the distribution of $I(t_1)$, $I(t_2)$, $I(t_3)$. Since this distribution is normal its characteristic function is

$$\begin{aligned}\text{Average exp } [iz_1 I_1 + iz_2 I_2 + iz_3 I_3] \\ = \exp -\Big[\frac{\psi_0}{2}(z_1^2 + z_2^2 + z_3^2) + \psi(t_2 - t_1) z_1 z_2 \\ + \psi(t_3 - t_1) z_1 z_3 + \psi(t_3 - t_2) z_2 z_3\Big]\end{aligned} \tag{3.9–12}$$

From the definition of the characteristic function it follows that

$$\begin{aligned}\overline{I_1^2 I_2^2 I_3^2} &= -\text{coeff. of } \frac{z_1^2 z_2^2 z_3^2}{2!2!2!} \text{ in ch. f.} \\ &= \psi_0^3 + 2\psi_0(\psi_{21}^2 + \psi_{31}^2 + \psi_{32}^2) \\ &\quad + 8\psi_{21}\psi_{31}\psi_{32}\end{aligned} \tag{3.9–13}$$

where we have written ψ_{21} for $\psi(t_2 - t_1)$, etc. When (3.9–13) is multiplied by $dt_1\, dt_2\, dt_3$, the variables integrated from 0 to T, and the above double integral expression for σ_T^2 used, we find

$$\overline{(E - \bar{E})^3} = 2!2^2 \int_0^T dt_1 \int_0^T dt_2 \int_0^T dt_3 \psi_{21}\psi_{31}\psi_{32}\,.$$

Denoting the triple integral on the right by J and differentiating,

$$\begin{aligned}\frac{dJ}{dT} &= 3\int_0^T dt_1 \int_0^T dt_2 \psi(t_2 - t_1)\psi(T - t_1)\psi(T - t_2) \\ &= 3\int_0^T dx \int_0^T dy \psi(x - y)\psi(x)\psi(y) \\ &= 6\int_0^T dx \int_0^x dy \psi(x - y)\psi(x)\psi(y)\end{aligned}$$

In going from the first line to the second t_1 and t_2 were replaced by $T - x$ and $T - y$, respectively. In going from the second to the third use was made of the relations symbolized by

$$\begin{aligned}\int_0^T dx \int_0^T dy &= \int_0^T dx \int_0^x dy + \int_0^T dx \int_x^T dy \\ &= \int_0^T dx \int_0^x dy + \int_0^T dy \int_0^y dx\end{aligned}$$

and of the fact that the integrand is symmetrical in x and y. Integrating dJ/dT with respect to T from 0 to T_1, using the formula

$$\int_0^{T_1} dT \int_0^T f(x)\,dx = \int_0^{T_1} (T_1 - x)f(x)\,dx,$$

noting that J is zero when T is zero, and dropping the subscript on T_1 finally gives

$$\overline{(E - \bar{E})^3} = 48 \int_0^T dx \int_0^x dy(T - x)\psi(x)\psi(y)\psi(x - y).$$

$\overline{E^4}$ may be treated in a similar way. It is found that

$$\overline{(E - \bar{E})^4} - 3\overline{(E - \bar{E})^2}^2 = 3!2^3 \int_0^T dt_1 \int_0^T dt_2 \int_0^T dt_3 \int_0^T dt_4 \psi_{21}\psi_{31}\psi_{42}\psi_{43}$$

which may be reduced to the sum of two triple integrals. It is interesting to note that the expression on the left is the fourth semi-invariant of the random variable E and gives us a measure of the peakedness of the distribution (kurtosis). Likewise, the second and third moments about the mean are the second and third semi-invariants of E. This suggests that possibly the higher semi-invariants may also be expressed as similar multiple integrals.

So far, in this section, we have been speaking of the statistical constants of E. The determination of an exact expression for the probability density of E, in which T occurs as a parameter, seems to be quite difficult.

When T is very small E is approximately $I^2(t)T$. The probability that E lies in dE is the probability that the current lies in $-I$, $-I - dI$ plus the probability that the current lies in I, $I + dI$:

$$\frac{2dI}{\sqrt{2\pi\psi_0}} \exp -\frac{I^2}{2\psi_0} = (2\pi\psi_0 ET)^{-1/2} \exp -\frac{E}{2\psi_0 T}\,dE \qquad (3.9\text{–}14)$$

where E is positive,

$$I = \left(\frac{E}{T}\right)^{1/2}, \qquad dI = \frac{1}{2}(ET)^{-1/2}\,dE$$

and T is assumed to be so small that $I(t)$ does not change appreciably during an interval of length T.

When T is very large we may divide it into a number of intervals, say n, each of length T/n. Let E_r be the contribution of the r th interval. The energy E for the entire interval is then

$$E = E_1 + E_2 + \cdots + E_n$$

If the sub-intervals are large enough the E_r's are substantially independent random variables. If in addition n is large enough E is distributed nor-

mally, approximately. Hence when T is very large the probability that E lies in dE is

$$\frac{dE}{\sigma_T\sqrt{2\pi}} \exp - \frac{(E - m_T)^2}{2\sigma_T^2} \tag{3.9–15}$$

where

$$\begin{aligned} m_T &= T\int_0^\infty w(f)\, df \\ \sigma_T^2 &= T\int_0^\infty w^2(f)\, df \end{aligned} \tag{3.9–16}$$

the second relation being obtained by letting $T \to \infty$ in (3.9–9). The analogy with Campbell's theorem, section 1.2, is evident. When we deal with a band pass filter we may use (3.9–10) and (3.9–11).

Consider a relatively narrow band pass filter such that we may find a T for which $Tf_a >> 2\pi$ but $T(f_b - f_a) << .64$. Thus several cycles of frequency f_a are contained in T but, from (3.8–15), the envelope does not change appreciably during this interval. Thus throughout this interval $I(t)$ may be considered to be a sine wave of amplitude R. The corresponding value of E is approximately

$$E = T\frac{R^2}{2}$$

where the distribution of the envelope R is given by (3.7–10). From this it follows that the probability of E lying in dE is

$$\frac{dE}{\psi_0 T} \exp - \frac{E}{\psi_0 T} = \frac{dE}{m_T} e^{-E/m_T} \tag{3.9–17}$$

when E is small but not too small.

When we look at (3.9–14) and (3.9–17) we observe that they are of the form

$$\frac{a^{n+1}E^n}{\Gamma(n+1)} e^{-aE}\, dE \tag{3.9–18}$$

Moreover, the normal law (3.9–15), may be obtained from this by letting n become large. This suggests that an approximate expression for the distribution of E is given by (3.9–18) when a and n are selected so as to give the values of m_T and σ_T obtained from (3.9–3) and (3.9–9). This gives

$$a = \frac{m_T}{\sigma_T^2}, \qquad n + 1 = \frac{m_T^2}{\sigma_T^2} \tag{3.9–19}$$

and if we drop the subscript T and substitute the value of a in (3.9–18) we get

$$\frac{\left(\frac{mE}{\sigma^2}\right)^n}{\Gamma(n+1)} \exp\left(-\frac{mE}{\sigma^2}\right) d\left(\frac{mE}{\sigma^2}\right), \qquad n = \frac{m^2}{\sigma^2} - 1 \qquad (3.9\text{–}20)$$

An idea of how this distribution behaves may be obtained from the following table:

n	$T(f_b - f_a)$	$x_{.25}$	$x_{.50}$	$x_{.75}$	$\frac{x_{.25}}{x_{.50}}$	$\frac{x_{.75}}{x_{.50}}$
0	0	.29	.695	1.39	.415	2.00
1	1.45	.96	1.68	2.69	.572	1.60
2	2.4	1.73	2.67	3.94	.647	1.47
3	3.4	2.54	3.67	5.12	.692	1.39
5	5.4	4.22	5.67	7.42	.744	1.31
10	10.5	8.63	10.67	13.02	.808	1.22
24	25	21.47	24.67	28.17	.870	1.14
48	50	44.1	48.7	53.5	.905	1.10

where n is the exponent in (3.9–20). The column $T(f_b - f_a)$ holds only for a narrow band pass filter and was obtained by reading the curve y_A in Fig. 1 of the above mentioned paper. The figures in this column are not very accurate. The next three columns give the points which divide the distribution into four intervals of equal probability:

$$x_{.25} = \frac{mE_{.25}}{\sigma^2}, \quad E_{.25} = \text{energy exceeded } 75\% \text{ of time}$$

$$x_{.50} = \frac{mE_{.50}}{\sigma^2}, \quad E_{.50} = \text{energy exceeded } 50\% \text{ of time}$$

$$x_{.75} = \frac{mE_{.75}}{\sigma^2}, \quad E_{.75} = \text{energy exceeded } 25\% \text{ of time}$$

The values in these columns were obtained from Pearson's table of the incomplete gamma function. The last two columns show how the distribution clusters around the average value as the normal law is approached.

For the larger values of n we expected the normal law (3.9–15) to be approached. Since, for this law the 25, 50, and 75 per cent points are at $m - .675\sigma$, m, and $m + .675\sigma$ we have to a first approximation

$$\begin{aligned} x_{.50} &= \frac{m^2}{\sigma^2} = (n+1) \approx T(f_b - f_a) \\ x_{.25} &= \frac{m}{\sigma^2}(m - .675\sigma) = x_{.50} - .675\sqrt{x_{.50}} \\ x_{.75} &= x_{.50} + .675\sqrt{x_{.50}} \end{aligned} \qquad (3.9\text{–}21)$$

This agrees with the table.

Thiede[36] has studied the mean square value of the fluctuations of the integral

$$A(t) = \int_{-\infty}^{t} I^2(\tau) e^{-\alpha(t-\tau)}\, d\tau \qquad (3.9\text{–}22)$$

The reading of a hot wire ammeter through which a current I is passing is proportional to $A(t)$. α is a constant of the meter. Here we study $A(t)$ by

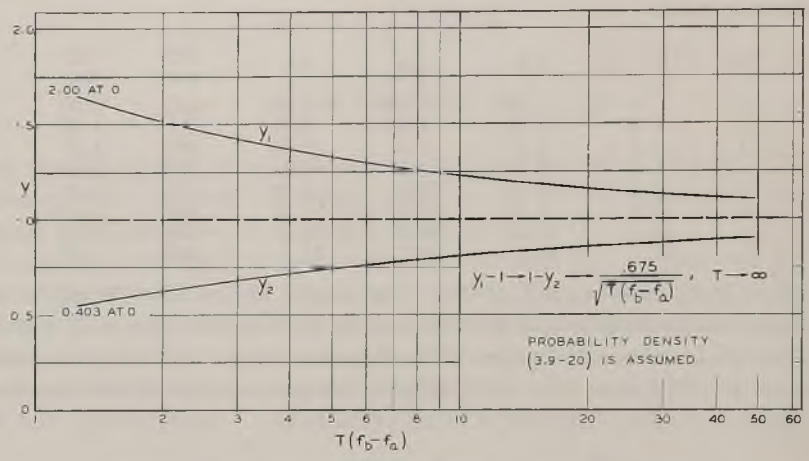

Fig. 5*—Filtered thermal noise—spread of energy fluctuation

$E = \int_{t_1}^{t_1+T} I^2(t)\, dt$, t_1 random, I is noise current.
$y_1 = E_{.75}/E_{.50}$, $y_2 = E_{.25}/E_{.50}$.
$f_b - f_a$ = band width of filter.

first obtaining its correlation function. This method of approach enables us to extend Thiede's results

The distributed portion of the power spectrum of $A(t)$ is given by (3.9–30). When the power spectrum $w(f)$ of $I(t)$ is zero except over the band $f_a < f < f_b$ where it is w_0, the power spectrum of $A(t)$ is

$$\frac{2w_0^2(f_b - f_a - f)}{\alpha^2 + 4\pi^2 f^2} \quad \text{for} \quad 0 < f < f_b - f_a$$

and is zero from $f_b - f_a$ up to $2f_a$. The spectrum from $2f_a$ to $2f_b$ is not zero, and may be obtained from (3.9–34). The mean square fluctuation of $A(t)$ is given, in the general case, by (3.9–28) and (3.9–32). For the band pass case, when $(f_b - f_a)/\alpha$ is large,

$$\text{r.m.s.}\ \frac{A(t) - \bar{A}}{\bar{A}} = \left[\frac{\alpha}{2(f_b - f_a)}\right]^{1/2}$$

[36] *Elec. Nachr. Tek.*, 13 (1936), 84–95. This is an excellent article.
* Note added in proof. The value of y_2 at 0 should be .415 instead of .403.

We start by setting $\tau = t - u$ which transforms the integral for $A(t)$ into

$$A(t) = \int_0^\infty I^2(t - u)e^{-\alpha u}\, du \tag{3.9-23}$$

In order to obtain the correlation function $\Psi(\tau)$ for $A(t)$ we multiply $A(t)$ by $A(t + \tau)$ and average over all the possible currents

$$\begin{aligned}\Psi(\tau) &= \overline{A(t)A(t + \tau)} \\ &= \int_0^\infty e^{-\alpha u}\, du \int_0^\infty e^{-\alpha v}\, dv \text{ ave. } I^2(t - u)I^2(t + \tau - v)\end{aligned}$$

Just as in (3.9–4) the average in the integrand is the correlation function of $I^2(t)$, the argument being $t + \tau - v - t + u = \tau + u - v$. From (3.9–7) it is seen that this is

$$\psi_0^2 + 2\psi^2(\tau + u - v)$$

where $\psi(\tau)$ is the correlation function of $I(t)$. Hence

$$\Psi(\tau) = \frac{\psi_0^2}{\alpha^2} + 2\int_0^\infty du \int_0^\infty dv\, e^{-\alpha u - \alpha v}\psi^2(\tau + u - v) \tag{3.9–24}$$

From the integral (3.9–23) for $A(t)$ it is seen that the average value of $A(t)$ is

$$\bar{A} = \frac{\bar{I}^2}{\alpha} = \frac{\psi_0}{\alpha} \tag{3.9–25}$$

where we have used

$$\psi_0 = \psi(0) = \int_0^\infty w(f)\, df = \bar{I}^2$$

Using this result again, only this time applying it to $A(t)$, gives

$$\begin{aligned}\overline{A^2(t)} &= \Psi(0) \\ &= \bar{A}^2 + 2\int_0^\infty du \int_0^\infty dv\, e^{-\alpha u - \alpha v}\psi^2(u - v)\end{aligned} \tag{3.9–26}$$

The double integrals may be transformed by means of the change of variable $u + v = x$, $u - v = y$. Then (3.9–24) becomes

$$\begin{aligned}\Psi(\tau) &= \bar{A}^2 + \left[\int_0^\infty dy \int_y^\infty dx + \int_{-\infty}^0 dy \int_{-y}^\infty dx\right] e^{-\alpha x}\psi^2(\tau + y) \\ &= \bar{A}^2 + \frac{1}{\alpha}\int_0^\infty e^{-\alpha y}[\psi^2(\tau + y) + \psi^2(\tau - y)]\, dy\end{aligned} \tag{3.9–27}$$

When we make use of the fact that $\psi(y)$ is an even function of y we see, from (3.9–26), that the mean square fluctuation of $A(t)$ is

$$\overline{(A(t) - \bar{A})^2} = \overline{A^2(t)} - \bar{A}^2 = \frac{2}{\alpha}\int_0^\infty e^{-\alpha y}\psi^2(y)\,dy \qquad (3.9\text{–}28)$$

$\Psi(\tau)$ may be expressed in terms of integrals involving the power spectrum $w(f)$ of $I(t)$. The work starts with (3.9–24) and is much the same as in going from (3.9–8) to (3.9–9). The result is

$$\Psi(\tau) = \bar{A}^2 + \int_0^\infty df_1 \int_0^\infty df_2 w(f_1)w(f_2) \left[\frac{\cos 2\pi(f_1 + f_2)\tau}{\alpha^2 + [2\pi(f_1 + f_2)]^2} + \frac{\cos 2\pi(f_1 - f_2)\tau}{\alpha^2 + [2\pi(f_1 - f_2)]^2}\right]$$

It is convenient to define $w(-f)$ for negative frequencies to be equal to $w(f)$. The integration with respect to f_2 may then be taken from $-\infty$ to $+\infty$ and we get

$$\Psi(\tau) = \bar{A}^2 + \int_0^\infty df_1 \int_{-\infty}^{+\infty} df_2 w(f_1)w(f_2) \frac{\cos 2\pi(f_1 - f_2)\tau}{\alpha^2 + [2\pi(f_1 - f_2)]^2} \qquad (3.9\text{–}29)$$

The power spectrum $W(f)$ of $A(t)$ may be obtained by integrating $\Psi(\tau)$:

$$W(f) = 4\int_0^\infty \Psi(\tau)\cos 2\pi f\tau\,d\tau$$

Let us concern ourselves with the fluctuating portion $A(t) - \bar{A}$ of $A(t)$. Its power spectrum $W_c(f)$ is

$$W_c(f) = 4\int_0^\infty (\Psi(\tau) - \bar{A}^2)\cos 2\pi f\tau\,d\tau$$

The integration is simplified by using Fourier's integral formula in the form

$$\int_0^\infty d\tau \int_{-\infty}^{+\infty} df_2 F(f_2)\cos 2\pi(u - f_2)\tau = \tfrac{1}{2}F(u)$$

We get

$$W_c(f) = \frac{1}{\alpha^2 + 4\pi^2 f^2}\int_0^\infty df_1[w(f_1)w(f + f_1) + w(f_1)w(-f + f_1)] = \frac{1}{\alpha^2 + 4\pi^2 f^2}\int_{-\infty}^{+\infty} w(f_1)w(f - f_1)\,df_1 \qquad (3.9\text{–}30)$$

The simplicity of this result suggests that a simpler derivation may be found. If we attempt to use the result

$$w(f) = \operatorname*{Limit}_{T\to\infty} \frac{\overline{2|S(f)|^2}}{T} \qquad (2.5\text{–}3)$$

where $S(f)$ is given by (2.1–2) we find that we need the result

$$\operatorname*{Limit}_{T\to\infty} \frac{2}{T}\int_0^T dt_1 \int_0^T dt_2\, e^{2\pi i f(t_2-t_1)}\, I^2(t_1)I^2(t_2) = \int_{-\infty}^{+\infty} w(f_1)w(f-f_1)\,df_1 \tag{3.9–31}$$

where $f > 0$ and $I(t)$ is a noise current with $w(f)$ as its power spectrum. This may be proved by using (3.9–7) and

$$8\int_0^\infty \psi^2(\tau)\cos 2\pi f\tau\, d\tau = \int_{-\infty}^{+\infty} w(x)w(f-x)\,dx$$

which is given by equation (4C-6) in Appendix 4C.

An expression for the mean square fluctuation of $A(t)$ in terms of $w(f)$ may be obtained by setting τ equal to zero in (3.9–29)

$$\overline{(A(t)-\bar{A})^2} = \Psi(0) - \bar{A}^2 = \int_0^\infty df_1 \int_{-\infty}^{+\infty} df_2 \frac{w(f_1)w(f_2)}{\alpha^2 + 4\pi^2(f_1-f_2)^2} \tag{3.9–32}$$

The same result may be obtained by integrating $W_c(f)$, (3.9–30), from 0 to ∞:

$$\int_0^\infty \frac{df}{\alpha^2+4\pi^2f^2}\int_{-\infty}^{+\infty} df_1 w(f_1)w(f-f_1) \tag{3.9–33}$$

Although this differs in appearance from (3.9–32) it may be transformed into that expression by making use of $w(-f) = w(f)$.

Suppose that $I(t)$ is the current through an ideal band pass filter so that $w(f)$ is zero except in the band $f_a < f < f_b$ where it is w_0. Then, if $3f_a > f_b$,

$$\bar{A} = \frac{w_0}{\alpha}(f_b - f_a) \tag{3.9–34}$$

$$\int_{-\infty}^{+\infty} w(x)w(f-x)\,dx = \begin{cases} 2w_0^2(f_b - f_a - f) & 0 < f \le f_b - f_a \\ w_0^2(f - 2f_a) & 2f_a \le f \le f_b + f_a \\ w_0^2(2f_b - f) & f_b + f_a \le f \le 2f_b \end{cases}$$

and is zero outside these ranges. The power spectrum $W_c(f)$ may be obtained immediately from (3.9–30) by dividing these values by $\alpha^2 + 4\pi^2f^2$.

From (3.9–33)

$$\overline{(A(t)-\bar{A})^2} = 2w_0^2\int_0^{f_b-f_a}\frac{(f_b-f_a-f)\,df}{\alpha^2+4\pi^2f^2} + w_0^2\int_{2f_a}^{f_b+f_a}\frac{(f-2f_a)}{\alpha^2+4\pi^2f^2}\,df + w_0^2\int_{f_b+f_a}^{2f_b}\frac{(2f_b-f)}{\alpha^2+4\pi^2f^2}\,df$$

If an exact answer is desired the integrations may be performed. When we assume that $f_b - f_a << f_b + f_a$ we may obtain approximations for the last two integrals.

$$\overline{(A(t) - \bar{A})^2} \approx w_0^2 \left[\frac{f_b - f_a}{\pi\alpha} \tan^{-1} \frac{2\pi(f_b - f_a)}{\alpha} - \frac{1}{4\pi^2} \log \frac{\alpha^2 + 4\pi^2(f_b - f_a)^2}{\alpha^2} + \frac{(f_b - f_a)^2}{\alpha^2 + 4\pi^2(f_b + f_a)^2} \right]$$

Furthermore, if $2\pi(f_b - f_a)/\alpha$ is large we have

$$\overline{(A(t) - \bar{A})^2} \approx w_0^2 \frac{f_b - f_a}{2\alpha}$$

and the relative r.m.s. fluctuation is

$$\text{r.m.s. of } \left[\frac{(A(t) - \bar{A})}{\bar{A}} \right] \approx \left[\frac{\alpha}{2(f_b - f_a)} \right]^{1/2}$$

This result may also be obtained from (3.9–10) and (3.9–11) by assuming α so small that the integral for $A(t)$ may be broken into a great many integrals each extending over an interval T. αT is assumed so small that $e^{-\alpha u}$ is substantially constant over each interval.

3.10 Distribution of Noise Plus Sine Wave

Suppose we have a steady sinusoidal current

$$I_p = I_p(t) = P \cos(\omega_p t - \varphi_p) \tag{3.10–1}$$

We pick times $t_1, t_2, \cdots$ at random and note the corresponding values of the current. How are these values distributed? Picking the times at random in (3.10–1) is the same, statistically, as holding t constant and picking the phase angles φ_p at random from the range 0 to 2π. If I_p be regarded as a random variable defined by the random variable φ_p, its characteristic function is

$$\begin{aligned} \text{ave. } e^{izI_p} &= \frac{1}{2\pi} \int_0^{2\pi} e^{izP \cos(\omega_p t - \varphi)} \, d\varphi \\ &= J_0(Pz) \end{aligned} \tag{3.10–2}$$

and its probability density is

$$\frac{1}{2\pi} \int_{-\infty}^{+\infty} e^{-izI_p} J_0(Pz) \, dz = \begin{cases} \frac{1}{\pi}(P^2 - I_p^2)^{-1/2} & |I_p| < P \\ 0 & |I_p| > P \end{cases} \tag{3.10–3}$$

In this case it is simpler to obtain the probability density directly from (3.10–1) instead of from the characteristic function.

Now suppose that we have a noise current I_N plus a sine wave. By combining our representation (2.8–6) for I_N with the idea of φ_p being random mentioned above we are led to the representation

$$I(t) = I = I_p + I_N$$

$$= P \cos(\omega_p t - \varphi_p) + \sum_1^M c_n \cos(\omega_n t - \varphi_n), \qquad (3.10\text{–}4)$$

$$c_n^2 = 2w(f_n)\Delta f$$

where φ_p and $\varphi_1, \cdots \varphi_M$ are independent random angles.

If we note I at the random times $t_1, t_2 \cdots$ how are the observed values distributed? Since I_p and I_N may be regarded as independent random variables and since the characteristic function for the sum of two such variables is the product of their characteristic functions we have from (3.1–6) and (3.10–2)

$$\text{ave. } e^{izI} = \text{ave. } e^{iz(I_p+I_N)}$$

$$= J_0(Pz) \exp\left(\frac{-\psi_0 z^2}{2}\right) \qquad (3.10\text{–}5)$$

which gives the characteristic function of I. The probability density of I is[37]

$$\frac{1}{2\pi}\int_{-\infty}^{+\infty} e^{-izI-(\psi_0 z^2/2)} J_0(Pz)\, dz = \frac{1}{\pi\sqrt{2\pi\psi_0}}\int_0^{\pi} e^{-(I-P\cos\theta)^2/2\psi_0}\, d\theta \qquad (3.10\text{–}6)$$

In the same way the two-dimensional probability density of (I_1, I_2), where $I_1 = I(t)$ is a sine wave plus noise (3.10–4) and $I_2 = I(t + \tau)$ is its value at a constant interval τ later, may be shown to be

$$\frac{(\psi_0^2 - \psi_\tau^2)^{-1/2}}{2\pi}\int_0^{2\pi} d\theta \exp\left[-\frac{B(\theta)}{2(\psi_0^2 - \psi_\tau^2)}\right] \qquad (3.10\text{–}7)$$

where

$$B(\theta) = \psi_0[(I_1 - P\cos\theta)^2 + (I_2 - P\cos(\theta + \omega_p\tau))^2]$$

$$- 2\psi_\tau(I_1 - P\cos\theta)(I_2 - P\cos(\theta + \omega_p\tau))$$

The characteristic function for I_1 and I_2 is

$$\text{ave. } e^{iuI_1+ivI_2} = J_0\left(P\sqrt{u^2 + v^2 + 2uv\cos\omega_p\tau}\right)$$

$$\times \exp\left[-\frac{\psi_0}{2}(u^2 + v^2) - \psi_\tau uv\right] \qquad (3.10\text{–}8)$$

[37] A different derivation of this expression is given by W. R. Bennett. *Jour. Acous. Soc. Amer.*, Vol. 15, p. 165 (Jan. 1944); *B.S.T.J.*, Vol. 23, p. 97 (Jan. 1944).

Sometimes the distribution of the envelope of

$$I = P \cos pt + I_N \tag{3.10–9}$$

is of interest. Here we have replaced ω_p by p and have set φ_p to zero. By the envelope we mean $R(t)$ given by

$$R^2(t) = R^2 = (P + I_c)^2 + I_s^2 \tag{3.10–10}$$

where I_c is the component of I_N "in phase" with cos pt and I_s is the component "in phase" with sin pt:

$$I_c = \sum c_n \cos [(\omega_n - p)t - \varphi_n]$$

$$I_s = \sum c_n \sin [(\omega_n - p)t - \varphi_n]$$

$$I_N = I_c \cos pt - I_s \sin pt$$

$$\overline{I_N^2} = \overline{I_c^2} = \overline{I_s^2} = \psi_0$$

Since I_c and I_s are distributed normally about zero with a variance of ψ_0, the probability densities of the variables

$$x = P + I_c$$

$$y = I_s$$

are

$$(2\pi\psi_0)^{-1/2} \exp - \frac{(x - P)^2}{2\psi_0}$$

$$(2\pi\psi_0)^{-1/2} \exp - \frac{y^2}{2\psi_0}$$

respectively. Setting

$$x = R \cos \theta$$

$$y = R \sin \theta$$

and using these distributions shows that the probability of a point (x, y) lying in the ring R, $R + dR$ is

$$\frac{R\,dR}{2\pi\psi_0} \int_0^{2\pi} \exp\left[-\frac{1}{2\psi_0}(R^2 + P^2 - 2RP \cos\theta)\right] d\theta$$

$$= \frac{R\,dR}{\psi_0} \exp\left[-\frac{R^2 + P^2}{2\psi_0}\right] I_0\left(\frac{RP}{\psi_0}\right) \tag{3.10–11}$$

where I_0 is the Bessel function with imaginary argument.

$$I_0(z) = \sum_{n=0}^{\infty} \frac{z^{2n}}{2^{2n}\, n!\, n!}$$

and is a tabulated function. Thus (3.10–11) gives the probability density of the envelope R.

The average value of R^n may be obtained by multiplying (3.10–11) by R^n and integrating from 0 to ∞. Expansion of the Bessel function and term-wise integration gives

$$\overline{R^n} = (2\psi_0)^{n/2}\Gamma\left(\frac{n}{2}+1\right)e^{-P^2/2\psi_0}\,{}_1F_1\left(\frac{n}{2}+1;\,1;\,\frac{P^2}{2\psi_0}\right)$$

$$= (2\psi_0)^{n/2}\Gamma\left(\frac{n}{2}+1\right){}_1F_1\left(-\frac{n}{2};\,1;\,-\frac{P^2}{2\psi_0}\right) \qquad (3.10\text{–}12)$$

where ${}_1F_1$ is a hypergeometric function.[38] In going from the first line to the second we have used Kummer's first transformation of this function. A special case is

$$\overline{R^2} = P^2 + 2\psi_0 \qquad (3.10\text{–}13)$$

When only noise is present, $P = 0$ and

$$\overline{R} = (2\psi_0)^{1/2}\Gamma(\tfrac{3}{2}) = \left(\frac{\psi_0\pi}{2}\right)^{1/2}$$
$$\overline{R^2} = 2\psi_0 \qquad (3.10\text{–}14)$$

Before going further with (3.10–11) it is convenient to make the following change of notation

$$v = \frac{R}{\psi_0^{1/2}}, \qquad dv = \frac{dR}{\psi_0^{1/2}}, \qquad a = \frac{P}{\psi_0^{1/2}} \qquad (3.10\text{–}15)$$

"a" is the ratio (sine wave amplitude)/(r.m.s. noise current).
Instead of the random variable R we now have the random variable v whose probability density is

$$p(v) = v\exp\left[-\frac{v^2+a^2}{2}\right]I_0(av) \qquad (3.10\text{–}16)$$

Curves of $p(v)$ versus v are plotted in Fig. 6 for the values 0, 1, 2, 3, 5 of a. Curves showing the probability that v is less than a stated amount, i.e., distribution curves for v, are given in Fig. 7. These curves were obtained by integrating $p(v)$ numerically. The following useful expression for this probability has been given by W. R. Bennett in some unpublished work.

$$\int_0^v p(u)\,du = \exp\left[-\frac{v^2+a^2}{2}\right]\sum_{n=1}^{\infty}\left(\frac{v}{a}\right)^n I_n(av) \qquad (3.10\text{–}17)$$

[38] Curves of this function are given in "Tables of Functions", Jahnke and Emde (1938), p. 275, and some of its properties are stated in Appendix 4C.

This is obtained by integration by parts using

$$\int u^n I_{n-1}(au)\, du = u^n I_n(au)/a$$

When $av >> 1$ but $1 << a - v$, Bennett has shown that (3.10–17) leads to

$$\int_0^v p(u)\, du \approx \left(\frac{v}{2\pi a}\right)^{1/2} \frac{1}{a - v} \exp\left[-\frac{(v - a)^2}{2}\right] \left(1 - \frac{3(a + v)^2 - 4v^2}{8av(a - v)^2} \cdots\right) \tag{3.10–18}$$

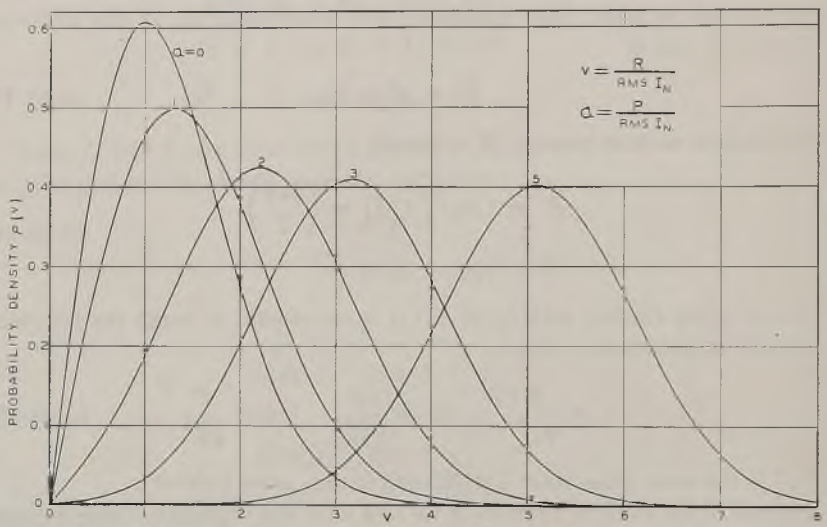

Fig. 6—Probability density of envelope R of $I(t) = P \cos pt + I_N$

This formula may also be obtained by putting the asymptotic expansion (3.10–19) for $p(v)$ in (3.10–17), integrating by parts twice, and neglecting higher order terms.

When av becomes large we may replace $I_0(av)$ by its asymptotic expression. The expression for $p(v)$ is then

$$p(v) \sim \left(1 + \frac{1}{8av}\right)\left(\frac{v}{2\pi a}\right)^{1/2} \exp\left[-\frac{(v - a)^2}{2}\right] \tag{3.10–19}$$

Thus when either a becomes large or v is far out on the tail of the probability density curve, the distribution behaves like a normal law. In terms of the original quantities, the normal law has an average of P and a standard deviation of $\psi_0^{1/2}$. This standard deviation is the same as the standard deviation

of the instantaneous values of I_N. When $av \gg 1$ and $a \gg | v - a |$ we may expand the coefficient of the exponential term in (3.10–19) in powers of

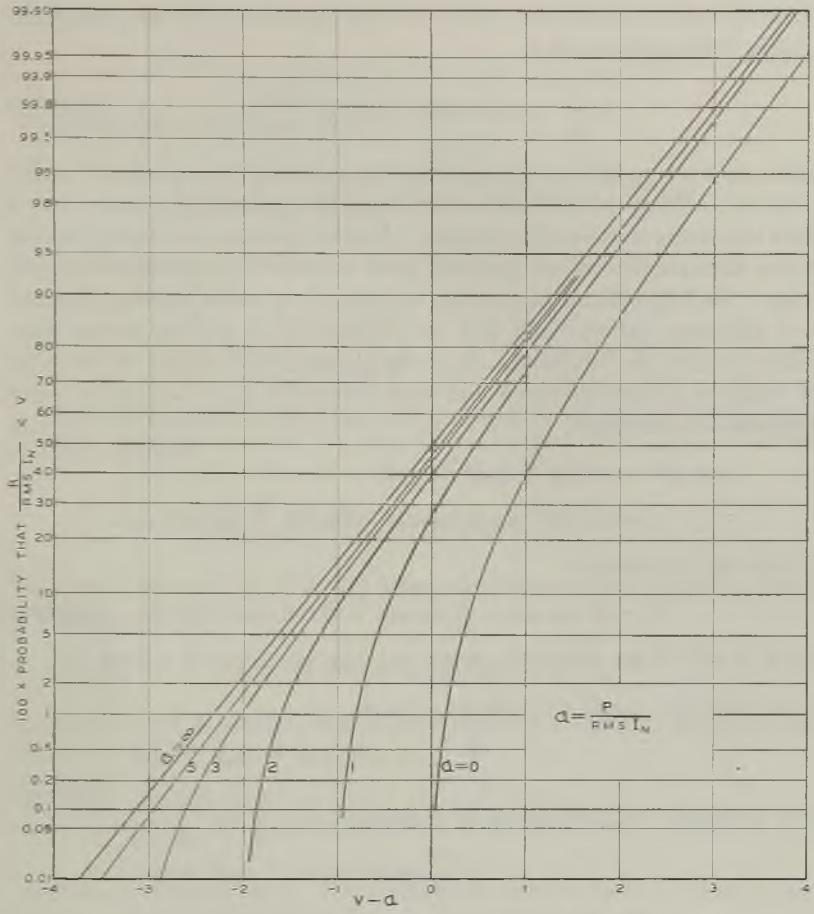

Fig. 7—Distribution function of envelope R of $I(t) = P \cos pt + I_N$

$(v - a)/a$. Integrating this expansion termwise gives, when terms of magnitude less than a^{-3} are neglected,

$$\int_0^v p(u)\,du \approx \frac{1}{2} + \frac{1}{2}\,erf\,\frac{v-a}{\sqrt{2}} - \frac{1}{2a\sqrt{2\pi}}\left[1 - \frac{v-a}{4a} + \frac{1+(v-a)^2}{8a^2}\right]\exp\left[-\frac{(v-a)^2}{2}\right]$$

When I consists of two sine waves plus noise

$$I = P \cos pt + Q \sin qt + I_N , \tag{3.10–20}$$

where the radian frequencies p and q are incommensurable, the probability density of the envelope R is

$$R \int_0^\infty r J_0(Rr) J_0(Pr) J_0(Qr) e^{-\psi_0 r^2/2}\, dr \tag{3.10–21}$$

where ψ_0 is $\overline{I_N^2}$. When Q is zero the integral may be evaluated to give (3.10–11). When both P and Q are zero the probability density for R when only noise is present is obtained. If there are three sine waves instead of two then another Bessel function must be placed in the integrand, and so on. To define R it is convenient to think of the noise as being confined to a relatively narrow band and the frequencies of the sine waves lying within, or close to, this band. As in equations (3.7–2) to (3.7–4), we refer all terms to a representative mid-band frequency $f_m = \omega_m/2\pi$ by using equations of the type

$$\begin{aligned} \cos pt &= \cos [(p - \omega_m)t + \omega_m t] \\ &= \cos (p - \omega_m)t \cos \omega_m t - \sin (p - \omega_m)t \sin \omega_m t. \end{aligned}$$

In this way we obtain

$$V = A \cos \omega_m t - B \sin \omega_m t = R \cos (\omega_m t + \theta) \tag{3.10–22}$$

where A and B are relatively slowly varying functions of t given by

$$\begin{aligned} A &= P \cos (p - \omega_m)t + Q \cos (q - \omega_m)t \\ &\qquad + \sum_n c_n \cos (\omega_n t - \omega_m t - \varphi_n) \\ B &= P \sin (p - \omega_m)t + Q \sin (q - \omega_m)t \\ &\qquad + \sum_n c_n \sin (\omega_n t - \omega_m t - \varphi_n) \end{aligned} \tag{3.10–23}$$

and

$$\begin{aligned} R^2 &= A^2 + B^2, \qquad R > 0 \\ \tan \theta &= B/A \end{aligned} \tag{3.10–24}$$

As might be expected, (3.10–21) is closely associated with the problem of random flights and may be obtained from Kluyver's result[39] by assuming

[39] G. N. Watson, "Theory of Bessel Functions" (Cambridge, 1922), p. 420.

the noise to correspond to a very large number of very small random displacements.

Another way of deriving (3.10–21) is to assume $(p - \omega_m)t$, $(q - \omega_m)t$, φ_1, φ_2, $\cdots$ are independent random angles. The characteristic function of A, B is

$$\text{ave. } e^{iuA+ivB} = J_0(P\sqrt{u^2 + v^2})J_0(Q\sqrt{u^2 + v^2})e^{-(\psi_0/2)(u^2+v^2)}$$

The probability density of A, B is

$$\left(\frac{1}{2\pi}\right)^2 \int_{-\infty}^{+\infty} du \int_{-\infty}^{+\infty} dv\, e^{-iuA-ivB} \text{ ave. } e^{iuA+ivB}$$

When the change of variables

$$A = R\cos\theta \qquad u = r\cos\varphi$$

$$B = R\sin\theta \qquad v = r\sin\varphi$$

is made the integration with respect to φ may be performed. The double integral becomes

$$\frac{1}{2\pi}\int_0^{\infty} rJ_0(Pr)J_0(Qr)J_0(Rr)e^{-(\psi_0/2)r^2}\,dr$$

This leads directly to (3.10–21) when we observe that $dAdB = RdRd\theta$.

Incidentally, if

$$I = Q(1 + k\cos pt)\cos qt + I_N$$

in which $p << q$, similar considerations show that the probability density of R is

$$\frac{R}{2\pi}\int_0^{2\pi} d\alpha \int_0^{\infty} rJ_0(Rr)J_0[Qr(1 + k\cos\alpha)]e^{-(\psi_0/2)r^2}\,dr$$

when ω_m is taken to be q. The integration with respect to r may be performed. This relation is closely connected with (3.10–11).

Returning now to the case in which I is the sum of two sine waves plus noise, we may show from (3.10–21) and

$$\int_0^{\infty} R^{n+1}J_0(Rr)\,dR = \frac{2^{n+1}\Gamma\left(1 + \frac{n}{2}\right)}{r^{n+2}\Gamma\left(-\frac{n}{2}\right)}$$

that the average value of R^n is, when $-2 < re\ (n) < -\frac{3}{2}$,

$$\overline{R^n} = \frac{2^{n+1}\Gamma\left(1+\frac{n}{2}\right)}{\Gamma\left(-\frac{n}{2}\right)} \int_0^\infty r^{-n-1} J_0(Pr) J_0(Qr) e^{-\psi_0 r^2/2}\, dr$$

$$= (2\psi_0)^{n/2}\Gamma\left(\frac{n}{2}+1\right) \sum_{k=0}^{\infty}\sum_{m=0}^{\infty} \frac{\left(-\frac{n}{2}\right)_{k+m} (-x)^k (-y)^m}{k!\,k!\,m!\,m!} \qquad (3.10\text{–}25)$$

$$= (2\psi_0)^{n/2}\Gamma\left(\frac{n}{2}+1\right) \sum_{k=0}^{\infty} \frac{\left(-\frac{n}{2}\right)_k (y-x)^k}{k!\,k!} P_k\left(\frac{x+y}{x-y}\right)$$

It appears very probable that this result could be extended, by analytic continuation, to positive integer values of n. We have used the notation

$$(\alpha)_0 = 1, \qquad (\alpha)_k = \alpha(\alpha+1)\cdots(\alpha+k-1)$$
$$x = \frac{P^2}{2\psi_0}, \qquad y = \frac{Q^2}{2\psi_0} \qquad (3.10\text{–}26)$$

and have denoted the Legendre polynomial by $P_k(z)$. The series converge for all values of P, Q, and ψ_0 and terminate when n is an even positive integer.

When x or y, or both, are large in comparison with unity we may use the integral for $\overline{R^n}$ to obtain the asymptotic expansion, assuming $Q < P$ so that $y < x$,

$$\overline{R^n} \sim P^n \sum_{k=0}^{\infty} \frac{\left(-\frac{n}{2}\right)_k \left(-\frac{n}{2}\right)_k}{k!\,x^k} {}_2F_1\left(k-\frac{n}{2}, k-\frac{n}{2}; 1; \frac{y}{x}\right) \qquad (3.10\text{–}27)$$

When n is an even positive integer this series terminates and gives the same expression as (3.10–25). When n is an odd integer the ${}_2F_1$ may be expressed in terms of the complete elliptic functions E and K of modulus $y^{1/2}x^{-1/2}$:

$${}_2F_1\left(-\tfrac{1}{2}, -\tfrac{1}{2}; 1; \frac{y}{x}\right) = \frac{4}{\pi}E - \frac{2}{\pi}\left(1-\frac{y}{x}\right)K$$
$${}_2F_1\left(\tfrac{1}{2}, \tfrac{1}{2}; 1; \frac{y}{x}\right) = \frac{2}{\pi}K \qquad (3.10\text{–}28)$$

The higher terms may be computed from

$$a(1-z)^2\,{}_2F_1(a+1, a+1; 1; z) = (2a-1)(1+z)\,{}_2F_1(a, a; 1; z)$$
$$+ (1-a)\,{}_2F_1(a-1, a-1; 1; z) \qquad (3.10\text{–}29)$$

which is a special case of

$$ab(\gamma+1)(1-z)^2\,{}_2F_1(a+1,b+1;c;z) = A\,{}_2F_1(a,b;c;z) - (\gamma-1)(c-a)(c-b)\,{}_2F_1(a-1,b-1;c;z) \quad (3.10\text{–}30)$$

where $\gamma = c - a - b$ and

$$A = (\gamma^2-1)\gamma + (1-z)[(\gamma-1)(c-b)(b-1) + (\gamma+1)a(c-a-1)]$$

Although this expression does not show it, A is really symmetrical in a and b. A symmetrical form may be obtained by using the expression obtained by putting $z = 0$ in (3.10–30).

3.11 Shot Effect Representation

In most of the work in this part the representations (2.8–1) or (2.8–6) have been used as a starting point. Here we point out that the shot effect representation used in Part I may also be used as a starting point.

For example, suppose we wish to find the two dimensional distribution of $I(t)$ and $I(t+\tau)$ discussed in Section 3.2. This is a special case of the distribution of the two variables

$$\begin{aligned} I(t) &= \sum_{k=-\infty}^{+\infty} F(t-t_k) \\ J(t) &= \sum_{k=-\infty}^{+\infty} G(t-t_k) \end{aligned} \quad (3.11\text{–}1)$$

where we now assume

$$\int_{-\infty}^{+\infty} F(t)\,dt = \int_{-\infty}^{+\infty} G(t)\,dt = 0 \quad (3.11\text{–}2)$$

in order that the average values of I and J may be zero. In fact, to get $I(t+\tau)$ from $J(t)$ we set $G(t)$ equal to $F(t+\tau)$.

The distribution of I and J may be obtained in much the same manner as was the distribution of I alone in section 1.4. The characteristic function of the distribution is

$$\begin{aligned} f(u,v) &= \text{ave. } e^{iuI+ivJ} \\ &= \exp\ \nu \int_{-\infty}^{+\infty} [e^{iuF(t)+ivG(t)} - 1]\,dt \end{aligned} \quad (3.11\text{–}3)$$

where ν is the expected number of events (electron arrivals in the shot effect) per second. The probability density of I and J is

$$\frac{1}{4\pi^2}\int_{-\infty}^{+\infty} du \int_{-\infty}^{+\infty} dv\, e^{-iuI-ivJ} f(u,v) \quad (3.11\text{–}4)$$

The semi-invariants $\lambda_{m,n}$ are given by the generating function

$$\log f(u, v) = \sum_{m,n=1}^{k} \frac{\lambda_{m,n}}{m!\,n!} (iu)^m (iv)^n + o[(iu)^k, (iv)^k]$$

and are

$$\lambda_{m,n} = \nu \int_{-\infty}^{+\infty} F^m(t) G^n(t)\, dt \tag{3.11–5}$$

As $\nu \longrightarrow \infty$ the distribution of I and J approaches a two dimensional normal law. The approximation to this normal law may be obtained in much the same manner as in section 1.6. From our assumption (3.11–2) it follows that λ_{10} and λ_{01} are zero. From the relation between the second moments and semi-invariants λ we have

$$\begin{aligned} \mu_{11} &= \lambda_{20} + \lambda_{10}^2 = \nu \int_{-\infty}^{+\infty} F^2(t)\, dt \\ \mu_{12} &= \lambda_{11} + \lambda_{10}\lambda_{01} = \nu \int_{-\infty}^{+\infty} F(t)G(t)\, dt \\ \mu_{22} &= \lambda_{02} + \lambda_{01}^2 = \nu \int_{-\infty}^{+\infty} G^2(t)\, dt \end{aligned} \tag{3.11–6}$$

where the notation in the subscripts of the μ's differs from that of the λ's, the change being made to bring it in line with sections 2.9 and 2.10 so that we may write down the normal distribution at once.

The formulas (3.11–6) are closely related to Rowland's generalization of Campbell's theorem mentioned just below equation (1.5–9).

PART IV

NOISE THROUGH NON-LINEAR DEVICES

4.0 Introduction

We shall consider two problems which concern noise passing through detectors or other non-linear devices. The first deals with the statistical properties of the output of a non-linear device, that is, with its average value, its fluctuation about this average and so on. The second problem may be stated more definitely: Given a non-linear device and an input consisting of noise alone, or of noise plus a signal. What is the power spectrum of the output?

There does not seem to be much published material on the first problem. However, from conversation with other people, I have learned that it has been studied independently by several investigators. The same is probably true of the second problem although here the published material is somewhat more plentiful. This makes it difficult to assign credit where credit is due. Much of the material given here had its origin in discussions with friends, especially with W. R. Bennett, J. H. Van Vleck, and David Middleton. Help was obtained from the recent paper[37] by Bennett, and also from the manuscript of a forthcoming paper by Middleton.[40]

4.1 Low Frequency Output of a Square Law Device

Let the output current I of the device be related to the input voltage V by

$$I = \alpha V^2 \tag{4.1-1}$$

where α is a constant. When the power spectrum of V is confined to a relatively narrow band, the power spectrum of I consists of two portions. One portion clusters around twice the mid-band frequency of V and the other around zero frequency. We are interested in the low frequency portion. The current corresponding to this portion will be denoted by $I_{t\ell}$, and is the current which would flow if a low pass filter were inserted in the output to remove the upper portion of the spectrum. It is convenient to divide $I_{t\ell}$ into two components:

$$I_{t\ell} = I_{dc} + I_{tf} \tag{4.1-2}$$

[37] Loc. cit. (Section 3.10).

[40] Cruft Laboratory and the Research Laboratory of Physics, Harvard University, Cambridge, Mass. In the following sections references to Bennett's paper and Middleton's manuscript are made by simply giving the authors' names.

where the subscripts stand for "total low" frequency, "direct current." and "low frequency," respectively. We have

$$I_{dc} = \text{average } I_{t\ell} = \overline{I}_{t\ell} \tag{4.1-3}$$

$$\text{Mean Square } I_{\ell f} = \text{average } (I_{t\ell} - I_{dc})^2 = \overline{I^2_{t\ell}} - I^2_{dc}$$

Probably the simplest method of obtaining I_{dc} is to square the given expression for V and pick out the terms independent of time. Thus if

$$V = P \cos pt + Q \cos qt + V_N \tag{4.1-4}$$

we have

$$I_{dc} = \alpha\left(\frac{P^2}{2} + \frac{Q^2}{2} + \overline{V_N^2}\right) \tag{4.1-5}$$

$I_{\ell f}$ may also be obtained by picking out the low frequency terms. However, here we wish to use the square law device, and the linear rectifier in the next section, to illustrate a general method of dealing with the statistical properties of the output of a non-linear device when the input voltage is restricted to a relatively narrow band.

If none of the low frequency spectrum is removed by filters,

$$I_{t\ell} = \alpha \frac{R^2}{2} \tag{4.1-6}$$

where R is the envelope of V. The probability density and the statistical properties of $I_{t\ell}$ may be derived from this relation when the distribution function of R is known.[41] Before discussing these properties we shall establish (4.1–6).

Equation (4.1–6) is a special case of a more general result established in Section 4.3. However, its truth may be seen by taking the example

$$V = P \cos pt + Q \cos qt + V_N \tag{4.1-4}$$

where $f_p = p/2\pi$ and $f_q = q/2\pi$ lie within, or close to, the band of the noise voltage V_N.

By using formulas of the type

$$\begin{aligned} \cos pt &= \cos [(p - \omega_m)t + \omega_m t] \\ &= \cos (p - \omega_m)t \cos \omega_m t - \sin (p - \omega_m)t \sin \omega_m t \end{aligned} \tag{4.1-7}$$

[41] When part of the low-frequency spectrum is removed, the problem becomes much more difficult. I_{dc} may be obtained as above, but to get $\overline{I^2_{\ell f}}$ it is necessary to first determine the power spectrum of I (Section 4.5) and then integrate over the appropriate portion of it. Concerning the distribution of $I_{\ell f}$, our present knowledge tells us only that it lies between the one given by (4.1–6) and the normal law which it approaches when only a narrow portion of the low frequency spectrum is passed by the audio frequency filter (Section 4.3).

we may refer all terms to the mid-band frequency $f_m = \omega_m/2\pi$, as is done in equations (3.7–2) to (3.7–4).

In this way we obtain

$$V = A \cos \omega_m t - B \sin \omega_m t = R \cos (\omega_m t + \theta), \tag{4.1–8}$$

where A and B are relatively slowly varying functions of t given by

$$A = P \cos (p - \omega_m)t + Q \cos (q - \omega_m)t + \sum_n c_n \cos (\omega_n t - \omega_m t - \varphi_n),$$

$$B = P \sin (p - \omega_m)t + Q \sin (q - \omega_m)t + \sum_n c_n \sin (\omega_n t - \omega_m t - \varphi_n)$$

and

$$\begin{aligned} R^2 &= A^2 + B^2, \qquad R > 0 \\ \tan \theta &= B/A. \end{aligned} \tag{4.1–9}$$

This definition of R has also been given in equations (3.10–22, 23, 24). The envelope of V is R and the output current is

$$I = \alpha R^2 \left[\frac{1}{2} + \frac{1}{2} \cos (2\omega_m t + 2\theta)\right] \tag{4.1–10}$$

Since R is a slowly varying function of time, so is R^2. The power spectrum of R^2 is confined to frequencies much lower than $2f_m$ and consequently the power spectrum of $R^2 \cos (2\omega_m t + 2\theta)$ is clustered around $2f_m$. Thus the only term in I contributing to the low frequency output is $\alpha R^2/2$ which is what we wished to show.

We now return to the statistical properties of $I_{t\ell}$. First, consider the case in which V consists of noise only, $V = V_N$, so that the probability density of the envelope R is

$$\frac{R}{\psi_0} e^{-R^2/2\psi_0} \tag{3.7–10}$$

where

$$\psi_0 = [rms\ V_N]^2 = \overline{V_N^2} \tag{4.1–11}$$

Hence

$$\begin{aligned} I_{dc} = \overline{I}_{t\ell} &= \frac{\alpha \overline{R^2}}{2} \\ &= \int_0^\infty \frac{\alpha R^2}{2} \frac{R}{\psi_0} e^{-R^2/2\psi_0}\, dR \\ &= \alpha \psi_0 \\ \overline{I_{\ell\ell}^2} = \overline{I_{t\ell}^2} - I_{dc}^2 &= \int_0^\infty \frac{\alpha^2 R^5}{4\psi_0} e^{-R^2/2\psi_0}\, dR - I_{dc}^2 \\ &= \alpha^2 \psi_0^2 \end{aligned} \tag{4.1–12}$$

Second, consider the case in which

$$V = V_N + P \cos pt \tag{4.1–13}$$

where $p/2\pi$ lies near the noise band of V_N. The probability density of the envelope R is

$$\frac{R}{\psi_0} \exp\left[-\frac{R^2 + p^2}{2\psi_0}\right] I_0\left(\frac{RP}{\psi_0}\right) \tag{3.10–11}$$

From this and equations (3.10–12), (3.10–13), we find

$$I_{dc} = \frac{\alpha\overline{R^2}}{2} = \alpha\psi_0 + \frac{\alpha P^2}{2} \tag{4.1–14}$$

$$\overline{I_{i\ell}^2} = \frac{\alpha^2}{4}\overline{R^4} = \alpha^2\left[2\psi_0^2 + 2P^2\psi_0 + \frac{P^4}{4}\right]$$

$$\overline{I_{\ell f}^2} = \overline{I_{i\ell}^2} - I_{dc}^2 = \alpha^2[\psi_0 + P^2]\psi_0 \tag{4.1–15}$$

In (4.1–14) ψ_0 is the mean square value of V_N and $P^2/2$ is the mean square value of the signal. These two equations show that I_{dc} and the rms value of $I_{\ell f}$ are independent of the distribution of the noise power spectrum in V_N as long as the input V is confined to a relatively narrow band. In other words, although this distribution does affect the power spectrum of the output, it does not affect the d.c. and rms $I_{\ell f}$ when ψ_0 and P are given. That the same is also true for a large class of non-linear devices was first pointed out by Middleton (see end of Section 4.9).

When the voltage is[42]

$$V = V_N + P \cos pt + Q \cos qt, \tag{4.1–4}$$

$p \neq q$, we obtain from equation (3.10–25)

$$I_{dc} = \frac{\alpha}{2}\overline{R^2} = \alpha\left(\psi_0 + \frac{P^2}{2} + \frac{Q^2}{2}\right)$$

$$\overline{I_{i\ell}^2} = \frac{\alpha^2}{4}\overline{R^4} \tag{4.1–16}$$

$$\overline{I_{\ell f}^2} = \alpha^2\left[\psi_0^2 + P^2\psi_0 + Q^2\psi_0 + \frac{P^2Q^2}{2}\right]$$

[42] These results are special cases, obtained by assuming no audio frequency filter, of formulas given by F. C. Williams, *Jour. Inst.* of *E. E.*, 80 (1937), 218–226. Williams also discusses the response of a linear rectifier to (4.1–4) when $P \gg Q + V_N$. An account of Williams' work is given by E. B. Moullin, "Spontaneous Fluctuations of Voltage," Oxford (1938), Chap. 7.

4.2 Low Frequency Output of a Linear Rectifier

In the case of the linear rectifier

$$I = \begin{cases} 0, & V < 0 \\ \alpha V, & V > 0 \end{cases} \tag{4.2-1}$$

the low frequency output current, assuming no audio frequency filter, is

$$I_{\ell} = \frac{\alpha R}{\pi} \tag{4.2-2}$$

This formula, like its analogue (4.1–6) for the square law device, assumes that the applied signal and noise lie within a relatively narrow band. It may be used to compute the probability density and statistical properties of I_{ℓ} when the corresponding information regarding the envelope R of the applied voltage is known.

The truth of (4.2–2) may be seen by considering the output I. It consists of the positive halves of the oscillations of αV. The envelope of I is the same as that of αV. However, the area under the loops of I is only about $1/\pi$ of the area under αR, this being the ratio of the area under a loop of $\sin x$ to the area of a rectangle of unit height and length 2π. From the low frequency point of view these loops of I merge into a current which varies as $\alpha R/\pi$.

When V is a sine wave plus noise,

$$V = V_N + P \cos pt \tag{4.1–13}$$

the average value of I_{ℓ} is[43]

$$\begin{aligned} I_{dc} &= \frac{\alpha}{\pi}\overline{R} = \alpha\left(\frac{\psi_0}{2\pi}\right)^{1/2} {}_1F_1\left(-\frac{1}{2}; 1; -\frac{P^2}{2\psi_0}\right) \\ &= \alpha\left(\frac{\psi_0}{2\pi}\right)^{1/2} e^{-x/2}\left[(1+x)I_0\left(\frac{x}{2}\right) + xI_1\left(\frac{x}{2}\right)\right] \end{aligned} \tag{4.2–3}$$

where I_0, I_1 are Bessel functions of imaginary argument and

$$x = \frac{P^2}{2\psi_0} = \frac{\text{ave. sine wave power}}{\text{ave. noise power}} \tag{4.2–4}$$

[43] This result was discovered independently by several investigators, among whom we may mention W. R. Bennett and D. O. North. The latter has applied it to noise measurement work. He has found that the diode detector, when adapted to noise metering, is a great improvement over the thermocouple, and has used noise meters of this type satisfactorily since 1940. See D. O. North, "The Modification of Noise by Certain Non-Linear Devices", Paper read before I.R.E., Jan. 28, 1944.

ψ_0 being the average value of V_N^2. Equation (4.2–3) follows from the formulas (3.10–12) and (4B–9). When x is large the asymptotic expansion (4B–3) of the ${}_1F_1$ gives

$$I_{dc} \sim \frac{\alpha}{\pi}\left[P + \frac{\psi_0}{2P} + \frac{\psi_0^2}{8P^3} + \cdots\right] \tag{4.2–5}$$

Similarly, the mean square value of $I_{i\ell}$ is

$$\overline{I_{i\ell}^2} = \frac{\alpha^2}{\pi^2}\overline{R^2} = \frac{\alpha^2}{\pi^2}(P^2 + 2\psi_0) \tag{4.2–6}$$

and the mean square value of the low frequency current $I_{\ell f}$, excluding the d.c., is given by

$$\overline{I_{\ell f}^2} = \overline{I_{i\ell}^2} - I_{dc}^2$$

When x is large we have

$$\overline{I_{\ell f}^2} \sim \frac{\alpha^2}{\pi^2}\left[\psi_0 - \frac{\psi_0^2}{2P^2}\cdots\right] = \frac{\alpha^2}{\pi^2}\psi_0\left[1 - \frac{1}{4x}\cdots\right] \tag{4.2–7}$$

and when $x = 0$,

$$\overline{I_{\ell f}^2} = \frac{\alpha^2}{\pi^2}\psi_0\left(2 - \frac{\pi}{2}\right) \tag{4.2–8}$$

Curves for I_{dc} are given in Figures 1, 2 and 3 of Bennett's paper. He also gives curves, in Fig. 4, showing $\overline{I_{\ell f}^2}$ versus x. These show that the effect of the higher order modulation terms is small when $I_{\ell f}$ is computed by adding low frequency modulation products.

When V consists of two sine waves plus noise,

$$V = V_N + P\cos pt + Q\cos qt, \tag{4.1–4}$$

the average value of $I_{i\ell}$ is, from (3.10–25), a sort of double ${}_1F_1$ function:

$$\begin{aligned} I_{dc} = \frac{\alpha}{\pi}\overline{R} &= \alpha\left(\frac{\psi_0}{2\pi}\right)^{1/2}\sum_{k=0}^{\infty}\sum_{m=0}^{\infty}\frac{(-\tfrac{1}{2})_{k+m}}{k!\,k!\,m!\,m!}(-x)^k(-y)^m \\ &= \alpha\left(\frac{\psi_0}{2\pi}\right)^{1/2}\sum_{k=0}^{\infty}\frac{(-\tfrac{1}{2})_k}{k!\,k!}(y-x)^k P_k\left(\frac{x+y}{x-y}\right) \end{aligned} \tag{4.2–9}$$

where

$$x = \frac{P^2}{2\psi_0}, \qquad y = \frac{Q^2}{2\psi_0}, \qquad P_k(z) = \text{Legendre polynomial} \tag{4.2–10}$$

If x is large and $y < x$, we have from (3.10–27) the asymptotic expression

$$I_{dc} \sim \frac{\alpha}{\pi}P\sum_{k=0}^{\infty}\frac{(-\tfrac{1}{2})_k(-\tfrac{1}{2})_k}{k!\,x^k}\,{}_2F_1\left(k-\tfrac{1}{2}, k-\tfrac{1}{2}; 1; \frac{y}{x}\right) \tag{4.2–11}$$

The ${}_2F_1$ may be expressed in terms of the complete elliptic functions E and K of modulus $y^{1/2}x^{-1/2}$. Thus

$$
\begin{aligned}
{}_2F_1\left(-\tfrac{1}{2}, -\tfrac{1}{2}; 1; \frac{y}{x}\right) &= \frac{4}{\pi} E - \frac{2}{\pi}\left(1 - \frac{y}{x}\right) K, \\
{}_2F_1\left(\tfrac{1}{2}, \tfrac{1}{2}; 1; \frac{y}{x}\right) &= \frac{2}{\pi} K
\end{aligned}
\tag{3.10-28}
$$

and the higher terms may be computed from the recurrence relation (3.10–29). The first term, $k = 0$, in (4.2–11) gives I_{dc} when the noise is absent.[44]

The mean square value of I_{ℓ} is

$$
\overline{I_{\ell}^2} = \frac{\alpha^2}{\pi^2}\overline{R^2} = \frac{\alpha^2}{\pi^2}[2\psi_0 + P^2 + Q^2] \tag{4.2-14}
$$

From this expression and our expression for I_{dc}, the rms value of the low frequency current, $I_{\ell f}$, excluding the d.c., may be computed. For example, when the noise is small,

$$
\begin{aligned}
\overline{I_{\ell f}^2} \sim \frac{\alpha^2}{\pi^2}\Bigg[& P^2 + Q^2 - \left(P\,{}_2F_1\left(-\tfrac{1}{2}, -\tfrac{1}{2}; 1; \frac{y}{x}\right)\right)^2 \\
& + 2\psi_0\left(1 - {}_2F_1\left(-\tfrac{1}{2}, -\tfrac{1}{2}; 1; \frac{y}{x}\right)\frac{K}{\pi}\right)\Bigg]
\end{aligned}
\tag{4.2-15}
$$

The term independent of ψ_0 gives the mean square low frequency current in the absence of noise. As Q goes to zero (4.2–15) approaches the leading term in (4.2–7), as it should. When $P = Q$ our formula breaks down and it appears that we need the asymptotic behavior of[45]

$$
I_{dc} = \alpha\left(\frac{\psi_0}{2\pi}\right)^{1/2}\sum_{k=0}^{\infty}\frac{(-\tfrac{1}{2})_k(2k)!}{[k!]^4}(-x)^k
$$

In view of the questionable nature of the derivation given in Section 3.10 of equations (4.2–9) and (4.2–11) it was thought that a numerical check on their equivalence would be worth while. Accordingly, the values $x = 4$, $y = 3$ were used in the second series of (4.2–9). It was found that the largest term (about 130) in the summation occurred at $k = 11$. In all, 24 terms were taken. The result obtained was

$$
\frac{\overline{R}}{\sqrt{2\psi_0}} = 2.5502
$$

[44] See W. R. Bennett, *B.S.T.J.*, Vol. 12 (1933), 228–243.

[45] This may be done by the method given by W. B. Ford, Asymptotic Developments, Univ. of Mich. Press (1936), Chap. VI.

For the same values of x and y the asymptotic series (4.2–11) gave

$$2.40 + 0.171 + .075 + 0.52 + \cdots$$

If we stop just before the smallest term we get 2.57 for the sum. If we include the smallest term we get 2.65. This agreement indicates that (4.2–11) is actually the asymptotic expansion of (4.2–9).

When the voltage is of the form

$$V = Q(1 + k \cos pt) \cos qt + V_N$$

we may use

$$\overline{R^n} = (2\psi_0)^{n/2} \Gamma\left(1 + \frac{n}{2}\right) \frac{1}{2\pi} \int_0^{2\pi} {}_1F_1\left[-\frac{n}{2}; 1; -y(1 + k \cos\theta)^2\right] d\theta \tag{4.2–16}$$

where R is the envelope with respect to the frequency $q/2\pi$ and y is given by (4.2–10). The integral may be evaluated by writing ${}_1F_1$ as a power series and integrating termwise using the result

$$\frac{1}{2\pi} \int_0^{2\pi} (1 + k \cos\theta)^\ell \cos m\theta \, d\theta = \frac{(-\ell)_m}{2^m m!} (-k)^m \, {}_2F_1\left[\frac{m - \ell}{2}, \frac{m - \ell + 1}{2}; m + 1; k^2\right] \tag{4.2–17}$$

where m is a non-negative integer, ℓ any number,

$$(\alpha)_m = \alpha(\alpha + 1) \cdots (\alpha + m - 1), \qquad (\alpha)_0 = 1, \qquad \text{and} \qquad (0)_0 = 1.$$

The integral may also be evaluated in terms of the associated Legendre function.

By applying the methods of Section 3.10 to (4.2–16) we are led to

$$\overline{R^2} = Q^2\left(1 + \frac{k^2}{2}\right) + 2\psi_0$$
$$\overline{R} \sim Q \sum_{s=0}^{\infty} \frac{(-\frac{1}{2})_s (-\frac{1}{2})_s}{s!\, y^s} \, {}_2F_1(s - \tfrac{1}{2}, s; 1; k^2) \tag{4.2–18}$$

where the asymptotic series holds when y is very large and k is not too close to unity. These expressions give

$$\overline{I_{\ell f}^2} \sim \frac{\alpha^2}{\pi^2}\left(Q^2 \frac{k^2}{2} + \psi_0[2 - (1 - k^2)^{-1/2}] + \cdots\right) \tag{4.2–19}$$

The reader might be tempted to associate the coefficient of ψ_0 in (4.2–19) with the continuous portion of the output power spectrum. However, this would not be correct. It appears that the principal contribution of the continuous portion of the power spectrum to $\overline{I_{\ell f}^2}$ is $\alpha^2\psi_0/\pi^2$, just as in (4.2–7) when k is zero. The difference between this and the corresponding term in (4.2–19) seems to arise from the fact that the amplitude of the recovered signal is not exactly $\alpha Qk/\pi$ but is modified by the presence of the noise. This general type of behavior might be expected on physical grounds since changing P, say doubling it, in (4.2–7) does not appreciably affect the $\overline{I_{\ell f}^2}$ in (4.2–7) (which is due entirely to the continuous portion of the noise spectrum). The modulating wave may be regarded as slowly making changes of this sort in P.

4.3 Some Statistical Properties of the Output of a General Non-Linear Device

Our general problem is this: Given a non-linear device whose output I is related to its input V by the relation

$$I = \frac{1}{2\pi}\int_C F(iu)e^{iVu}\,du \qquad (4A–1)$$

which is discussed in Appendix 4A. Let the input V contain noise in addition to the signal. Choose some frequency band in the output for study. What are the statistical properties of the current flowing in this band?

It seems to be difficult to handle this general problem. However, it appears that the two following results are true.

1. As the output band is chosen narrower and narrower the statistical properties of the corresponding current approach those of the random noise current discussed in Part III (provided no signal harmonic lies within the band). In particular, the instantaneous current values are distributed normally.

2. When the input V is confined to a relatively narrow band the power spectrum of the output I is clustered around the 0^{th} (d.c.), 1st, 2nd, etc. harmonics of the midband frequency of V. The low frequency output including the d.c. is

$$I_{t\ell} = A_0(R) = \frac{1}{2\pi}\int_C F(iu)J_0(uR)\,du \qquad (4.3–11)$$

where R is the envelope of V.

The envelope of the nth harmonic of the output, when $n > 0$, is

$$A_n(R) = \frac{1}{\pi}\int_C F(iu)J_n(uR)\,du \qquad (4.3–1)$$

The mathematical statement is

$$I = \sum_{n=0}^{\infty} A_n(R) \cos (n\omega_m t + n\theta) \tag{4.3-9}$$

where $f_m = \omega_m/(2\pi)$ is the representative mid-band frequency of V and θ is a relatively slowly varying phase angle. The results of Sections 4.1 and 4.2 are special cases of this.

Middleton's result that the noise power in each of the output bands (in the entire band corresponding to a given harmonic) depends only on $\overline{V_N^2} = \psi_0$ and not on the spectrum of V_N, where V_N is the noise voltage component of V, may also be obtained from (4.3-9). We note that the total power in the n^{th} band depends only on the mean square value of its envelope $A_n(R)$, and that the probability density of the envelope R of the input involves V_N only through ψ_0.

The argument we shall use in discussing the first result is not very satisfactory. It runs as follows. The output current I may be divided into two parts. One consists of sinusoidal terms due to the signal. The other consists of noise. We shall be concerned only with the latter which we shall call I_N. The correlation between two values of I_N separated by an interval of time approaches zero as the interval becomes large. Let τ be an interval long enough to ensure that the two values of I_N are substantially independent. Choose an interval of time T long enough to contain many intervals of length τ. Expand I_N as a Fourier series over this interval. We have

$$\begin{aligned} I_N &= \frac{a_0}{2} + \sum_{n=1}^{\infty} \left[a_n \cos \frac{2\pi nt}{T} + b_n \sin \frac{2\pi nt}{T} \right] \\ a_n - ib_n &= \frac{2}{T} \int_0^T e^{-i2\pi nt/T} I_N(t)\, dt \end{aligned} \tag{4.3-2}$$

Let the band chosen for study be $f_0 - \frac{\beta}{2}$ to $f_0 + \frac{\beta}{2}$ and let

$$T\left(f_0 - \frac{\beta}{2}\right) = n_1, \qquad T\left(f_0 + \frac{\beta}{2}\right) = n_2 \tag{4.3-3}$$

where n_1 and n_2 are integers. The number of components in the band is $(n_2 - n_1)$. We suppose β is such that this is small in comparison with T/τ. The output of the band is

$$J_N = \sum_{n=n_1}^{n_2} \left[a_n \cos \frac{2\pi n}{T} t + b_n \sin \frac{2\pi nt}{T} \right] \tag{4.3-4}$$

where

$$a_n - ib_n = \frac{2}{T}\int_0^T e^{-i2\pi((n/T)-f_0)t} e^{-i2\pi f_0 t} I_N(t)\, dt$$
$$n = \frac{n_1 + n_2}{2} + n - \frac{n_1 + n_2}{2} = f_0 T + (n - f_0 T) \tag{4.3-5}$$

We choose the band so narrow that

$$n_2 - n_1 \ll T/\tau \quad \text{or} \quad \beta\tau \ll 1 \tag{4.3-6}$$

This enables us to write approximately

$$a_n - ib_n = \sum_{r=1}^{r_1} e^{-i2\pi((n/T)-f_0)r\tau} \frac{2}{T}\int_{(r-1)\tau}^{r\tau} e^{-i2\pi f_0 t} I_N(t)\, dt$$

$r_1 = T/\tau$, T being chosen to make r_1 an integer. Suppose we do this for a large number of intervals of length T. Then $I_N(t)$ will differ from interval to interval. The set of integrals for $r = 1$ gives us an array of values which we regard as defining the distribution of a complex random variable, say x_1. Similarly the set of integrals for $r = 2$ defines the distribution of a second random variable x_2, and so on to x_{r_1}. Because we have chosen τ so large that $I_N(t)$ in any one integral is practically independent of its values in the other integrals we may say that $x_1, x_2, \cdots x_{r_1}$ are independent.

We have

$$a_{n_1} - ib_{n_1} = \sum_{r=1}^{r_1} e^{-i2\pi((n_1/T)-f_0)r\tau} x_r$$
$$a_{n_1+1} - ib_{n_1+1} = \sum_{r=1}^{r_1} e^{-i2\pi((n_1+1/T)-f_0)r\tau} x_r$$
$$\vdots \qquad\qquad \vdots$$
$$a_{n_2} - ib_{n_2} = \sum_{r=1}^{r_1} e^{-i2\pi((n_2/T)-f_0)r\tau} x_r$$

and if $n_2 - n_1 \ll r_1$, as was assumed in (4.3–6), we may apply the central limit theorem to show that $a_{n_1}, b_{n_1}, a_{n_1+1}, \cdots a_{n_2}, b_{n_2}$ tend to become independent and normally distributed about zero as we let the band width $\beta \to 0$ and $T \to \infty$ (and hence $r_1 \to \infty$) in such a way as to keep $n_2 - n_1$ fixed. In this work we make use of the fact that $I_N(t)$ is such that the real and imaginary parts of $x_1, x_2, \cdots x_r$ all have the same average and standard deviation. It is convenient to assume $f_0 T$ is an integer.

Thus as the band width β approaches zero the band output J_N given by (4.3–4) may be represented in the same way, namely as (2.8–1), as was the random noise current studied in Part III. Hence J_N tends to have the

same properties as the random noise current studied there. For example, the distribution of J_N tends towards a normal law. In our discussion we had to assume that $\beta\tau \ll 1$. If the voltage V applied to the non-linear device is confined to a relatively narrow frequency band, say $f_b - f_a$, it appears that the interval τ (chosen above so that $I(t)$ and $I(t + \tau)$ are substantially independent) may be taken to be of the order of $1/(f_b - f_a)$. In this case J_N tends to behave like a random noise current if $\beta/(f_b - f_a)$ is much smaller than unity.

We now turn our attention to the second statement made at the beginning of this section. Let the applied voltage be confined to a relatively narrow band so that it may be represented by equation (4.1–8) of Section 4.1,

$$V = R \cos (\omega_m t + \theta), \qquad R \geq 0, \tag{4.1–8}$$

where $f_m = \omega_m/(2\pi)$ is some representative frequency within the band and R and θ are functions of time which vary slowly in comparison with $\cos \omega_m t$. We call R the envelope of V.

From equation (4A–1)

$$I = \frac{1}{2\pi} \int_C F(iu) e^{iuR \cos (\omega_m t + \theta)}\, du \tag{4.3–7}$$

We expand the integrand by means of

$$e^{ix \cos \varphi} = \sum_{n=0}^{\infty} \epsilon_n i^n \cos n\varphi J_n(x) \tag{4.3–8}$$

where ϵ_0 is 1 and ϵ_n is 2 when $n > 0$ and $J_n(x)$ is a Bessel function. Thus

$$I = \sum_{n=0}^{\infty} A_n(R) \cos (n\omega_m t + n\theta) \tag{4.3–9}$$

where

$$A_n(R) = \epsilon_n \frac{i^n}{2\pi} \int_C F(iu) J_n(uR)\, du \tag{4.3–10}$$

Since R is a relatively slowly varying function of time we expect the same to be true of $A_n(R)$, at least for moderately small values of n. Thus from (4.3–9) we see that the power spectrum of I will consist of a succession of bands, the n^{th} band being clustered around the frequency nf_m. If we eliminate all of the bands except the n^{th} by means of a filter we see that the output will have the envelope $A_n(R)$ when $n \geqq 1$. Taking n to be zero, shows that the low frequency output is simply

$$A_0(R) = \frac{1}{2\pi} \int_C F(iu) J_0(uR)\, du \tag{4.3–11}$$

Taking n to be one shows that the band around f_m is given by

$$\frac{A_1(R)}{R} V \tag{4.3-12}$$

The statistical properties of the low frequency output and of the envelopes of the output bands may be obtained from those of R. For example, the probability density of $A_n(R)$ is of the form

$$p(R) \Big/ \frac{dA_n(R)}{dR} \tag{4.3-13}$$

where $p(R)$ is the probability density of R. In this expression R is considered as a function of A_n.

It should be noted that we have been assuming that all of the band surrounding the harmonic frequency nf_m is taken. When we take only a portion of it, presumably the statistical properties will tend to approach those of a random noise current in accordance with the first statement made at the beginning of this section.

When we apply (4.3–11) to the square law device we have

$$F(iu) = \frac{2\alpha}{(iu)^3}$$

$$A_0(R) = -\frac{2\alpha}{2\pi i} \int^{(0+)} \frac{J_0(uR)}{u^3}\, du$$

$$= \frac{\alpha}{2} R^2$$

When we apply (4.3–11) to the linear rectifier:

$$F(iu) = -\frac{\alpha}{u^2}$$

$$A_0(R) = -\frac{\alpha}{2\pi} \int_{-\infty}^{+\infty} \frac{J_0(uR)}{u^2}\, du = \frac{\alpha R}{\pi}$$

where the path of integration passes under the origin. These two results agree with those obtained in Section 4.1 and 4.2 from simple considerations. As a final example we find the low frequency output of a biased linear rectifier in terms of the envelope R of the applied voltage. From the table of $F(iu)$ given in Appendix 4A we see that $F(iu)$ corresponding to

$$I = 0, \qquad V < B$$

$$I = V - B, \qquad V > B$$

is

$$F(iu) = -\frac{e^{-iuB}}{u^2}$$

Consequently, the low frequency output is

$$A_0(R) = -\frac{1}{2\pi}\int_{-\infty}^{+\infty} e^{-iuB} J_0(uR) u^{-2}\, du$$

where the path of integration is indented downwards at the origin. When $B > R$ the value of the integral is zero since then the path of integration may be closed in the lower half plane by an infinite semi-circle This value also follows at once from the physics of the problem. When $-R < B < R$ we may integrate by parts and get

$$\begin{aligned} A_0(R) &= \frac{1}{2\pi}\int_{-\infty}^{+\infty} e^{-iuB}[iBJ_0(uR) + RJ_1(uR)]u^{-1}\, du \\ &= -\frac{B}{2} + \frac{1}{\pi}\int_0^{\infty} [B \sin uBJ_0(uR) + R\cos uBJ_1(uR)]u^{-1}\, du \\ &= -\frac{B}{2} + \frac{B}{\pi}\arcsin\frac{B}{R} + \frac{1}{\pi}\sqrt{R^2 - B^2} \\ &= -\frac{B}{2} + \frac{R}{\pi} F\left(-\frac{1}{2}, -\frac{1}{2}; \frac{1}{2}; \frac{B^2}{R^2}\right), \qquad -R < B < R \end{aligned} \tag{4.3-14}$$

This hypergeometric function turns up again in equation (4.7–6). Also in the range $-R < B < R$,

$$\frac{dA_0}{dR} = \frac{1}{\pi}\sqrt{1 - \frac{B^2}{R^2}}$$

When B is negative and $R < -B$, the path of integration may be closed by an infinite semicircle in the upper half plane and the value of the integral is proportional to the residue of the pole at the origin:

$$\begin{aligned} A_0(R) &= 2\pi i\left(-\frac{1}{2\pi}\right)(-iB) \\ &= -B \end{aligned}$$

Thus, to summarize, the low frequency output for our linear rectifier is, for $B > 0$, (R is always positive)

$$\begin{aligned} A_0(R) &= 0, \qquad R < B \\ A_0(R) &= -\frac{B}{2} + \frac{B}{\pi}\arcsin\frac{B}{R} + \frac{1}{\pi}\sqrt{R^2 - B^2}, \qquad B < R \end{aligned} \tag{4.3-15}$$

and for $B < 0$ it is

$$A_0(R) = |B|, \quad R < |B|$$

$$A_0(R) = +\frac{|B|}{2} + \frac{|B|}{\pi} \arcsin \frac{|B|}{R} + \frac{1}{\pi}\sqrt{R^2 - B^2}, \quad |B| < R \tag{4.3–16}$$

where the arc sines lie between 0 and $\pi/2$. $A_0(R)$ and its first derivative with respect to R are continuous.

From (4.3–15), the d.c. output current is, for $B > 0$,

$$I_{dc} = \int_B^\infty \left[-\frac{B}{2} + \frac{B}{\pi} \arcsin \frac{B}{R} + \frac{1}{\pi}\sqrt{R^2 - B^2}\right] p(R)\, dR \tag{4.3–15}$$

where $p(R)$ is the probability density of the envelope of the input V, e.g., $p(R)$ is of the form (3.7–10) for noise alone, and of the form (3.10–11) for noise plus a sine wave. Similarly, the rms value of the low frequency current $I_{\ell f}$, excluding d.c., may be computed from

$$\overline{I_{\ell f}^2} = \overline{I_{i\ell}^2} - I_{dc}^2$$

where, if $B > 0$,

$$\overline{I_{i\ell}^2} = \int_B^\infty \left[-\frac{B}{2} + \frac{B}{\pi} \arcsin \frac{B}{R} + \frac{1}{\pi}\sqrt{R^2 - B^2}\right]^2 p(R)\, dR \tag{4.3–16}$$

If V consists of a sine wave of amplitude P plus noise V_N, so it may be represented as (4.1–13), and if $P \gg$ rms V_N, the distribution of R is approximately normal. If, in addition, $P - B \gg$ rms $V_N > 0$, (4.3–15), (4.3–16), and (3.10–19) lead to the approximations

$$\begin{aligned} I_{dc} &\approx -\frac{B}{2} + \frac{B}{\pi} \arcsin \frac{B}{P} + \frac{1}{\pi}\sqrt{P^2 - B^2} + \frac{\psi_0}{2\pi\sqrt{P^2 - B^2}} \\ &\approx -\frac{B}{2} + \frac{P}{\pi} + \frac{B^2 + \psi_0}{2\pi P} \qquad (4.3–17) \\ \overline{I_{\ell f}^2} &\approx \frac{P^2 - B^2}{\pi^2 P^2}\,\psi_0 \end{aligned}$$

The second expression for I_{dc} assumes $P \gg B$. When $B = 0$, these reduce to the first terms of (4.2–5) and (4.2–7). By using a different method Middleton has obtained a more precise form of this result.

Incidentally, for a given applied voltage, $I_{dc}(+)$ for a positive bias $|B|$ is related to $I_{dc}(-)$ for a negative bias $-|B|$ by

$$I_{dc}(-) = |B| + I_{dc}(+) \tag{4.3–18}$$

Also r.m.s. $I_{\ell f}(+)$ is equal to r.m.s. $I_{\ell f}(-)$. Equation (4.3–18) follows from a physical argument based on the areas underneath a curve of I for

the two cases. Both of the above relations follow from formulas given by Middleton when V is the sum of a sine wave plus noise. They may also be derived from (4.3–15) and (4.3–16).

4.4 Output Power Spectrum

The remainder of Part IV will be concerned with methods of solving the following problem: Given a non-linear device and an input voltage consisting of noise alone or of a signal plus noise. What is the power spectrum of the output?

In some ways the answer to this problem gives us less information than the methods discussed in the first three sections. For example, beyond giving the rms value, it tells us very little about the probability density of the current corresponding to a given frequency band of the output. On the other hand, this rms value may be found (by integrating the power spectrum) for any band we choose to study. The methods described earlier depended on the input being confined to a relatively narrow band and gave information regarding only the entire band corresponding to a given harmonic (0th, 1st, 2nd, etc.) of the input. There was no way to study the output when part of a band was eliminated by filters except by obtaining the power spectrum of some function of the envelope.

At present there appear to be two general methods available for the determination of the output power spectrum each with its own advantages and disadvantages. First there is the direct method which has been used by W. R. Bennett*, F. C. Williams**, J. R. Ragazzini[46] and others. The noise is represented as the sum of a finite number of sinusoidal components. The typical modulation product is computed and the output power spectrum is obtained by considering the density and amplitude of these products. The chief advantage of this method lies in its close relation to the known theory of modulation in non-linear circuits. Generally, the lower order modulation products are the only ones which contribute significantly to the output power and when they are known, the problem is well along towards solution. The main disadvantage is the labor of counting the modulation products falling in a given interval. However, Bennett has developed a method for doing this.[47]

The fundamental idea of the second method is to obtain the correlation function for the output current. From this the output power spectrum may be obtained by Fourier's transform. The correlation function method and its variations are of more recent origin than the direct method. They have

* Cited in Section 4.0. Also much of this writer's work on interference in broad band communication systems may be carried over to noise theory without any change in the methods used.

** Cited in Section 4.1.

[46] *Proc. I.R.E.* Vol. 30, pp. 277–288 (June 1942), "The Effect of Fluctuation Voltages on the Linear Detector."

[47] *B.S.T.J.*, Vol. 19 (1940), pp. 587–610, Appendix B.

been discovered independently and at about the same time, by several workers. In a paper read before the I.R.E., Jan. 28, 1944, D. O. North described results obtained by using the correlation function. J. H. Van Vleck and D. Middleton have been using the two variations of the method which we shall describe in Sections 4.7 and 4.8, since early in 1943. A primitive form of the method of Section 4.8 had been used by A. D. Fowler and the writer in some unpublished material written in 1942. Recently, I have learned that a method similar to the one used by Fowler and myself had already been used by Kurt Fränz in 1941.[48]

The correlation function method avoids the problem of counting the modulation products. However, in some cases it becomes rather unwieldy. Probably it is best to have both methods in mind when investigating any particular problem. The direct method will be illustrated by applying it to the square law detector. Two approaches to the correlation function method will then be described and applied to examples.

4.5 Noise Through Square Law-Device

Probably the most direct method of obtaining the power spectrum $W(f)$ of I, where

$$I = \alpha V^2, \tag{4.1-1}$$

V being a noise voltage, is to square the expression

$$V = V_N = \sum_1^M c_m \cos(\omega_m t - \varphi_m) \tag{2.8-6}$$

in which c_m^2 is $2w(f_m)\Delta f$, $\omega_m = 2\pi f_m$, $f_m = m\Delta f$ and $\varphi_1, \varphi_2, \cdots \varphi_M$ are random phase angles.

Considerable simplification of the algebra results when we replace the representation (2.8–6) by

$$V_N = \frac{1}{2}\sum_{-\infty}^{\infty} c_m e^{ima t - i\varphi_m} \tag{4.5-1}$$

Here we have added a term $c_0/2$ so as to not have any gaps in the summation and have introduced the definitions

$$\begin{aligned} c_{-m} &= c_m \\ \varphi_{-m} &= -\varphi_m \\ a &= 2\pi\Delta f \end{aligned} \tag{4.5-2}$$

[48] "Die Übertragung von Rauschspannung über den linearen Gleichrichter," *Hochfr. u. Elektroakyst.*, June 1941. Other articles by Fränz are (I am indebted to Dr. North for the following references) "Beitrage zur Berechnung des Verhaltnisses von Signal spannung zu Rauschspannung am Ausgang von Empfängern", *E.N.T.*, 17, 215, 1940 and 19, 285, 1942. "Die Amplituden von Geräuschspannungen", *E.N.T.*, 19, 166, 1942. The May 1944 (p. 237), issue of the Wireless Engineer contains an abstract of "The Influence of Carrier Waves on the Noise on the Far Side of Amplitude-Limiters and Linear Rectifiers" by Fränz and Vellat, *E.N.T.*, Vol. 20, pp. 183–189 (Aug. 1943).

Squaring (4.5–1) gives the double series

$$V_N^2 = \frac{1}{4} \sum_{-\infty}^{+\infty} \sum_{-\infty}^{+\infty} c_m c_n e^{i(m+n)at - i\varphi_m - i\varphi_n}$$

$$= \frac{1}{4} \sum_{k=-\infty}^{+\infty} \sum_{n=-\infty}^{+\infty} c_{k-n} c_n e^{ikat - i\varphi_{k-n} - i\varphi_n}$$

Suppose we wish to consider the component of V_N^2 of frequency $f_k = k\Delta f$. It is seen to be

$$A_k \cos(\omega_k t - \psi_k) = \frac{1}{2} \sum_{n=-\infty}^{+\infty} c_{k-n} c_n \cos(kat - \varphi_{k-n} - \varphi_n) \qquad (4.5\text{–}3)$$

The power spectrum $W(f)$ of I at frequency f_k is α^2 times the coefficient of Δf in the mean square value of (4.5–3) where the average is taken over the φ's. Thus

$$W(f_k)\Delta f = \frac{\alpha^2}{4} \sum_{-\infty}^{+\infty} \sum_{-\infty}^{+\infty} c_{k-n} c_n c_{k-m} c_m$$

$$\times \text{ ave. } \cos(kat - \varphi_{k-n} - \varphi_n) \cos(kat - \varphi_{k-m} - \varphi_m)$$

where the summations extend over m and n. Let n be fixed and consider those values of m which give an average different from zero. We see that $m = n$ and $m = k - n$ are two such values. The only other possibilities are $m = -n$ and $m = -k + n$, but these lead to terms containing (except when n or k equal zero) three different angles, φ_n, φ_{k-n}, and φ_{k+n} which average to zero. Using the fact that the average of cosine squared is one-half and that for a given n there are two such terms, we get

$$W(f_k)\Delta f = \frac{\alpha^2}{4} \sum_{n=-\infty}^{+\infty} c_{k-n}^2 c_n^2$$

$$= \alpha^2 \Delta f \sum_{n=-\infty}^{+\infty} w(f_k - f_n) w(f_n) \Delta f \qquad (4.4\text{–}5)$$

where in the last step we have used

$$f_{k-n} = (k - n)\Delta f = f_k - f_n$$

and have implied, from $c_{-n} = c_n$, that

$$w(f_{-n}) = w(-n\Delta f) = w(-f_n)$$

is equal to $w(f_n)$.

Thus, from (4.5–4), we get for the power spectrum of I

$$W(f) = \alpha^2 \int_{-\infty}^{+\infty} w(x) w(f - x)\, dx \qquad (4.5\text{–}5)$$

with the understanding that f is not zero and

$$w(-x) = w(x). \tag{4.5-6}$$

The result which is obtained by using (2.8–6), involving the cosines and only positive values of m, is

$$W(f) = \alpha^2 \int_0^f w(x)w(f - x)\,dx + 2\alpha^2 \int_0^\infty w(x)w(f + x)\,dx \tag{4.5-7}$$

This contains only positive values of frequency. (4.5–5) and (4.5–7) are equivalent and may readily be transformed into each other.

The first integral in (4.5–7) arises from second order modulation products of the sum type and the second integral from products of the difference type. This may be seen by writing the current as

$$\begin{aligned} I = \alpha V^2 &= \alpha \sum_{m=1}^{\infty} \sum_{n=1}^{\infty} c_m c_n \cos(\omega_m t - \varphi_m) \cos(\omega_n t - \varphi_n) \\ &= \frac{\alpha}{2} \sum_{m=1}^{\infty} \sum_{n=1}^{\infty} c_m c_n [\cos[(\omega_m - \omega_n)t - \varphi_m + \varphi_n] \\ &\qquad + \cos[(\omega_m + \omega_n)t + \varphi_m + \varphi_n]\} \end{aligned} \tag{4.5-8}$$

The power in the range $f_k, f_k + \Delta f$ is the power due to modulation products of the difference type, $\omega_{k+\ell} - \omega_\ell$, plus the power due to the modulation products of the sum type, $\omega_{k-\ell} + \omega_\ell$. In the first type ℓ runs from 1 to ∞ and in the second type ℓ runs from 1 to $k - 1$.

Consider the difference type first, and for the moment take both k and ℓ to be fixed. The two sets $m = k + \ell$, $n = \ell$ and $m = \ell$, $n = k + \ell$ are the only values of m and n in (4.5–8) leading to $\omega_{k+\ell} - \omega_\ell$. The two corresponding terms in (4.5–8) are equal because $\cos(-x)$ is equal to $\cos x$. The average power contributed by these two terms is

$$\begin{aligned} &\left(\frac{\alpha}{2} c_{k+\ell}\, c_\ell\right)^2 \times \{\text{Average of } (2\cos[(\omega_{k+\ell} - \omega_\ell)t - \varphi_{k+\ell} + \varphi_\ell])^2\} \\ &\qquad = \tfrac{1}{2}(\alpha c_{k+\ell}\, c_\ell)^2 \end{aligned} \tag{4.5-9}$$

The power contributed to $f_k, f_k + \Delta f$ by the difference modulation products is obtained by summing ℓ from 1 to ∞:

$$\begin{aligned} \frac{\alpha^2}{2} \sum_{\ell=1}^{\infty} c_{k+\ell}^2 c_\ell^2 &= 2\alpha^2 \sum_{\ell=1}^{\infty} w(f_{k+\ell})w(f_\ell)(\Delta f)^2 \\ &\to 2\alpha^2 \Delta f \int_0^\infty w(f_k + f)w(f)\,df \end{aligned}$$

This leads to the second term in (4.5–7).

Now consider the modulation products of the sum type. The terms of this type in (4.5–8) which give rise to the frequency ω_k are those for which $m + n$ is equal to k. Let n be 1 then $m = k - 1$. The phase of this term is random with respect to all the other terms except the one given by $n = k - 1$, $m = 1$ which has the same phase. The average power contributed by these two terms in (4.5–8) is, as in (4.5–9),

$$\tfrac{1}{2}(\alpha c_1 c_{k-1})^2$$

This disposes of two terms for which $m + n$ is equal to k. Taking n to be 2 and going through the same process gives two more. Thus, assuming for the moment that k is an odd number, the power contributed to the interval f_k, $f_k + \Delta f$ by the sum modulation products is

$$\frac{1}{2}\sum_{n=1}^{(k-1)/2}(\alpha c_n c_{k-n})^2 = \frac{1}{4}\sum_{n=1}^{k-1}(\alpha c_n c_{k-n})^2 \to \alpha^2 \Delta f \int_0^{f_k} w(f)w(f_k - f)\,df$$

and this leads to the second term in (4.5–7).

When the voltage V applied to the square law device is the sum of a noise voltage V_N and a sine wave:

$$V = P\cos pt + V_N, \tag{4.1–13}$$

we have

$$V^2 = P^2\cos^2 pt + 2PV_N\cos pt + V_N^2 \tag{4.5–10}$$

From the two equations

$$\cos^2 pt = \frac{1}{2} + \frac{1}{2}\cos 2pt$$

$$\text{ave. } V_N^2 = \sum_1^M c_m^2 \frac{1}{2} \to \int_0^\infty w(f)\,df$$

we see that I, or αV^2, has a dc component of

$$\frac{\alpha P^2}{2} + \alpha\int_0^\infty w(f)\,df \tag{4.5–11}$$

which agrees with (4.1–14), and a sinusoidal component

$$\frac{\alpha P^2}{2}\cos 2pt \tag{4.5–12}$$

The continuous power spectrum $W_c(f)$ of the remaining portion of I may be computed from

$$2PV_N\cos pt + V_N^2.$$

Using the representation (2.8–6) we see

$$2PV_N \cos pt = P \sum_1^M c_m[\cos(\omega_m t + pt - \varphi_m) + \cos(\omega_m t - pt - \varphi_m)]$$

For the moment, we take $p = 2\pi r\Delta f$. The terms pertaining to frequency $f_n = n\Delta f$ are those for which

$$\omega_m + p = 2\pi f_n \qquad |\omega_m - p| = 2\pi f_n$$
$$m + r = n \qquad |m - r| = n$$
$$m = n - r \qquad m = r \pm n$$

where only positive values of m are to be taken: If $n > r$, then m is $n - r$ or $r + n$. If $n < r$, then m is $r - n$ or $r + n$. In either case the values of m are $|n - r|$ and $n + r$. The terms of frequency f_n in $2PV_N \cos pt$ are therefore

$$Pc_{|n-r|} \cos(2\pi f_n t - \varphi_{|n-r|}) + Pc_{n+r} \cos(2\pi f_n t - \varphi_{n+r})$$

and the mean square value of this expression, the average being taken over the φ's, is

$$\frac{P^2}{2}(c^2_{|n-r|} + c^2_{n+r}) = P^2\Delta f[w(f_{|n-r|}) + w(f_{n+r})]$$
$$= P^2\Delta f[w(|f_n - f_p|) + w(f_n + f_p)]$$

where f_p denotes $p/2\pi$.

By combining this with the expression (4.5–5) which arises from V_N^2 we see that the continuous portion $W_c(f)$ of the power spectrum of I is

$$W_c(f) = \alpha^2 P^2[w(f - f_p) + w(f + f_p)] + \alpha^2 \int_{-\infty}^{+\infty} w(x)w(f - x)\,dx \qquad (4.5\text{–}13)$$

where $w(-f)$ has the same value as $w(f)$.

Equation (4.5–13) has been used to compute $W_c(f)$ as shown in Fig. 8. The input noise is assumed to be uniform over a band of width β centered at f_p, cf. Filter c, Appendix C. By noting the area under the low frequency portion of the spectrum we find

$$\int_0^\beta W_c(f)\,df = \alpha^2\beta w_0(P^2 + \beta w_0)$$

Since the mean square value of the input V_N is $\psi_0 = \beta w_0$, it is seen that this equation agrees with the expression (4.1–15) for the mean square value of $I_{\ell f}$, the low frequency current, excluding the d.c. If audio frequency

filters cut out part of the spectrum, $W_c(f)$ may be integrated over the remaining portion to give the mean square value of the corresponding output current. This idea is mentioned in the footnote pertaining to equation (4.1–6).

If V consists of V_N plus two sinusoidal voltages of incommensurable frequencies, say

$$V = P \cos pt + Q \cos qt + V_N ,$$

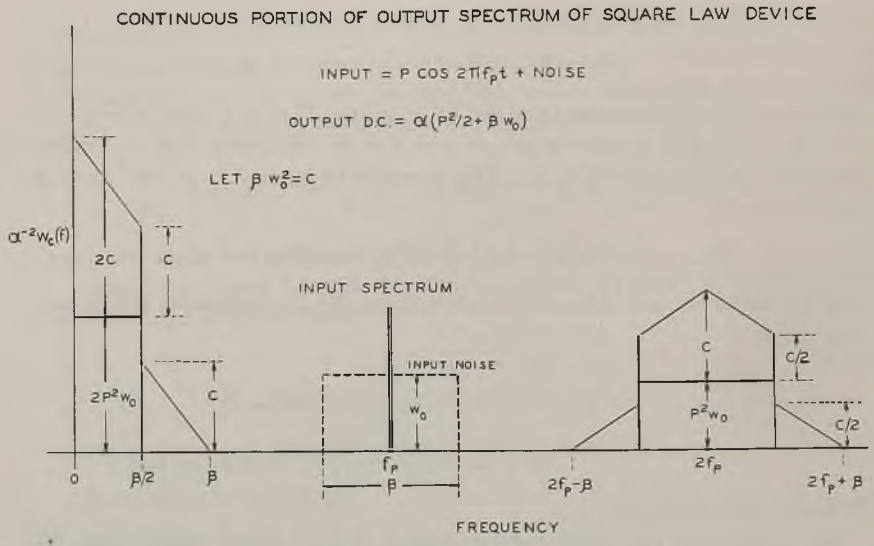

Fig. 8

the continuous portion $W_c(f)$ of the power spectrum of I may be shown to be (4.5–13) plus the additional terms

$$\alpha^2 Q^2 [w(f - f_q) + w(f + f_q)] \tag{4.5–14}$$

where f_q denotes $q/2\pi$.

When the voltage applied to the square law device (4.1–1) is[49]

$$\begin{aligned} V(t) &= Q(1 + k \cos pt) \cos qt + V_N \\ &= Q \cos qt + \frac{Qk}{2} \cos (p + q)t + \frac{Qk}{2} \cos (p - q)t + V_N \end{aligned}$$

the resulting current contains the *dc* component

$$\frac{\alpha}{2} Q^2 \left(1 + \frac{k^2}{2}\right) + \alpha \int_0^\infty w(f)\, df \tag{4.5–16}$$

[49] A complete discussion of this problem is given by L. A. MacColl in a manuscript being prepared for publication.

The sinusoidal terms of I are obtained by squaring

$$Q(1 + k \cos pt) \cos qt$$

and multiplying by α. The remaining portion of I has a continuous power spectrum given by

$$\begin{aligned} W_c(f) = \alpha^2 Q^2 \Big[& w(f - f_q) + w(f + f_q) \\ & + \frac{k^2}{4} w(f - f_p - f_q) + \frac{k^2}{4} w(f + f_p + f_q) \\ & + \frac{k^2}{4} w(f - f_p + f_q) + \frac{k^2}{4} w(f + f_p - f_q) \Big] \\ & + \alpha^2 \int_{-\infty}^{+\infty} w(x) w(f - x)\, dx \end{aligned} \tag{4.5-17}$$

where f_p denotes $p/2\pi$ and f_q denotes $q/2\pi$.

4.6 Two Correlation Function Methods

As mentioned in Section 4.4 these methods for determining the output power spectrum are based on finding the correlation function $\Psi(\tau)$ for the output current. From this the power spectrum, $W(f)$, of the output current may be obtained from (2.1–5), rewritten as

$$W(f) = 4 \int_0^\infty \Psi(\tau) \cos 2\pi f\tau \, d\tau \tag{4.6–1}$$

It will be recalled that $W(f)\Delta f$ may be regarded as the average power which would be dissipated by those components of I in the band $f, f + \Delta f$ if I were to flow through a resistance of one ohm.

The input of the non-linear device is taken to be a voltage $V(t)$. It may, for example, consist of a noise voltage $V_N(t)$ plus sinusoidal components. The output is taken to be a current $I(t)$. The non-linear device is specified by a relation between $V(t)$ and $I(t)$. In this work $I(t)$ at time t is assumed to be completely determined by the value of $V(t)$ at time t.

Two methods of obtaining $\Psi(\tau)$ will be described.

(a) Integrating the two-dimensional probability density of $V(t)$ and $V(t + \tau)$ over the values allowed by the non-linear device. This method, which is especially direct when applied to noise alone through rectifiers, was discovered independently by Van Vleck and North.

(b) Introducing and using the characteristic function, which for the sake of brevity will be abbreviated to ch. f., of the two-dimensional probability distribution of $V(t)$ and $V(t + \tau)$.

4.7 Linear Detection of Noise—The Van Vleck-North Method

The method due to Van Vleck and North will be illustrated by using it to determine the output power spectrum of a linear detector when the input consists of noise alone.

The linear detector is specified by

$$I(t) = \begin{cases} 0, & V(t) < 0 \\ V(t), & V(t) > 0, \end{cases} \tag{4.7-1}$$

which may be obtained from (4.2–1) by setting α equal to one, and the input voltage is

$$V(t) = V_N(t) \tag{4.7-2}$$

where $V_N(t)$ is a noise voltage whose correlation function is $\psi(\tau)$ and whose power spectrum is $w(f)$.

The correlation function $\Psi(\tau)$ is the average value of $I(t)I(t+\tau)$. This is the same as the average value of the function

$$F(V_1, V_2) = \begin{cases} V_1 V_2, & \text{when both } V_1, V_2 > 0 \\ 0, & \text{all other } V\text{'s}, \end{cases} \tag{4.7-3}$$

where we have set

$$V_1 = V(t)$$

$$V_2 = V(t+\tau)$$

The two-dimensional distribution of V_1 and V_2 is given by (3.2–4), and from this it follows that the average value of any function $F(V_1, V_2)$ is

$$\int_{-\infty}^{+\infty} dV_1 \int_{-\infty}^{+\infty} dV_2 \frac{F(V_1, V_2)}{2\pi |M|^{1/2}} \exp\left[-\frac{1}{2|M|}(\psi_0 V_1^2 + \psi_0 V_2^2 - 2\psi_\tau V_1 V_2)\right] \tag{4.7-4}$$

where

$$|M| = \psi_0^2 - \psi_\tau^2.$$

For the linear rectifier case, where $F(V_1, V_2)$ is given by (4.7–3), the integral is

$$|M|^{-1/2} \frac{1}{2\pi} \int_0^\infty dV_1 \int_0^\infty dV_2 V_1 V_2 \exp\left[-\frac{1}{2|M|}(\psi_0 V_1^2 + \psi_0 V_2^2 - 2\psi_\tau V_1 V_2)\right]$$

$$= \frac{1}{2\pi}\left([\psi_0^2 - \psi_\tau^2]^{1/2} + \psi_\tau \cos^{-1}\left[\frac{-\psi_\tau}{\psi_0}\right]\right)$$

where we have used (3.5–4) to evaluate the integral. The arc cosine is taken to be between 0 and π. We therefore have for the correlation function of $I(t)$,

$$\Psi(\tau) = \frac{1}{2\pi}\left([\psi_0^2 - \psi_\tau^2]^{1/2} + \psi_\tau \cos^{-1}\left[\frac{-\psi_\tau}{\psi_0}\right]\right) \tag{4.7–5}$$

The power spectrum $W(f)$ may be obtained from this by use of (4.6–1). For this purpose it is convenient to write (4.7–5) in terms of a hypergeometric function. By expanding and comparing terms it is seen that

$$\begin{aligned}\Psi(\tau) &= \frac{\psi_\tau}{4} + \frac{\psi_0}{2\pi} F\left(-\tfrac{1}{2}, -\tfrac{1}{2}; \tfrac{1}{2}; \frac{\psi_\tau^2}{\psi_0^2}\right) \\ &= \frac{\psi_\tau}{4} + \frac{\psi_0}{2\pi} + \frac{\psi_\tau^2}{4\pi\psi_0} + \text{terms involving } \psi_\tau^4, \psi_\tau^6, \text{ etc.}\end{aligned} \tag{4.7–6}$$

As will be discussed more fully in Section 4.8, a constant term A^2 in $\psi(\tau)$ indicates a direct current component of $I(t)$ of A amperes. Thus $I(t)$ has a *dc* component equal to

$$\left[\frac{\psi_0}{2\pi}\right]^{1/2} = \frac{1}{\sqrt{2\pi}} \times \text{rms value of } V(t) \tag{4.7–7}$$

This agrees with (4.2–3) when the P of that equation is set equal to zero.

Integrals of the form

$$G_n(f) = \int_{J_0}^{\infty} \psi_\tau^n \cos 2\pi f\tau \, d\tau$$

which result when (4.7–6) is put in (4.6–1) and integrated termwise are discussed in Appendix 4C. From the results given there it is seen that if we neglect ψ_τ^4 and higher powers we obtain an approximation for the continuous portion $W_c(f)$ of $W(f)$:

$$\begin{aligned}W_c(f) &\approx G_1(f) + \frac{G_2(f)}{\pi\psi_0} \\ &= \frac{w(f)}{4} + \frac{1}{4\pi\psi_0}\cdot\frac{1}{2}\int_{-\infty}^{+\infty} w(x)w(f-x)\,dx\end{aligned} \tag{4.7–8}$$

where $w(-f)$ is defined as $w(f)$.

When $V_N(t)$ is uniform over a relatively narrow band extending from f_a to f_b so that $w(f)$ is equal to w_0 in this band and is zero outside it, we may use the results for Filter c of Appendix 4C. The f_0 and β given there are related to f_a and f_b by

$$f_a = f_0 - \frac{\beta}{2}, \qquad f_b = f_0 + \frac{\beta}{2}$$

and the value of w_0 taken there is the same as here and is ψ_0/β. The value of $G_2(f)$ given there leads to the approximation, for low frequencies:

$$W_c(f) \approx \frac{1}{\pi\psi_0}\frac{\psi_0^2}{4\beta}\left(1 - \frac{f}{\beta}\right) = \frac{w_0}{4\pi}\left(1 - \frac{f}{f_b - f_a}\right) \tag{4.7–9}$$

when $0 < f < f_b - f_a$, and to $W_0(f) \approx 0$ for $f_b - f_a < f < f_a$. By setting P equal to zero in the curve given in Fig. 8 for $W_c(f)$ corresponding to the square law detector, we see that the low frequency portion of the power spectrum is triangular in shape and is zero at $f = \beta$. Thus, looking at (4.7–9), we see that to a first approximation the shape of the output power spectrum is the same for a linear detector as for a square law detector when the input consists of a relatively narrow band of noise.

An approximate rms value of the low frequency output current may be obtained by integrating (4.7–9)

$$\overline{I_{lf}^2} = \int_0^{f_b - f_a} W_c(f)\, df \approx \frac{w_0(f_b - f_a)}{8\pi} = \frac{\psi_0}{8\pi}$$

$$\text{rms low freq. current} \approx \frac{1}{\sqrt{8\pi}} \times \text{rms applied voltage} \tag{4.7–10}$$

It is seen that this is half of the direct current. It must be kept in mind that (4.7–10) is an approximation because we have neglected ψ_τ^4 and higher powers. The true value may be obtained from (4.2–8). It is seen that the coefficient $(8\pi)^{-1/2} = 0.200$ should be replaced by

$$\frac{1}{\pi}\left(2 - \frac{\pi}{2}\right)^{1/2} = 0.209$$

$W_c(f)$ for other types of band pass filters may be obtained by using the corresponding G's given in appendix 4C. It turns out that (4.7–10) holds for all three types of filters. This is a special case of Middleton's theorem, mentioned several times before, that the total power in any modulation product (it will be shown later in Section 4.9 that the term ψ_τ^n in (4.7–6) corresponds to the n^{th} order modulation products) depends only on the total input power of the applied noise, not on its spectral distribution.

4.8 The Characteristic Function Method

As mentioned in the preceding parts, especially in connection with equation (1.4–3), the ch. f. of a random variable x is the average value of exp

(iux). This is a function of u. The ch. f. of two random variables x and y is the average value of $\exp(iux + ivy)$ and is a function of u and v. The ch. f. which we shall use here is the ch. f. of the two random variables $V(t)$ and $V(t+\tau)$ where $V(t)$ is the voltage applied to the non-linear device, and the randomness is introduced by t being selected at random, τ remaining fixed. We may write this characteristic function as

$$g(u, v, \tau) = \operatorname*{Limit}_{T\to\infty} \frac{1}{T}\int_0^T \exp\left[iuV(t) + ivV(t+\tau)\right] dt \quad (4.8\text{–}1)$$

If $V(t)$ contains a noise voltage $V_N(t)$, as it always does in this section, and if we use the representation (2.8–1) or (2.8–6) a large number of random parameters (a_n's and b_n's or φ_n's) will appear in (4.8–1). In accordance with our use of such representations we may average over these parameters without changing the value of (4.8–1) and may thereby simplify the integration.

For example suppose

$$V(t) = V_s(t) + V_N(t) \quad (4.8\text{–}2)$$

where $V_s(t)$ is some regular voltage which may, e.g., consist of one or more sine waves. Substituting this in (4.8–1) and using the result (3.2–7) that the ch. f. of $V_N(t)$ and $V_N(t+\tau)$ is

$$\begin{aligned} g_N(u, v, \tau) &= \text{ave. } \exp\left[iuV_N(t) + ivV_N(t+\tau)\right] \\ &= \exp\left[-\frac{\psi_0}{2}(u^2 + v^2) - \psi_\tau uv\right] \end{aligned} \quad (4.8\text{–}3)$$

$\psi_\tau \equiv \psi(\tau)$ being the correlation function of $V_N(t)$, we obtain for the ch. f. of $V(t)$ and $V(t+\tau)$,

$$\begin{aligned} g(u, v, \tau) &= \exp\left[-\frac{\psi_0}{2}(u^2 + v^2) - \psi_\tau uv\right] \\ &\quad \times \operatorname*{Limit}_{T\to\infty} \frac{1}{T}\int_0^T \exp\left[iuV_s(t) + ivV_s(t+\tau)\right] dt \\ &= g_N(u, v, \tau) g_s(u, v, \tau) \end{aligned} \quad (4.8\text{–}4)$$

In the last line we have used $g_s(u, v, \tau)$ to denote the limit in the line above:

$$g_s(u, v, \tau) = \operatorname*{Limit}_{T\to\infty} \frac{1}{T}\int_0^T \exp\left[iuV_s(t) + ivV_s(t+\tau)\right] dt \quad (4.8\text{–}5)$$

The principal reason we use the ch. f. is because quite a few non-linear devices may be described by the integral

$$I = \frac{1}{2\pi}\int_C F(iu) e^{iVu}\, du \quad (4A\text{–}1)$$

where the function $F(iu)$ and the path of integration C are chosen to fit the device. Examples of such devices are given in Appendix 4A. The correlation function $\Psi(\tau)$ of $I(t)$ is given by

$$\begin{aligned}\Psi(\tau) &= \operatorname*{Limit}_{T\to\infty} \frac{1}{T}\int_0^T I(t)I(t+\tau)\,dt \\ &= \operatorname*{Limit}_{T\to\infty} \frac{1}{4\pi^2 T}\int_0^T dt \int_C F(iu)e^{iuV(t)}\,du \int_C F(iv)e^{ivV(t+\tau)}\,dv \\ &= \frac{1}{4\pi^2}\int_C F(iu)\,du \int_C F(iv)\,dv \qquad (4.8\text{–}6) \\ &\qquad \operatorname*{Limit}_{T\to\infty} \frac{1}{T}\int_0^T \exp\left[iuV(t) + ivV(t+\tau)\right] dt \\ &= \frac{1}{4\pi^2}\int_C F(iu)\,du \int_C F(iv)g(u, v, \tau)\,dv\end{aligned}$$

This is the fundamental formula of the ch. f. method.

When $V(t)$ is the sum of a noise voltage and a regular voltage, as in (4.8–2), (4.8–6) becomes

$$\begin{aligned}\Psi(\tau) = \frac{1}{4\pi^2}\int_C F(iu)e^{-(\psi_0/2)u^2}\,du \int_C F(iv)e^{-(\psi_0/2)v^2} \\ e^{-\frac{1}{2}\tau uv} g_s(u, v, \tau)\,dv\end{aligned} \qquad (4.8\text{–}7)$$

where $g_s(u, v, \tau)$ is the ch. f. of $V_s(t)$ and $V_s(t+\tau)$ given by (4.8–5). This is a definite expression for $\Psi(\tau)$. All that follows is devoted to the evaluation of this integral and to the evaluation of

$$W(f) = 4\int_0^\infty \Psi(\tau)\cos 2\pi f\tau\,d\tau \qquad (4.6\text{–}1)$$

for the power spectrum of I.

Quite often $I(t)$ will contain *dc* and periodic components. It seems convenient to deal with these separately since they correspond to terms in $\Psi(\tau)$ which cause the integral (4.6–1) for $W(f)$ to diverge. In fact, from Section 2.2 it follows that a correlation function of the form

$$A^2 + \frac{C^2}{2}\cos 2\pi f_0\tau \qquad (2.2\text{–}3)$$

corresponds to a current

$$A + C\cos\left(2\pi f_0 t - \varphi\right) \qquad (2.2\text{–}2)$$

where the phase angle φ cannot be determined from (2.2–3) since it does not affect the average power.

Consider the correlation function for $V(t) = V_s(t) + V_N(t)$ given by (4.8–2). It is

$$\operatorname*{Limit}_{T\to\infty} \frac{1}{T}\left[\int_0^T V_s(t)V_s(t+\tau)\,dt + \int_0^T V_s(t)V_N(t+\tau)\,dt + \int_0^T V_N(t)V_s(t+\tau)\,dt + \int_0^T V_N(t)V_N(t+\tau)\,dt\right] \tag{4.8–8}$$

Since $V_s(t)$ and $V_N(t)$ are unrelated the contributions of the second and third integrals vanish leaving us with the result

$$\text{Correlation function of } V(t) = \text{Correlation function of } V_s(t) + \text{Correlation function of } V_N(t). \tag{4.8–9}$$

Now as $\tau \to \infty$ the correlation function of $V_N(t)$ becomes zero while that of $V_s(t)$ becomes of the type (2.2–3) given above. Hence the correlation function of the regular voltage $V_s(t)$ may be obtained from $V(t)$ by letting $\tau \to \infty$ and picking out the non-vanishing terms. Although we have been speaking of $V(t)$, the same results hold for $I(t)$ and this process may be used to pick out those parts of $\Psi(\tau)$ which correspond to the *dc* and periodic components of $I(t)$. Thus, if we look at (4.8–7) we see that as $\tau \to \infty$, $\psi_\tau \to 0$, while the $g_s(u, v, \tau)$ corresponding to $V_s(t)$ given by (4.8–5) remains unchanged in general magnitude. This last statement may be hard to see, but examination of the cases discussed later show that it is true, at least for these cases. Thus the portion of $\Psi(\tau)$ corresponding to the *dc* and periodic components of $I(t)$ is, setting $\psi_\tau = 0$ in (4.8–7),

$$\Psi_\infty(\tau) = \frac{1}{4\pi^2}\int_C F(iu)e^{-(\psi_0/2)u^2}\,du \int_C F(iv)e^{-(\psi_0/2)v^2} g_s(u, v, \tau)\,dv \tag{4.8–10}$$

where the subscript ∞ indicates that $\Psi_\infty(\tau)$ is that part of $\Psi(\tau)$ which does not vanish as $\tau \to \infty$.

We may write (4.8–9), when applied to $I(t)$, as

$$\Psi(\tau) = \Psi_\infty(\tau) + \Psi_c(\tau) \tag{4.8–11}$$

where $\Psi_c(\tau)$ is the correlation function of the "continuous" portion of the power spectrum of $I(t)$.

Incidentally, the separation of $\Psi(\tau)$ into the two parts shown in (4.8–11) may be avoided if one is willing to use the $\delta(f)$ functions in order to interpret the integral in (4.6–1) as explained in Section 2.2. This method gives the proper *dc* and sinusoidal components even though (4.6–1) does not converge (because of the presence of the terms leading to $\Psi_\infty(\tau)$).

4.9 Noise Plus Sine Wave Applied to Non-Linear Device

In order to illustrate the characteristic function method described in Section 4.8 we shall consider the case of a non-linear device specified by

$$I = \frac{1}{2\pi} \int_C F(iu) e^{iVu}\, du \tag{4A-1}$$

when V consists of a noise voltage plus a sine wave:

$$V(t) = P \cos pt + V_N(t) \tag{4.1-13}$$

As usual, $V_N(t)$ has the power spectrum $w(f)$ and the correlation function $\psi(\tau)$. $\psi(\tau)$ is often written as ψ_τ for the sake of shortness. Comparing (4.1–13) with (4.8–2) gives

$$V_s(t) = P \cos pt \tag{4.9-1}$$

Our first task is to compute the ch. f. $g_s(u, v, \tau)$ for the pair of random variables $V_s(t)$ and $V_s(t + \tau)$. We do this by using the integral (4.8–5):

$$\begin{aligned} g_s(u, v, \tau) &= \operatorname*{Limit}_{T\to\infty} \frac{1}{T} \int_0^T \exp\left[iuP \cos pt + ivP \cos p(t + \tau)\right] dt \\ &= J_0(P\sqrt{u^2 + v^2 + 2uv \cos p\tau}) \end{aligned} \tag{4.9-2}$$

where J_0 is a Bessel function. The integration is performed by writing

$$\begin{aligned} u \cos pt + v \cos p\,(t + \tau) &= (u + v \cos p\tau) \cos pt - v \sin p\tau \sin pt \\ &= \sqrt{u^2 + v^2 + 2uv \cos p\tau}\, \cos\,(pt + \text{phase angle}) \end{aligned}$$

and using the integral

$$J_0(z) = \frac{1}{2\pi} \int_0^{2\pi} e^{iz \cos t}\, dt$$

The correlation function for (4.1–13) has also been given in Section 3.10.

The correlation function $\Psi(\tau)$ for $I(t)$ may now be obtained by substituting the above expressions in (4.8–7)

$$\begin{aligned} \Psi(\tau) = \frac{1}{4\pi^2} \int_C du\, F(iu) e^{-(\psi_0/2)u^2} \int_C dv\, F(iv) e^{-(\psi_0/2)v^2} \\ e^{-\psi_\tau uv} J_0(P\sqrt{u^2 + v^2 + 2uv \cos p\tau}). \end{aligned} \tag{4.9-3}$$

$\Psi_\infty(\tau)$, the correlation function for the d.c. and periodic components of I, may, according to (4.8–10), be obtained from this by setting ψ_τ equal to zero.

When we have a particular non-linear device in mind the appropriate $F(iu)$ may often be obtained from Appendix 4*A*. For example, $F(iu)$ for a linear rectifier is $-u^{-2}$. Inserting this value in (4.9–3) gives a definite

double integral for $\Psi(\tau)$. If there were some easy way to evaluate this integral then everything would be fine. Unfortunately, no simple method of evaluation has yet been found. However, one method is available which is closely related to the direct method used by Bennett. It is based on the expansion

$$g_s(u, v, \tau) = J_0(P\sqrt{u^2 + v^2 + 2uv \cos p\tau})$$
$$= \sum_{n=0}^{\infty} \epsilon_n (-)^n J_n(Pu) J_n(Pv) \cos np\tau \qquad (4.9\text{–}4)$$
$$\epsilon_0 = 1, \quad \epsilon_n = 2 \quad \text{for} \quad n \geq 1$$

This expansion enables us to write the troublesome terms in (4.9–3) as

$$e^{-\psi_\tau uv} J_0(P\sqrt{u^2 + v^2 + 2uv \cos p\tau})$$
$$= \sum_{n=0}^{\infty} \sum_{k=0}^{\infty} (-)^{n+k} \epsilon_n \cos np\tau \frac{(\psi_\tau uv)^k}{k!} J_n(Pu) J_n(Pv) \qquad (4.9\text{–}5)$$

The virtue of this double sum is that it simplifies the integration. Thus, putting it in (4.9–3) and setting

$$h_{nk} = \frac{i^{n+k}}{2\pi} \int_c F(iu) u^k J_n(Pu) e^{-(\psi_0/2)u^2} du \qquad (4.9\text{–}6)$$

gives

$$\Psi(\tau) = \sum_{n=0}^{\infty} \sum_{k=0}^{\infty} \frac{1}{k!} \psi_\tau^k h_{nk}^2 \epsilon_n \cos np\tau \qquad (4.9\text{–}7)$$

The correlation function $\Psi_\infty(\tau)$ for the dc and periodic components of I are obtained by letting $\tau \to \infty$ where $\psi_\tau \to 0$. Only the terms for which $k = 0$ remain:

$$\Psi_\infty(\tau) = \sum_{n=0}^{\infty} \epsilon_n h_{n0}^2 \cos np\tau \qquad (4.9\text{–}8)$$

Comparing this with the known fact that the correlation function of

$$A + C \cos (2\pi f_0 t - \varphi) \qquad (2.2\text{–}2)$$

is

$$A^2 + \frac{C^2}{2} \cos 2\pi f_0 \tau \qquad (2.2\text{–}3)$$

and remembering that ϵ_0 is one while ϵ_n is two for $n \geq 1$ shows that

$$\text{Amplitude of dc component of } I = h_{00}$$
$$\text{Amplitude of } \frac{np}{2\pi} \text{ component of } I = 2h_{n0} \qquad (4.9\text{–}9)$$

Incidentally, these expressions for the amplitudes follow almost at once from the direct method of solution. This will be shown in connection with equation (4.9–17).

Since the correlation function $\Psi_c(\tau)$ for the continuous portion $W_c(f)$ of the power spectrum for I is given by

$$\Psi_c(\tau) = \Psi(\tau) - \Psi_\infty(\tau), \tag{4.8–11}$$

we also have

$$\Psi_c(\tau) = \sum_{n=0}^{\infty} \sum_{k=1}^{\infty} \frac{1}{k!} \psi_\tau^k h_{nk}^2 \epsilon_n \cos np\tau \tag{4.9–10}$$

When this is substituted in

$$W_c(f) = 4 \int_0^\infty \Psi_c(\tau) \cos 2\pi f\tau \, d\tau \tag{4.9–11}$$

we obtain

$$W_c(f) = \sum_{n=0}^{\infty} \sum_{k=1}^{\infty} \frac{2\epsilon_n}{k!} h_{nk}^2 \left[G_k\left(f - \frac{np}{2\pi}\right) + G_k\left(f + \frac{np}{2\pi}\right)\right] \tag{4.9–12}$$

where

$$G_k(f) = \int_0^\infty \psi_\tau^k \cos 2\pi f\tau \, d\tau \tag{4.9–13}$$

is the function studied in Appendix 4C. $G_k(f)$ is an even function of f. The double series (4.9–12) for W_c looks rather formidable. However, when we are interested in a particular portion of the frequency spectrum often only a few terms of the series are needed.

It has been mentioned above that the direct method of obtaining the output power spectrum is closely related to the equations just derived. We now study this relation.

We start with the following result from modulation theory[50]: Let the voltage

$$\begin{aligned} V &= P_0 \cos x_0 + P_1 \cos x_1 + \cdots + P_N \cos x_N \\ x_k &= p_k t, \qquad k = 0, 1, \cdots N, \end{aligned} \tag{4.9–14}$$

where the p_k's are incommensurable, be applied to the device (4A–1). The output current is

$$I = \sum_{m_0=0}^{\infty} \cdots \sum_{m_N=0}^{\infty} \tfrac{1}{2} A_{m_0 \cdots m_N} \epsilon_{m_0} \cdots \epsilon_{m_N} \cos m_0 x_0 \cos m_1 x_1 \cdots \cos m_N x_N \tag{4.9–15}$$

[50] Bennett and Rice, "Note on Methods of Computing Modulation Products," *Phil. Mag.* S.7, V. 18, pp. 422–424, Sept. 1934, and Bennett's paper cited in Section 4.0.

where $\epsilon_0 = 1$ and $\epsilon_m = 2$ for $m \geq 1$. When the product of the cosines is expressed as a sum of cosines of the angles $m_0 x_0 \pm m_1 x_1 \cdots \pm m_N x_N$, it is seen that the coefficient of the typical term is $A_{m_0 \cdots m_N}$, except when all the m's are zero in which case it is $\frac{1}{2}A_{0\cdots 0}$. Thus

$$\begin{aligned} \tfrac{1}{2}A_{00\cdots 0} &= \text{dc component of } I \\ |\, A_{m_0 \cdots m_N} \,| &= \text{amplitude of component of frequency} \\ &\frac{1}{2\pi} |\, m_0 p_0 \pm m_1 p_1 \pm \cdots \pm m_N p_N \,| \end{aligned} \tag{4.9–16}$$

For all values of the m's,

$$\begin{aligned} A_{m_0 \cdots m_N} &= \frac{i^M}{\pi} \int_C F(iu) \prod_{r=0}^{N} J_{m_r}(P_r u)\, du \\ M &= m_0 + m_1 + \cdots + m_N \end{aligned} \tag{4.9–17}$$

Following Bennett's procedure, we identify V as given by (4.9–14), with

$$V = P \cos pt + V_N \tag{4.1–13}$$

by setting $P_0 = P$, $p_0 = p$, and representing the noise voltage V_N by the sum of the remaining terms. Since this makes P_1, P_N all very small, Laplace's process indicates that in (4.9–17) we may put

$$\begin{aligned} \prod_{r=1}^{N} J_0(P_r u) &\approx \exp -\frac{u^2}{4}(P_1^2 + \cdots + P_N^2) \\ &\approx e^{-\psi_0 u^2/2} \end{aligned} \tag{4.9–18}$$

We have used the fact that ψ_0 is the mean square value of V_N. It follows from these equations that

$$\text{dc component of } I = \frac{1}{2\pi} \int_C F(iu) J_0(Pu) e^{(-\psi_0/2)u^2}\, du$$

$$\text{Component of frequency } \frac{np}{2\pi} = \frac{i^n}{\pi} \int_C F(iu) J_n(Pu) e^{-\psi_0 u^2/2}\, du$$

These results are identical with those of (4.9–9).

The equations just derived show that h_{n0} is to be associated with the n^{th} harmonic of p. In much the same way it may be shown that h_{nk} is to be associated with the modulation products arising from the n^{th} harmonic of p and k of the elementary sinusoidal components representing V_N. We consider only combinations of the form $p_1 \pm p_2 \pm p_3$, taking $k = 3$ for example, and neglect terms of the form $3p_1$ and $2p_1 \pm p_2$. The former type is much more numerous, there being about N^3 of them while there are only about N and N^2, respectively, of the latter type.

We again take $k = 3$ and consider m_1, m_2, m_3 to be one, and m_4, $\cdots$ m_N to be zero, corresponding to the modulation product $np \pm p_1 \pm p_2 \pm p_3$. By making the same sort of approximations as Bennett does we find

$$A_{n,1,1,1,0,0,\cdots 0} = \frac{i^{n+3}}{\pi} \frac{P_1 P_2 P_3}{8} \int_C F(iu) J_n(Pu) u^3 e^{(-u^2/2)\psi_0} \, du$$

$$= \frac{P_1 P_2 P_3}{4} h_{n3}$$

When any other modulation product of the form $np \pm p_{r_1} \pm p_{r_2} \pm p_{r_3}$ is considered we get a similar expression in which $P_1 P_2 P_3$ is replaced by $P_{r_1} P_{r_2} P_{r_3}$. This may be done for any value of k. The result indicates that h_{nk}, and consequently also the $(n, k)^{\text{th}}$ terms in the double series (4.9–10) and (4.9–12) for $\Psi_c(\tau)$ and $W_c(f)$, are to be associated with the modulation products of order (n, k), the n referring to the signal and the k to the noise components.

We now may state a theorem due to Middleton regarding the total power in the modulation products of a given order. For a given non-linear device (i.e. $F(iu)$ is given), the total power which would be dissipated by all of the modulation products which are of order (n, k) if I were to flow through a resistance of one ohm is

$$\Psi_{nk}(0) = \frac{\epsilon_n [\psi(0)]^k}{k!} h_{nk}^2 = \frac{\epsilon_n [\overline{V_N^2}]^k h_{nk}^2}{k!} \tag{4.9–19}$$

The important feature of this expression is that it depends only on the r.m.s. value of V_N and on $F(iu)$. It depends not at all upon the spectral distribution of the noise power in the input.

The proof of (4.9–19) is based on the relation

$$\Psi_{nk}(0) = \int_0^\infty W_{nk}(f) \, df$$

between the total power dissipated by all the (n, k) order products and the corresponding correlation function obtained from (4.9–7).

This theorem has been used by Middleton to show that when the input is confined to a relatively narrow frequency band, so that the output spectrum consists of bands, the power in each band depends only on $\overline{V_N^2}$ and not on the spectrum of V_N.

4.10 Miscellaneous Results Obtained by Correlation Function Method

In this section a number of results which may be obtained from the theory given in the sections following 4.6 are given.

When the input to the square law device

$$I = \alpha V^2 \tag{4.1-1}$$

consists of noise only, so that $V = V_N$, the correlation function for I is

$$\Psi(\tau) = \alpha^2[\psi_0^2 + 2\psi_\tau^2] \tag{4.10-1}$$

where ψ_τ is the correlation function of V_N. This may be compared with equation (3.9–7). When V is general,

$$\begin{aligned}\Psi(\tau) &= \text{ave. } I(t)I(t+\tau)\\ &= \text{ave. } \alpha^2 V^2(t)V^2(t+\tau)\\ &= \alpha^2 \times \text{Coefficient of } \frac{(iu)^2}{2!}\frac{(iv)^2}{2!} \text{ in power series expansion}\\ &\qquad\qquad \text{of ch. f. of } V(t),\ V(t+\tau)\end{aligned} \tag{4.10-2}$$

where we have used a known property of the characteristic function. An expression for the ch. f., denoted by $g(u, v, \tau)$, is given by (4.8–4). For example, when V consists of a sine wave plus noise, (4.1–13), the ch. f. is obtainable from (4.9–3). Hence,

$$\begin{aligned}\Psi(\tau) &= \text{Coeff. of } \frac{u^2v^2}{4} \text{ in expansion of}\\ &\qquad \alpha^2 J_0\left(P\sqrt{u^2 + v^2 + 2uv\cos p\tau}\right)\\ &\qquad \times \exp\left[-\frac{\psi_0}{2}(u^2 + v^2) - \psi_\tau uv\right]\\ &= \alpha^2\left[\left(\frac{P}{2} + \psi_0\right)^2 + \frac{P^4}{8}\cos 2p\tau + 2P^2\psi_\tau \cos p\tau + 2\psi_\tau^2\right]\end{aligned} \tag{4.10-3}$$

The first two terms give the dc and second harmonic. The last two terms may be used to compute $W_o(f)$ as given by (4.5–13).

Expressions (4.10–1) and (4.10–3) are special cases of results obtained by Middleton who has studied the general theory of the quadratic rectifier by using the Van Vleck-North method, described in Section 4.7.

As an example to which the theory of Section 4.9 may be applied we consider the sine wave plus noise, (4.1–13), to be applied to the ν-law rectifier

$$\begin{aligned} I &= 0, \qquad V < 0\\ I &= V^\nu, \qquad V > 0\end{aligned} \tag{4.10-4}$$

From the table in Appendix 4*A* it is seen that

$$F(iu) = \Gamma(\nu + 1)(iu)^{-\nu-1}$$

and that the path of integration C runs along the real axis from $-\infty$ to ∞ with a downward indentation at the origin. The integral (4.9–6) for h_{nk} becomes

$$h_{nk} = \frac{i^{n+k-\nu-1}}{2\pi}\,\Gamma(\nu+1)\int_C u^{k-\nu-1}J_n(Pu)e^{-(\psi_0/2)u^2}\,du$$

$$= \frac{\left(\frac{\psi_0}{2}\right)^{(\nu-k)/2} x^{n/2}\,\Gamma(\nu+1)}{2\Gamma\left(\frac{2-k-n+\nu}{2}\right)n!}\,{}_1F_1\left(\frac{k+n-\nu}{2};\, n+1;\, -x\right) \qquad (4.10\text{–}5)$$

$$x = \frac{P^2}{2\psi_0}$$

where the integration has been performed by expanding $J_n(Pu)$ in powers of u and using

$$\int_C e^{-au^2}u^{2\lambda-1}\,du = ie^{-\lambda i\pi}a^{-\lambda}\sin\lambda\pi\Gamma(\lambda)$$

$$= \frac{a^{-\lambda}}{2}(1-e^{-2\lambda i\pi})\Gamma(\lambda) \qquad (4.10\text{–}6)$$

$$= \frac{i\pi e^{-\lambda i\pi}}{a^{\lambda}\Gamma(1-\lambda)}$$

it being understood that $\arg u = 0$ on the positive portion of C.

From (4.9–9), the dc component of I is

$$h_{00} = \frac{\Gamma(1+\nu)}{2\Gamma\left(1+\frac{\nu}{2}\right)}\left(\frac{\psi_0}{2}\right)^{\nu/2}{}_1F_1\left(-\frac{\nu}{2};\, 1;\, -x\right) \qquad (4.10\text{–}7)$$

which reduces to the expression (4.2–3) when $\nu = 1$ for the linear rectifier (aside from the factor α).

When the input (sine wave plus noise) is confined to a relatively narrow band, and when we are interested in the low frequency output, consideration of the modulation products suggests that we consider the difference products from the products of order (0, 0), (0, 2), (0, 4), $\cdots$ (1, 1), (1, 3), $\cdots$ (2, 0), (2, 2), $\cdots$ etc. where the typical product is of order (n, k). The orders (0, 0) and (2, 0) give the dc and second harmonic and hence are not considered in the computation of $W_c(f)$. Of the remaining terms, either (0, 2) or (1, 1) gives the greatest contribution to the series (4.9–12) and (4.9–10) for $W_c(f)$ and $\Psi_c(\tau)$. The remaining terms contribute less and less as n and

k increase. The low frequency portion of the continuous portion of the output power spectrum is then, from (4.9–12),

$$W_c(f) = \frac{4}{2!} h_{02}^2 G_2(f) + \frac{4}{4!} h_{04}^2 G_4(f) + \cdots$$

$$+ \frac{4}{1!} h_{11}^2 [G_1(f - f_0) + G_1(f + f_0)] + \frac{4}{3!} h_{13}^2 [G_3(f - f_0) \quad (4.10\text{–}8)$$

$$+ G_3(f + f_0)] + \frac{4}{2!} h_{22}^2 [G_2(f - 2f_0) + G_2(f + 2f_0)] + \cdots$$

From Table 2 of Appendix 4C we may pick out the low frequency portions of the G's. It must be remembered that $G_m(x)$ is an even function of x and that $0 < f \ll f_0$.

As an example we take the input noise V_N to have the same $w(f)$ and $\psi(\tau)$ as Filter a, the normal law filter, of Appendix 4C, so that

$$w(f) = \frac{1}{\sigma\sqrt{2\pi}} e^{-(f-f_0)^2/2\sigma^2}$$

and assume that the sine wave signal is at the middle of the band, giving $p = 2\pi f_0$. Thus, from (4.10–8), for low frequencies and the normal law distribution of the input noise power,

$$W_c(f) = \frac{1}{4\sigma\sqrt{\pi}} h_{02}^2 \psi_0^2 e^{-f^2/4\sigma^2} + \frac{1}{64\sigma\sqrt{2\pi}} h_{04}^2 \psi_0^4 e^{-f^2/8\sigma^2}$$

$$+ \frac{2}{\sigma\sqrt{2\pi}} h_{11}^2 \psi_0 e^{-f^2/2\sigma^2} + \frac{1}{4\sigma\sqrt{6\pi}} h_{13}^2 \psi_0^3 e^{-f^2/6\sigma^2} \quad (4.10\text{–}9)$$

$$+ \frac{1}{4\sigma\sqrt{\pi}} h_{22}^2 \psi_0^2 e^{-f^2/4\sigma^2} + \cdots$$

Although we have been speaking of the ν-law rectifier, equation (4.10–9) gives the low frequency portion of $W_c(f)$, corresponding to a normal law noise power, for any non-linear device provided the proper h_{nk}'s are inserted.

When we set ν equal to one in the expression (4.10–5) for h_{nk} we may obtain the results given by Bennett. Middleton has studied the output of a biased linear rectifier, when the input consists of a sine wave plus noise, and also the special case of the unbiased linear rectifier. He has computed the output for a wide range of the ratios P^2/ψ_0, B^2/ψ_0 where B is the bias. In order to cover the entire range he had to derive two series for the corresponding h_{nk}'s, each series being suitable for its particular portion of the range.

A special case of (4.10–9) occurs when noise alone is applied to a linear rectifier. The low frequency portion of the output power spectrum is

$$W_c(f) = \frac{\psi_0}{\pi} \sum_{m=1}^{\infty} \frac{(-\tfrac{1}{2})_m (-\tfrac{1}{2})_m}{m!\,m!} \frac{1}{\sigma\sqrt{4m\pi}} e^{-f^2/4m\sigma^2}$$

$$= \frac{\psi_0 \pi^{-3/2}}{2\sigma} \left[\tfrac{1}{4} e^{-f^2/4\sigma^2} + \frac{1}{64\sqrt{2}} e^{-f^2/8\sigma^2} + \frac{1}{256\sqrt{3}} e^{-f^2/12\sigma^2} + \cdots \right] \tag{4.10–10}$$

where we have used (4.7–6) and Table 2 of Appendix 4C.

The correlation function of

$$V_s = P \cos pt + Q \cos qt,$$

where p and q are incommensurable, is

$$J_0(P\sqrt{u^2 + v^2 + 2uv \cos p\tau}) \times J_0(Q\sqrt{u^2 + v^2 + 2uv \cos q\tau})$$

From equations (4.9–16) and (4.9–17) it is seen immediately that

$$h_{000} = \frac{1}{2\pi} \int_C F(iu) J_0(Pu) J_0(Qu) e^{-(u^2/2)\psi_0}\, du \tag{4.10–11}$$

is the d.c. component of I when the applied voltage is

$$P \cos pt + Q \cos qt + V_N\,. \tag{4.1–4}$$

J. R. Ragazzini has obtained an approximate expression for the output power spectrum when the voltage

$$\begin{aligned} V &= V_s + V_N \\ V_s &= Q(1 + r \cos pt)\cos qt \end{aligned} \tag{4.10–12}$$

is impressed on a linear rectifier.[46] In terms of our notation his expression for the continuous portion of the power spectrum is (for low frequencies)

$$W_c(f) = \frac{1}{\pi^2 \alpha^2 (Q^2 + 2\psi_0)} \times \left[\begin{array}{l} W_c(f) \text{ given by equation} \\ (4.5\text{–}17) \text{ for square law device} \end{array} \right] \tag{4.10–13}$$

The α^2 is put in the denominator to cancel the α^2 in the expression (4.5–17). We take the linear rectifier to be

$$I = \begin{cases} 0, & V < 0 \\ V, & 0 < V \end{cases} \tag{4.10–14}$$

and replace the index of modulation, k, in (4.5–17) by r.

[46] Equation (12), "The Effect of Fluctuation Voltages on the Linear Detector," *Proc. I.R.E.*, V. 30, pp. 277–288 (June 1942).

Ragazzini's formula is quite accurate when the index of modulation r is small, especially when $y = Q^2/(2\psi_0)$ is large. To show this we put $r = 0$ in (4.10–13) and obtain

$$W_c(f) = \frac{1}{\pi^2(Q^2 + 2\psi_0)}\left[Q^2 w(f_q - f) + Q^2 w(f_q + f) + \int_{-\infty}^{+\infty} w(x)w(f - x)\,dx\right] \tag{4.10–15}$$

where $f_q = q/(2\pi)$. This is to be compared with the low frequency portion of $W_c(f)$ obtained by specializing (4.10–8) to obtain the output power spectrum of a linear rectifier when the input consists of a sine wave plus noise. The leading terms in (4.10–8) give

$$W_c(f) = h_{11}^2[w(f_q - f) + w(f_q + f)] + h_{02}^2 \frac{1}{4}\int_{-\infty}^{+\infty} w(x)w(f - x)\,dx \tag{4.10–16}$$

The values of the h's appropriate to a linear rectifier are obtained by setting $\nu = 1$ in (4.10–5) and noticing that Q now plays the role of P.

$$\begin{aligned} h_{11} &= \frac{1}{2}\left(\frac{y}{\pi}\right)^{1/2} {}_1F_1(\tfrac{1}{2}; 2; -y) \\ h_{02} &= (2\pi\psi_0)^{-1/2}\, {}_1F_1(\tfrac{1}{2}; 1; -y) \\ y &= Q^2/(2\psi_0) \end{aligned} \tag{4.10–17}$$

Incidentally, the first approximation to the output of a linear rectifier given by (4.10–16) is interesting in its own right. Fig. 9 shows the low frequency portion of $W_c(f)$ as computed from (4.10–16) when the input noise is uniformly distributed over a narrow frequency band of width β, f_q being the mid-band frequency. h_{11} and h_{02} may be obtained from the curves shown in Fig. 10. In these figures P and x replace Q and y of (4.10–17) in order to keep the notation the same as in Fig. 8 for the square law device. These curves may also be obtained from equations (33) to (43) of Bennett's paper.

The following values are useful for our comparison.

When $x = 0$	When x is large
$h_{11} = 0$	$h_{11} = 1/\pi$
$h_{02} = (2\pi\psi_0)^{-1/2}$	$h_{02} = 1/(\pi Q)$.

(4.10–18)

The values for large x are obtained from the asymptotic expansion (4B – 3) given in Appendix 4B.

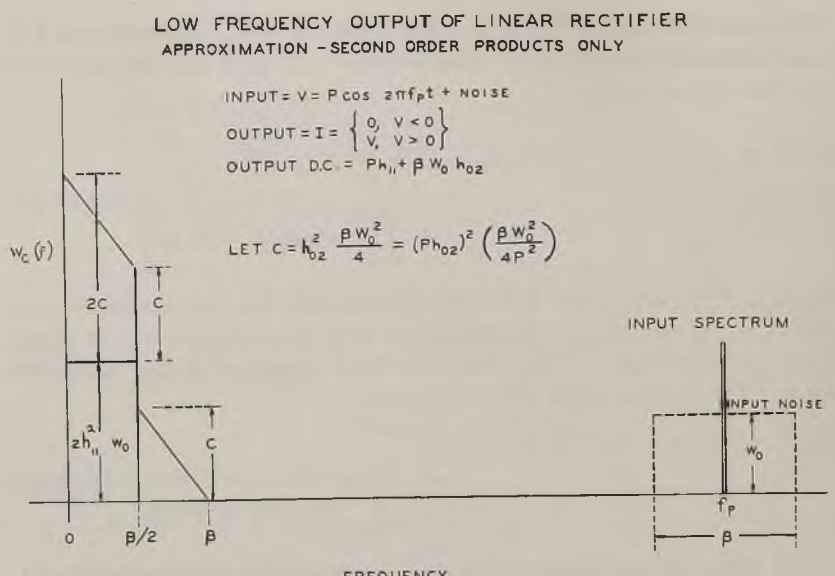

Fig. 9

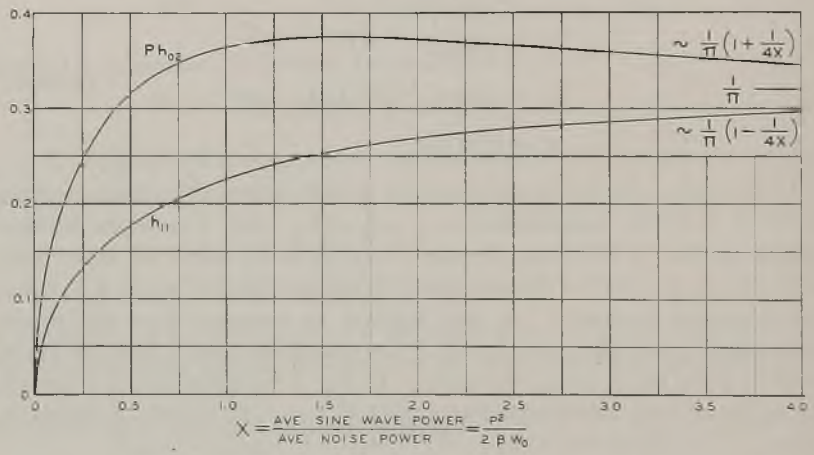

Fig. 10—Coefficients for linear detector output shown on Fig. 9

$$Ph_{02} = \sqrt{\frac{x}{\pi}}\,{}_1F_1(\tfrac{1}{2};\,1;\,-x) \qquad h_{11} = \frac{1}{2}\sqrt{\frac{x}{\pi}}\,{}_1F_1(\tfrac{1}{2};\,2;\,-x)$$

We make the first comparison between (4.10–15) and (4.10–16) by letting $Q \to \infty$. It is seen that both reduce to

$$W_c(f) = \frac{1}{\pi^2}\,[w(f_a - f) + w(f_a + f)] \qquad (4.10\text{–}19)$$

which shows that the agreement is perfect in this case. Next we let $Q = 0$. The two expressions then give

$$W_c(f) = \frac{1}{A 2\pi\psi_0} \int_{-\infty}^{+\infty} w(x)w(f - x)\, dx$$

where $A = \pi$ for Ragazzini's formula and $A = 4$ for (4.10–16). Thus the agreement is still quite good. The limiting value for (4.10–16) may also be obtained from (4.7–8).

Even if the index of modulation r is not negligibly small it may be shown that when $Q \to \infty$ $W_c(f)$ still approaches the value given by (4.10–19). Ragazzini's formula gives a somewhat larger answer because it includes the additional terms, shown in (4.5–17), which contain $k^2/4$, but this difference does not appear to be serious. If the $Q^2 + 2\psi_0$ in the denominator of (4.10–13) be replaced by $Q^2 + \frac{1}{2}Q^2k^2 + 2\psi_0$ the agreement is improved.

APPENDIX 4A

Table of Non-linear Devices Specified by Integrals

Quite a number of non-linear devices may be specified by integrals of the form

$$I = \frac{1}{2\pi} \int_C F(iu)e^{iVu}\, du \tag{4A–1}$$

where the function $F(iu)$ and the path of integration C are chosen to fit the device.* The table gives examples of such devices. Some important cases cannot be simply represented in this form. An example is the limiter

$$\begin{aligned} I &= -\alpha D, && V < -D \\ I &= \alpha V, && -D < V < D \\ I &= \alpha D, && D < V \end{aligned} \tag{4A–2}$$

which may be represented as

$$\begin{aligned} I &= \frac{2\alpha}{\pi} \int_0^{\infty} \sin Vu \sin Du \frac{du}{u^2} \\ &= -\alpha D + \frac{2\alpha}{2\pi i} \int_C e^{iVu} \sin Du \frac{du}{u^2} \end{aligned} \tag{4A–3}$$

where C runs from $-\infty$ to $+\infty$ and is indented downward at the origin. This is not of the form assumed in the theory of Part IV. However it appears that it would not be difficult to extend the theory in the particular case of the limiter.

* Reference 50 cited in Section 4.9.

Non-Linear Devices Specified by Integrals

$$I = \frac{1}{2\pi} \int_C F(iu) e^{iVu}\, du$$

I	$F(iu)$	C	Type of Device
$I = \alpha V^n$, n integer	$\frac{\alpha\, n!}{(iu)^{n+1}}$	Positive Loop around $u = 0$	nth power device
$I = \alpha(V - B)^n$, n integer	$\frac{\alpha\, n!}{(iu)^{n+1}} e^{-iuB}$	Positive Loop around $u = 0$	nth power device with bias
$I = 0, \quad V < 0$ $I = \alpha V, \quad 0 < V$	$\frac{\alpha}{(iu)^2} = -\frac{\alpha}{u^2}$	Real u axis from $-\infty$ to $+\infty$ with downward indentation at $u = 0$	Linear rectifier cut-off at $V = 0$
$I = 0, \quad V < B$ $I = \alpha(V - B)^\nu$, $V > B$ ν any positive number	$\frac{\alpha\Gamma(\nu + 1)}{(iu)^{\nu+1}} e^{-iuB}$	"	νth power rectifier with bias
$I = 0, \quad V < 0$ $I = \alpha V, \quad 0 < V < D$ $I = \alpha D, \quad D < V$	$\frac{\alpha(1 - e^{-iuD})}{(iu)^2}$	"	Linear rectifier plus limiter
$I = 0, \quad V < 0$ $I = \varphi(V), \quad V > 0$	$F(p) = \int_0^\infty e^{-pt}\varphi(t)\, dt$	"	

APPENDIX 4B

The Function ${}_1F_1(a; c; x)$

In problems concerning a sine wave plus noise the hypergeometric function

$${}_1F_1(a; c; z) = 1 + \frac{az}{c1!} + \frac{a(a + 1)}{c(c + 1)} \frac{z^2}{2!} + \cdots \tag{4B-1}$$

arises. Here we state some of its properties which are of use in the theory of Part IV. Curves of ${}_1F_1(a; c; z)$ are given for $a = -4, -3.5 \cdots, 3.5, 4.0$ and $c = -1.5, -.5, +.5, 1, 1.5, 2, 3, 4$ in the 1938 edition, page 275, of "Tables of Functions", by Jahnke and Emde. A list of properties of the function and other references are also given. In addition to these references we mention E. T. Copson, "Functions of a Complex Variable" (Oxford, 1935), page 260.

If c is not a negative integer or zero

$${}_1F_1(a; c; z) = e^z {}_1F_1(c - a; c; -z). \tag{4B-2}$$

When $R(z) > 0$ we have the asymptotic expansions

$$
\begin{aligned}
{}_1F_1(a; c; z) &\sim \frac{\Gamma(c)e^z}{\Gamma(a)z^{c-a}}\left[1 + \frac{(1-a)(c-a)}{1!z}\right. \\
&\left. + \frac{(1-a)(2-a)(c-a)(c-a+1)}{2!z^2} + \cdots\right] \\
{}_1F_1(a; c; -z) &\sim \frac{\Gamma(c)}{\Gamma(c-a)z^a}\left[1 + \frac{a(1+a-c)}{1!z}\right. \\
&\left. + \frac{a(a+1)(1+a-c)(2+a-c)}{2!z^2} + \cdots\right]
\end{aligned}
\tag{4B-3}
$$

Many of the hypergeometric functions encountered may be expressed in terms of Bessel functions of the first kind for imaginary argument. The connection may be made by means of the relation[51]

$${}_1F_1\left(\nu + \frac{1}{2}; 2\nu + 1; z\right) = 2^{2\nu}\Gamma(\nu+1)z^{-\nu}e^{z/2}I_\nu\left(\frac{z}{2}\right) \tag{4B-4}$$

together with the recurrence relations

	F_{a+}	F_{a-}	F_{c+}	F_{c-}	F
1.	a	$(a-c)$			$c - 2a - z$
2.	ac		$(c-a)z$		$-c(a+z)$
3.	a			$1-c$	$c - a - 1$
4.		$-c$	$-z$		c
5.		$a-c$		$c-1$	$1 - a - z$
6.			$(c-a)z$	$c(c-1)$	$c(1-c-z)$

For example, the first recurrence relation is obtained from line 1 as follows

$$
\begin{aligned}
&aF(a+1; c; z) + (a-c)F(a-1; c; z) \\
&\qquad + (c - 2a - z)F(a; c; z) = 0
\end{aligned}
\tag{4B-5}
$$

These six relations between the contiguous ${}_1F_1$ functions are analogous to the 15 relations, given by Gauss, between the contiguous ${}_2F_1$ hypergeometric functions and may be derived from these by using

$${}_1F_1(a; c; z) = \operatorname*{Limit}_{b\to\infty} {}_2F_1\left(a, b; c; \frac{z}{b}\right) \tag{4B-6}$$

A recurrence relation involving two ${}_1F_1$'s of the type (4B–4) may be obtained by replacing a by $a+1$ in the relation given by row four of the table

[51] G. N. Watson, "Theory of Bessel Functions" (Cambridge, 1922), p. 191.

and then eliminating ${}_1F_1(a+1;c;z)$ from this relation and the one obtained from row 3 of the table. There results

$$ {}_1F_1(a;c;z) = {}_1F_1(a;c-1;z) + \frac{za}{c(1-c)} F(a+1;c+1;z) \qquad (4B\text{–}7) $$

Setting ν equal to zero and one in (4B–4) and a equal to $\frac{1}{2}$, c equal to 2 in (4B–7) gives

$$ \begin{aligned} {}_1F_1\left(\frac{1}{2};1;z\right) &= e^{z/2} I_0\left(\frac{z}{2}\right) \\ {}_1F_1\left(\frac{3}{2};3;z\right) &= 4z^{-1}e^{z/2} I_1\left(\frac{z}{2}\right) \\ {}_1F_1\left(\frac{1}{2};2;z\right) &= e^{z/2}\left[I_0\left(\frac{z}{2}\right) - I_1\left(\frac{z}{2}\right)\right] \end{aligned} \qquad (4B\text{–}8) $$

Starting with these relations the relations in the table enable us to find an expression for ${}_1F_1(n+\frac{1}{2};m;z)$ where n and m are integers. A number of these are given in Bennett's paper. In particular, using (4B–2),

$$ {}_1F_1\left(-\frac{1}{2};1;-z\right) = e^{-z/2}\left[(1+z)I_0\left(\frac{z}{2}\right) + zI_1\left(\frac{z}{2}\right)\right]. \qquad (4B\text{–}9) $$

APPENDIX 4C

The Power Spectrum Corresponding to ψ_τ^n

Quite often we encounter the integral

$$ G_n(f) = \int_0^\infty [\psi(\tau)]^n \cos 2\pi f\tau \, d\tau \qquad (4C\text{–}1) $$

where $\psi(\tau)$ is the correlation function corresponding to the power spectrum $w(f)$. From the fundamental relation between $w(f)$ and $\psi(\tau)$ given by (2.1–5),

$$ G_1(f) = \frac{w(f)}{4} \qquad (4C\text{–}2) $$

The expression for the spectrum of the product of two functions enables us to write $G_n(f)$ in terms of $w(f)$. We shall use the following form of this expression: Let $F_r(f)$ be the spectrum of the function $\varphi_r(\tau)$ so that

$$ \begin{aligned} \varphi_r(\tau) &= \int_{-\infty}^{+\infty} F_r(f) e^{2\pi i f\tau} \, df, \quad r = 1, 2 \\ F_r(f) &= \int_{-\infty}^{+\infty} \varphi_r(\tau) e^{-2\pi i f\tau} \, dt \end{aligned} $$

Then

$$\int_{-\infty}^{+\infty} \varphi_1(\tau)\varphi_2(\tau)e^{-2\pi i f\tau}\,d\tau = \int_{-\infty}^{+\infty} F_1(x)F_2(f-x)\,dx \qquad \text{(4C-3)}$$

i.e., the spectrum of the product $\varphi_1(\tau)\varphi_2(\tau)$ is the integral on the right. If $\varphi_1(\tau)$ and $\varphi_2(\tau)$ are real even functions of τ, (4C-3) may be written as

$$\int_0^{\infty} \varphi_1(\tau)\varphi_2(\tau)\cos 2\pi f\tau\,d\tau = \frac{1}{2}\int_{-\infty}^{+\infty} F_1(x)F_2(f-x)\,dx \qquad \text{(4C-4)}$$

In order to obtain $G_2(f)$ we set $\varphi_1(\tau)$ and $\varphi_2(\tau)$ equal to $\psi(\tau)$. We may then use (4C-4) since $\psi(\tau)$ is an even real function of τ. When $\varphi_r(\tau)$ is an even real function of τ we see, from the Fourier integral for $F_r(f)$, that $F_r(f)$ must be an even real function of f. We therefore set

$$2F_r(f) = w(f), \qquad r = 1, 2$$

and define $w(f)$ for negative f by

$$w(-f) = w(f) \qquad \text{(4C-5)}$$

Equation (4C-4) then gives

$$\begin{aligned} G_2(f) &= \frac{1}{8}\int_{-\infty}^{+\infty} w(x)w(f-x)\,dx \\ &= \frac{1}{8}\int_0^f w(x)w(f-x)\,dx \\ &\quad + \frac{1}{4}\int_0^{\infty} w(x)w(f+x)\,dx \end{aligned} \qquad \text{(4C-6)}$$

where in the second equation only positive values of the argument of $w(f)$ appear.

In order to get $G_3(f)$ we set $\varphi_1(\tau)$ equal to $\psi(\tau)$, $2F_1(f)$ equal to $w(f)$, and $\varphi_2(\tau)$ equal to $\psi^2(\tau)$. Then

$$\begin{aligned} F_2(f) &= 2\int_0^{\infty} \varphi_2(\tau)\cos 2\pi f\tau\,d\tau \\ &= 2G_2(f) \end{aligned}$$

and from (4C-4) we obtain

$$\begin{aligned} G_3(f) &= \frac{1}{2}\int_{-\infty}^{+\infty} w(x)G_2(f-x)\,dx \\ &= \frac{1}{16}\int_{-\infty}^{+\infty} w(x)\,dx \int_{-\infty}^{+\infty} w(y)w(f-y)\,dy \end{aligned} \qquad \text{(4C-7)}$$

Equation (4C–7) suggests that we may write the expression for $G_2(f)$ as

$$G_2(f) = \frac{1}{2}\int_{-\infty}^{+\infty} w(x)G_1(f - x)\,dx \tag{4C–8}$$

This is seen to be true from (4C–2) and (4C–6). In fact it appears that

$$G_n(f) = \frac{1}{2}\int_{-\infty}^{+\infty} w(f - x)G_{n-1}(x)\,dx \tag{4C–9}$$

might be used for a step by step computation of $G_n(f)$.

We now consider $G_n(f)$ for the case of relatively narrow band pass filters. As examples we take filters whose characteristics give the following $w(f)$'s and $\psi(\tau)$'s

TABLE 1

Filter	$w(f)$ for $f > 0$	$\psi(\tau)$
a	$\frac{\psi_0}{\sigma\sqrt{2\pi}} e^{-(f-f_0)^2/2\sigma^2}$	$\psi_0 e^{-2(\pi\sigma\tau)^2} \cos 2\pi f_0 \tau$
b	$\frac{\psi_0 \alpha}{\pi} \frac{1}{\alpha^2 + (f - f_0)^2}$	$\psi_0 e^{-2\pi\alpha\lvert\tau\rvert} \cos 2\pi f_0 \tau$
c	$w(f) = w_0 = \psi_0/\beta$ for $f_0 - \frac{\beta}{2} < f < f_0 + \frac{\beta}{2}$; $w(f) = 0$ elsewhere	$\psi_0 \frac{\sin \pi\beta\tau}{\pi\beta\tau} \cos 2\pi f_0 \tau$

We shall refer to these filters as Filter a, Filter b, and Filter c, respectively. All have f_0 as the mid-frequency of the pass band. The constants have been chosen so that they all pass the same average power when a wide band voltage is applied:

$$\psi_0 = \int_0^\infty w(f)\,df = \text{mean square value of } I(t) \text{ or } V(t)$$

and it is assumed that $f_0 \gg \sigma$, $f_0 \gg \alpha$, $f_0 \gg \beta$ so that the pass bands are relatively narrow.

Expressions for $G_n(f)$ corresponding to several values of n are given in Table 2. When $n = 1$, $G_1(f)$ is simply $w(f)/4$. $G_2(f)$ is obtained by setting $n = 2$ in the definition (4C–1) for $G_n(f)$, squaring the $\psi(\tau)$'s of Table 1, and using

$$\cos^2 2\pi f_0\tau = \tfrac{1}{2} + \tfrac{1}{2}\cos 4\pi f_0\tau$$

TABLE 2

$G_n(f)$	Filter a	Filter b
$G_1(f)$	$\dfrac{\psi_0}{4\sigma\sqrt{2\pi}}\, e^{-(f-f_0)^2/2\sigma^2}$	$\dfrac{\alpha\psi_0}{4\pi}\,\dfrac{1}{\alpha^2+(f-f_0)^2}$
$G_2(f)$	$\dfrac{\psi_0^2}{8\sigma\sqrt{4\pi}}\,[2e^{-f^2/4\sigma^2}+e^{-(f-2f_0)^2/4\sigma^2}]$	$\dfrac{2\alpha\psi_0^2}{8\pi}\left[\dfrac{2}{4\alpha^2+f^2}+\dfrac{1}{4\alpha^2+(f-2f_0)^2}\right]$
$G_3(f)$	$\dfrac{\psi_0^3}{16\sigma\sqrt{6\pi}}\,[3e^{-(f-f_0)^2/6\sigma^2}+e^{-(f-3f_0)^2/6\sigma^2}]$	$\dfrac{3\alpha\psi_0^3}{16\pi}\left[\dfrac{3}{9\alpha^2+(f-f_0)^2}+\dfrac{1}{9\alpha^2+(f-3f_0)^2}\right]$
$G_4(f)$	$\dfrac{\psi_0^4}{32\sigma\sqrt{8\pi}}\,[6e^{-f^2/8\sigma^2}+4e^{-(f-2f_0)^2/8\sigma^2}+e^{-(f-4f_0)^2/8\sigma^2}]$	$\dfrac{4\alpha\psi_0^4}{32\pi}\left[\dfrac{6}{16\alpha^2+f^2}+\dfrac{4}{16\alpha^2+(f-2f_0)^2}+\dfrac{1}{16\alpha^2+(f-4f_0)^2}\right]$
$G_n(f)$ n odd f small	0	0
$G_n(f)$ n even f small	$\dfrac{\psi_0^n\, n!}{\left(\frac{n}{2}\right)!\left(\frac{n}{2}\right)!}\,\dfrac{e^{-f^2/2n\sigma^2}}{2^{n+1}\sigma\sqrt{2n\pi}}$	$\dfrac{\psi_0^n\, n!}{\left(\frac{n}{2}\right)!\left(\frac{n}{2}\right)!\,2^n}\,\dfrac{1}{2^{n+1}\,\pi n\alpha}\,\dfrac{1}{1+\left(\dfrac{f}{n\alpha}\right)^2}$
$G_n(f)$ n even n large f small	$\dfrac{1}{2\pi\sigma n}\, e^{-f^2/2n\sigma^2}$	$\dfrac{2}{\alpha(2\pi n)^{3/2}}\,\dfrac{1}{1+\left(\dfrac{f}{n\alpha}\right)^2}$
Filter c $G_1(f)$	$\dfrac{\psi_0}{4\beta}$ when $f_0-\dfrac{\beta}{2}<f<f_0+\dfrac{\beta}{2}$ 0 elsewhere	
Filter c $G_2(f)$		$\dfrac{\psi_0^2}{4\beta}\left(1-\dfrac{f}{\beta}\right)$ when $0\le f\le\beta$ $\dfrac{\psi_0^2}{8\beta^2}(f-2f_0+\beta)$ " $2f_0-\beta\le f\le 2f_0$ $\dfrac{\psi_0^2}{8\beta^2}(2f_0+\beta-f)$ " $2f_0\le f\le 2f_0+\beta$

The expression for $G_2(f)$ given in Table 2 corresponding to Filter c is exact. The expressions for Filters a and b give good approximations around $f = 0$ and $f = 2f_0$ where $G_2(f)$ is large. However, they are not exact because terms involving $f + 2f_0$ have been omitted. It is seen that all three G_2's behave in the same manner. Each has a peak symmetrical about $2f_0$ whose width is twice that of the original $w(f)$, is almost zero between 0 and $2f_0$, and rises to a peak at 0 whose height is twice that at $2f_0$.

$G_3(f)$ is obtained by cubing the $\psi(\tau)$ given in Table 1 and using

$$\cos^3 2\pi f_0\tau = \tfrac{3}{4}\cos 2\pi f_0\tau + \tfrac{1}{4}\cos 6\pi f_0\tau.$$

From the way in which the cosine terms combine with $\cos 2\pi f\tau$ in (4C–1) we see that $G_3(f)$, for our relatively narrow band pass filters, has peaks at f_0 and $3f_0$, the first peak being three times as high as the second. The expressions given for $G_3(f)$ and $G_4(f)$ are approximate in the same sense as are those for $G_2(f)$. It will be observed that the coefficients within the brackets, for Filters a and b, are the binomial coefficients for the value of n concerned. Thus for $n = 2$, they are 2 and 1, for $n = 3$ they are 3 and 1, and for $n = 4$ they are 6, 4, and 1.

The higher $G_n(f)$'s for Filters a and b may be computed in the same way. The integrals to be used are

$$\int_0^\infty e^{-2n(\pi\sigma\tau)^2}\cos 2\pi f\tau\, d\tau = \frac{e^{-f^2/2n\sigma^2}}{2\sigma\sqrt{2n\pi}}$$

$$\int_0^\infty e^{-2n\pi\alpha\tau}\cos 2\pi f\tau\, d\tau = \frac{1}{2\pi}\frac{n\alpha}{n^2\alpha^2 + f^2}$$

In many of our examples we are interested only in the values $G_n(f)$ for f near zero, i.e., only in that peak which is at zero. It is seen that $G_n(f)$ has such a peak only when n is even, this peak arising from the constant term in the expansion

$$\cos^{2k} x = \frac{1}{2^{2k-1}}\left[\cos 2kx + 2k\cos 2(k-1)x + \frac{(2k)(2k-1)}{2!}\cos 2(k-2)x + \cdots + \frac{(2k)!}{(k-1)!(k+1)!}\cos 2x + \frac{(2k)!}{k!k!2}\right]$$

Abstracts of Technical Articles by Bell System Authors

Historical Background of Electron Optics.[1] C. J. Calbick. The discovery of electron optics resulted from studies of the action, upon electrons or other charged particles, of electric and magnetic fields employed for the purpose of obtaining sharply defined beams. The original Braun tube (1896) employed gas-focusing, as did the low-voltage cathode-ray oscilloscope developed by Johnson in 1920. It was early discovered that an axial magnetic field could be used to concentrate the electrons into a beam, and this method came into wide use in the field of high-voltage cathode-ray oscillography. In 1927 Busch published a theoretical study of the action of an axially-symmetric magnetic field upon paraxial electrons, showing that the equation of the trajectories of the electrons was similar to that of the paths of light rays through an axially symmetric optical system. He concluded that such magnetic fields constituted lenses for electrons and presented experimental confirmation. In 1931 Knoll and Ruska presented a large amount of additional experimental material and used the words "electron optics" to describe the analogy. In 1932 Bruche and Johannson published the first electron micrographs.

The Davisson and Germer electron diffraction experiments (1927) employed electron beams formed by electron guns consisting of a thermionic cathode emitting electrons which were accelerated by potentials applied to a series of plates containing aligned apertures. The resultant beam was quite divergent. Davisson and Calbick made a theoretical and experimental study of the forms of such beams. They concluded that the distorted electric field in the vicinity of an aperture in a charged plate constituted a lens for charged particles (1931). The optical analogy was either a cylindrical or a spherical lens, according as the aperture was a slit or a circular hole. The theory was confirmed by photographing the forms of electron beams, and by construction of an electrostatic electron microscope whose experimental magnification agreed with the theoretical.

Coaxial Cables and Associated Facilities.[2] J. J. Pilliod. (*Summary of Talk before St. Louis Electrical Board of Trade*, October 17, 1944.) Coaxial cables provide means of transmitting frequency bands several million cycles in width over a metal tube a little larger than a lead pencil, with a copper wire extending along its axis. Several of these tubes can be placed in a lead sheath.

The frequency band transmitted over coaxial cables may be split up so as to provide several hundred telephone circuits or, without such division,

[1] *Jour. Applied Physics*, October 1944.
[2] *FM and Television*, November 1944.

coaxial cables will provide for broad-band transmission service such as is required for television.

A cable is now being installed between Terre Haute and St. Louis which contains six coaxial tubes to provide telephone circuits, and which may, in the future, find use in connection with the provision of intercity television networks.

The structure of the tubes used with coaxial cables consists of a central copper conductor within a copper tube about $\frac{1}{4}$ in. in diameter, made from flat copper strip which is formed around the insulating discs. Around each copper tube are two steel tapes which supplement the shielding of the copper tube in preventing interference between tubes in close proximity. The central conductor is separated from the outer conductor by slotted insulating disks which are forced onto the wire. The cables are formed with an appropriate number of these tubes along with some small gauge pairs used for control and operating purposes.

In the case of underground cables buried directly in the earth, jute or plastic protective coverings are used to assist in reducing sheath corrosion. In some parts of the country it is essential to add a metal covering outside the lead sheath and the plastic or jute to protect the cables against the operations of ground squirrels or pocket gophers. In certain areas these animals have been found to carry away long sections of the jute covering and will chew holes in the lead sheath unless other metal protection is provided. Copper is sometimes used for this metal covering to assist in lightning protection.

Repeaters in the coaxial system are now located at intervals of about five miles. Power for repeaters in the auxiliary stations is supplied from the adjacent main stations located at something over 50 miles at 60 cycles over the coaxial conductors themselves.

Coaxial cables are in regular operation between New York and Philadelphia and between Minneapolis and Stevens Point, Wisconsin, a total distance of nearly 300 miles. A network of such cables totaling about 7,000 route miles and including a second transcontinental cable route is being planned over additional routes. The requirements of the armed forces, general business conditions, the volume and distribution of long distance telephone messages, the availability of the necessary manufactured cable and equipment, and other factors may modify the extent of this construction, the time of starting, and the routes which will be undertaken.

Western Electric Recording System—U. S. Naval Photographic Science Laboratory.[3] R. O. Strock and E. A. Dickinson. This paper describes the complete 35-mm film and $33\frac{1}{3}$ or 78 rpm. disk recording and re-recording equipment installed for the U. S. Navy at the Photographic Science Laboratory, Anacostia, D. C. Modern design, excellent performance, and ease of operation are features of the installation.

[3] *Jour. Soc. Motion Picture Engineers,* December 1944.

Contributors to this Issue

WILLIAM A. EDSON. Kansas University, B.S. 1934; M.S. 1935. Harvard University, D.S. 1937. Bell Telephone Laboratories, 1937–1941 and 1943–. Assistant Professor of Electrical Engineering 1941–1942 at Illinois Institute of Technology, Chicago. Prior to 1941 Dr. Edson was concerned with carrier telephone terminal devices. At the present time he is engaged full time on war projects.

RICHARD C. EGGLESTON. Ph.B. 1909 and M.F. 1910, Yale University; U. S. Forest Service, 1910–1917; Pennsylvania Railroad, 1917–1920; First Lieutenant, Engineering Div., Ordnance Dept., World War I, 1918–1919; American Telephone and Telegraph Company, 1920–1927; Bell Telephone Laboratories, 1927–. Mr. Eggleston has been engaged chiefly with problems relating to the strength of timber and with statistical investigations in the timber products field.

S. O. RICE. B.S. in Electrical Engineering, Oregon State College, 1929; California Institute of Technology, 1929–30, 1934–35. Bell Telephone Laboratories, 1930–. Mr. Rice has been concerned with various theoretical investigations relating to telephone transmission theory.